INFORMATION TO USERS

This manuscript has been reproduced from the microfilm master. UMI films the text directly from the original or copy submitted. Thus, some thesis and dissertation copies are in typewriter face, while others may be from any type of computer printer.

The quality of this reproduction is dependent upon the quality of the copy submitted. Broken or indistinct print, colored or poor quality illustrations and photographs, print bleedthrough, substandard margins, and improper alignment can adversely affect reproduction.

In the unlikely event that the author did not send UMI a complete manuscript and there are missing pages, these will be noted. Also, if unauthorized copyright material had to be removed, a note will indicate the deletion.

Oversize materials (e.g., maps, drawings, charts) are reproduced by sectioning the original, beginning at the upper left-hand corner and continuing from left to right in equal sections with small overlaps. Each original is also photographed in one exposure and is included in reduced form at the back of the book.

Photographs included in the original manuscript have been reproduced xerographically in this copy. Higher quality 6" x 9" black and white photographic prints are available for any photographs or illustrations appearing in this copy for an additional charge. Contact UMI directly to order.

UMI

A Bell & Howell Information Company
300 North Zeeb Road, Ann Arbor MI 48106-1346 USA
313/761-4700 800/521-0600

Université d'Ottawa · University of Ottawa

The Use of Acid Sensitive Dyes to Monitor Acid Generation and Diffusion in Thin Polymer Films

Susan Virdee

A thesis presented to the

School of Graduate Studies and Research

In partial fulfillment of the requirements for the degree of

Master of Science

(Specialization in Chemical and Environmental Toxicology)

Université d'Ottawa · University of Ottawa

In the Ottawa-Carleton Chemistry Institute,

Department of Chemistry, University of Ottawa, Canada

Abstract

In integrated circuit fabrication, microlithography is used to image the various thin film materials which build up the device on a semiconductor substrate. To delineate exposed from unexposed areas in the film, chemically amplified resists use thermally activated acid catalytic reactions to change the local solubility of the resist's polymer. During exposure of the resist, an acid is photo-generated. At temperatures that are sufficient to activate the catalytic reaction, the acid diffuses within the resist. Since the sizes of integrated circuits are continually decreasing (down to 0.1 μm) the phenomenon of acid diffusion may become an increasing problem that would lead to degradation of the resist resolution and subsequent failure of the chip.

For purposes of understanding the diffusion behavior, we have developed the dyes and the basic knowledge that will allow the monitoring of acid diffusion in thin polymer films. We believe that fluorescence spectroscopy is the suitable tool for this purpose and have used acid-sensitive probes to monitor the presence of acid in thin polymer films. The three categories of compounds that were used were: 1) aromatic monoazines; 2-phenylpyridine, 2-phenylquinoline, and acridine, 2) xanthene dyes; fluorescein and rhodamine B base, and 3) various benzothiazole derivatives. The three main objectives of this part of the research were to choose the most appropriate sensors, observe images through fluorescence microscopy and study the feasibility of monitoring diffusion through fluorescence spectroscopy. All dyes were studied in polyhydroxy styrene (PHS) and/or polymethylmethacrylate (PMMA) films to monitor their abilities to change in the presence of added acid or photo-generated acid. All dyes were found to exhibit a change in spectral properties in the presence of acid. Fluorescence microscopy was used to observe images generated through a photomask onto photoacid generator (PAG)/polymer/dye systems. This yielded photographs of the generated images

ranging from 55 μm down to 1 μm lines. Diffusion experiments were conducted to monitor the diffusion from areas of image to areas of non-image. These results indicated that diffusion in an imaged sample can be monitored by such a method. Diffusion experiments were also done to monitor vertical diffusion or acid loss from irradiated polymer/PAG/dye systems.

The second part of this research also dealt with photoacid generation studies in thin polymer films. In this part of the research, an *in situ* method for quantifying acid-generation in photoresist sample was developed. The technique utilized a number of the acid-sensitive probes that were used for the diffusion studies but employed absorption spectroscopy. The dyes used were rhodamine B Base, fluorescein, Coumarin-6, DSB, DSBS and DMBB. The protonated form of each of these dyes has a spectrally different absorption than the neutral form. This change can be utilized to quantify the amounts of acid generated from a PAG, assuming that the change in absorption spectra is a direct result of acid-generation upon irradiation. Calibration plots for each of the dyes with increasing amounts of acid were made such that the PAG quantification could be done.

The last part of this thesis was done as a requirement to qualify for the Specialization in Environmental Chemistry and Toxicology. The toxicological properties of some of the components that are used to manufacture the photoresist compounds were reviewed. These included the solvents (diglyme, ethyl lactate) and some of the polymers (PMMA) used to manufacture photoresists. Furthermore, the toxicological properties of the some of the dyes (acridine, fluorescein, rhodamine B, 2-phenylquinoline, 2-phenylpyridine) proposed for purposes of monitoring acid quantification and acid diffusion, were reviewed.

Acknowledgments

The completion of this work cannot be considered without thanking a number of people to whom I am very grateful. First, and foremost, I would like to thank Tito Scaiano for giving me the opportunity to work in his lab, both on a CO-OP workterm and for the purposes of this work. Over the years, he has not only been a great supervisor, but also a very generous and understanding person. I am indebted to him for the experience he has given me and will always be grateful.

I would also like to thank my "pseudo-supervisor", Gerd Pohlers. Over the course of this M.Sc. he has helped me to a great extent in the completion of this work. His expertise and suggestions have always been valued. I would also like to thank him for some of the research he has done on the photophysical properties of the dyes studied in this research.

Furthermore, I would like to thank Roger Sinta for giving me the opportunity to conduct research at Shipley, Co. I would like to thank him, as well as Matt King and Jim Cameron for their work on the acid quantification studies. I would also like to thank everyone else at Shipley, who made the experience memorable and fun.

I would like to thank all the members and visitors of the Scaiano group with whom I have had the opportunity to work. I would especially like to thank Gerry Charette and Andre Simard for their amazing technical abilities and help through the years.

I would also like to thank my friends and family. Special thanks to Sham Syal for all the encouragement and good laughs he has given over the past years. Thanks to Mom, Dad, Amar and Rob for all their love and support. Finally, I would like to thank Gordon Rice, my soulmate, for being there and putting up with me during the writing of this thesis.

Table of Contents

List of Figures

Chapter 1

Chapter 2

Chapter 3

Chapter 4

List of Tables

Chapter 1

Chapter 2

Chapter 3

Chapter 1

Introduction

1.0. Objective

The main objective of this thesis is to use acid-sensitive probes to monitor acid diffusion and quantify acid generation in thin polymer films. The first part of this objective is to study acid-sensitive dyes that may be used to monitor acid diffusion in photoresist samples. Qualitative diffusion studies have been carried out to test the usefulness of the dyes studied. This thesis sets the stage to determine such diffusion coefficients by determining the feasibility of using acid-sensitive dyes. The second part of this objective, deals with the use of these acid-sensitive probes to quantify acid-generation in thin polymer films.

1.1. Historical Perspective

The microelectronics revolution has had a profound impact on our technological society over the latter half of the twentieth century in a number of diverse fields, such as automobiles, computers and communications, medicine, energy, and home entertainment[1]. The key innovation that initiated the microelectronics era was the invention of the monolithic integrated circuit in 1960. The invention provided a means for the internal interconnection of many solid-state devices on a semiconductor substrate to produce a working unit capable of performing complex electronic functions. Using this technology, the density of active devices making up an electronic circuit could be increased many thousands of times over that achievable with discrete or single-transistor devices.

The conventional means of increasing the level of integration of an integrated circuit, that is, of increasing the circuit density, has been to make the active elements in the devices smaller, thereby increasing the number of active circuits[2] that can be accommodated on a given

area of silicon. Overall, the size of the circuit elements in random access memories has continually decreased, with a concomitant increase in the number of active devices per chip. The reduction in feature size over time follows a linear trend that can be anticipated to continue for at least two more decades and lead to devices with minimum features as small as 0.1 μm[1].

The structure of an integrated circuit is quite complex, both in the topography of its surface and in its internal composition. Each element in such a device has an intricate three-dimensional architecture that must be reproduced exactly in every circuit. The structure is made up of many layers, each patterned in a manner required by the circuit design. Some of the layers lie within the substrate semiconductor wafer, and others are stacked on top. Fabrication of an integrated circuit, therefore, requires processes for depositing and patterning this sequence of layers.

In integrated circuit fabrication, microlithography is used to image the various thin film materials which build up the device on a semiconductor substrate. The primary step of the microlithographic process is the delineation of the desired circuit design in a resist layer, which generally consists of a photosensitive thin polymer film (or photoresist) spin coated on the semiconductor material. The lithographic process involves transferring a circuit pattern through a photomask into the polymer film (photoresist) and subsequently replicating that pattern in the underlying thin conductor or dielectric film. This process will be discussed in a further section of the introduction.

1.2. Lithographic Strategy

The basic goal of the lithographic process is the accurate and precise definition of three-dimensional patterns on the semiconductor substrate. These patterns delineate the areas for subsequent doping or thin-film etching to provide for the internal interconnection of devices. There are many techniques for creating these three-dimensional patterns. Photolithography,

was the first technique developed, and still continues to be the dominant technology but has undergone many innovations since it was first developed. Photolithography (contact, proximity or projection printing), uses ultraviolet radiation to transfer the pattern from the mask to a photosensitive resist. The size of the features that can be printed by photolithography is ultimately limited by the wavelength of the exposing radiation just as the resolution of an optical microscope is limited by the wavelength of the "white" light used for imaging. Photolithographic systems can print features about 1.3 times the exposure wavelength in size with good process latitude. With considerable reduction in overall process latitude, features comparable in size to the exposure wavelength can be printed. Most advanced circuits are currently manufactured with features of 0.5-0.7 μm dimensions by using G-line (λ = 436 nm) or ĭ-line (λ = 365 nm) and 5 times reduction step-and -repeat exposure tools. Where step and repeat photolithography involves exposing a small area and stepping this pattern over a large-diameter wafer. This technique was developed in the mid-1970's to accommodate larger wafers and to improve resolution. Advanced I-line technology can produce circuits with dimensions of 0.35-0.4 μm, but smaller geometries will require either new exposure-resist technologies or other technologies.

Furthermore, resolution can be improved by shifting to shorter wavelength UV light in the 240-250 nm region[3-5]. This is true because the resolution (R) is proportional to the exposing wavelength (λ), following the relationship ($R = k\lambda/NA$)[6]. Where the term NA refers to the numerical aperture of the lens and k is a constant. Thus higher resolutions can be obtained by either increasing the numerical aperture or by reducing the exposing wavelength. Increasingly, the industry is moving to lower wavelengths (i.e. 254 and 193 nm). Because the materials used in conventional refractive optical systems are too opaque at these wavelengths, quartz must be used. Deep-UV systems use either a line-arrowed excimer laser operating at 248 nm or a filtered Hg lamp as a light source.

Responding to the ever-increasing circuit density, other new high resolution exposure technologies such as ion beam, e-beam and X-Ray lithography have also been developed. These new technologies including the deep-UV systems require departure from the conventional diazoquinone / novolac based resists widely used[1]. Therefore, several new classes of chemically amplified resists have been developed[7-12] all of which utilize a so called photoacid generator (PAG), i.e. a substance that produces acid as one product of photolysis. In these formulations, during a thermally-assisted post-exposure baking step, an acid-catalyzed reaction is initiated that modifies the properties of the matrix to achieve the required difference in solubility between the exposed and unexposed resist areas.

1.3. Chemical Amplification

The use of deep-UV (DUV) resists have led to an improvement in resolution. However, the switch to lower wavelengths have led to changes that were required for successful use in terms of lens design, light source, and resist. Typically, diazoquinone-novolac systems were used for earlier resist systems specifically mid-UV resists cannot be tailored for deep-UV use. This is because of the strong absorbance of novolac resins and the strong and essentially unbleachable absorbance of the diazonapthoquinone chromophore in the DUV spectral region. For this reason, designing resist systems for DUV lithography required substantial departure from the previous systems.

Another major challenge was to design resist systems that were more photosensitive than the diazonaphthoquinone systems. This is because each photon in the DUV has about twice the energy of a photon in the near UV, about twice as many joules of DUV radiation are required to carry out a chemical transformation as in the near UV, if the absorbance and quantum efficiency for the photoreaction are assumed to be the same[1]. An improvement in sensitivity of about 100-fold is required to obtain the desired effect and this can only be achieved by a system with gain or chemical amplification[13,14].

In principle, systems with chemical amplification are those in which the initial photochemical event produces a catalyst. This catalyst then acts on the surrounding matrix to mediate a cascade of reactions or initiate a chain reaction that modifies the properties of the matrix in some way that can be exploited in relief image generation. In such systems, the quantum efficiency for formation of the species responsible for differential dissolution rate is the product of the quantum efficiency for generation of the catalytic species multiplied by the number of cycles the catalyst can mediate before it is lost or inactivated in some way. Since the catalytic length can be hundreds or even thousands of turnovers[13-16], the sensitivity of resists based on chemical amplification can be as much as 2 orders of magnitude (or more) greater than that of resists that consume at least one photon for every functional conversion, as in the case for the diazoketone-based systems[1]. In chemically amplified systems, basically, the exposing radiation generates a reactive species which catalyzes the formation of many chemical reactions in the exposed areas allowing image development by virtue of the acid catalyzed solubility differential. In such systems, the efficiency for formation of species responsible for image development is the product of the quantum efficiency for acid generation multiplied by the number of reactions the catalyst can initiate before being destroyed. The use of chemical amplification to increase resist sensitivity has been demonstrated in positive[17], negative[18], and pseudo-multilayer[19] resists.

Many substances produce acid as a product of photolysis with reasonable quantum efficiency. **Table 1.1** shows a representative sampling of the different chemically amplified resists that are available. The choice of the appropriate acid generator for a resist formulation depends on such factors as: the nature of the radiation to be used, the strength and nature of the acid required for catalysis in the system, thermal stability, solubility, and toxicity.

Name	Representative Structure	Acid produced
Diazonium salts	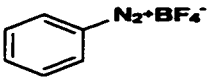	BF_3
Perhalomethyl triazines	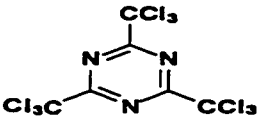	HCl
Diaryliodonium salts	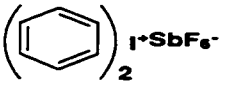	$HSbF_6$
Triarylsulfonium salts	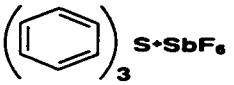	$HSbF_6$
o-Nitrobenzyl esters	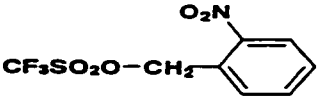	RSO_2OH
Phloroglucinol sulfonates	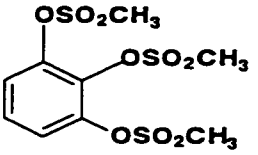	CH_3SO_2OH
Hydroxamic acid esters	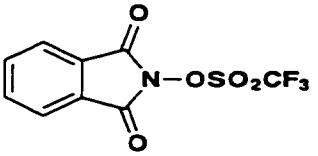	CF_3SO_2OH
Diazosulfonates	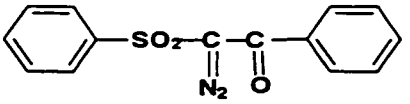	RSO_2OH
Bromobisphenol A	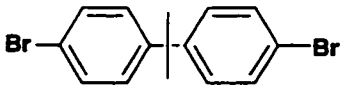	HBr

Table 1.1: Examples of types of substances that produce acid upon photolysis.

Photoacid generators may be divided into two main groups[20], i.e. ionic and non-ionic compounds. Ionic photoacid generators involve onium salts such as aryldiazonium, diaryliodonium, triarylsulfonium, and triarylphosphonium salts that contain complex metal

halides such as BF_4^-, SbF_6^-, AsF_6^- and PF_6^-. When onium salts are irradiated at wavelengths in the range of 200-300 nm, they undergo photolysis to form a protic acid. Onium salts have several advantages as photoacid generators. They are thermally stable and may be structurally modified to alter their spectral absorption characteristics. One serious disadvantage of onium salts is their limited solubility in common organic solvents.

The second group of PAGs are the systems that involve photoinduced generation from non-ionic compounds. These include the generation of carboxylic acids, sulfonic acids, phosphoric acids and hydrogen halides. Non-ionic photoacid generators have a much wider range of solubility in solvents and in polymer films than onium salt analogs. A disadvantage of the non-ionic photoacid generators arises because they are less thermally stable than the onium salts. However, this can be improved by their structural modification.

1.4. The Photolithographic Process

When a pattern is transferred to a photoresist, a photochemical reaction occurs in the areas exposed to light which generates a latent image in which the pattern information is stored chemically. When a developer is applied to the resist it differentiates between the chemistry of the exposed and unexposed areas in a way that converts one into an image and removes the other. The basic steps of the lithographic process are shown in **Figure 1.1**.

The diagram corresponds to a photolithography set-up in which the resist material is applied as a thin coating over some base and subsequently exposed through a photomask, such that light strikes selected areas of the resist material. A typical photomask for optical lithography consists of a chrome-coated glass plate 6-8 inches (15-20 cm) on a side, on which the chip pattern corresponding to the particular layer of the device has been repeated many times over its surface[1]. The exposed resist is then subjected to a development step, which

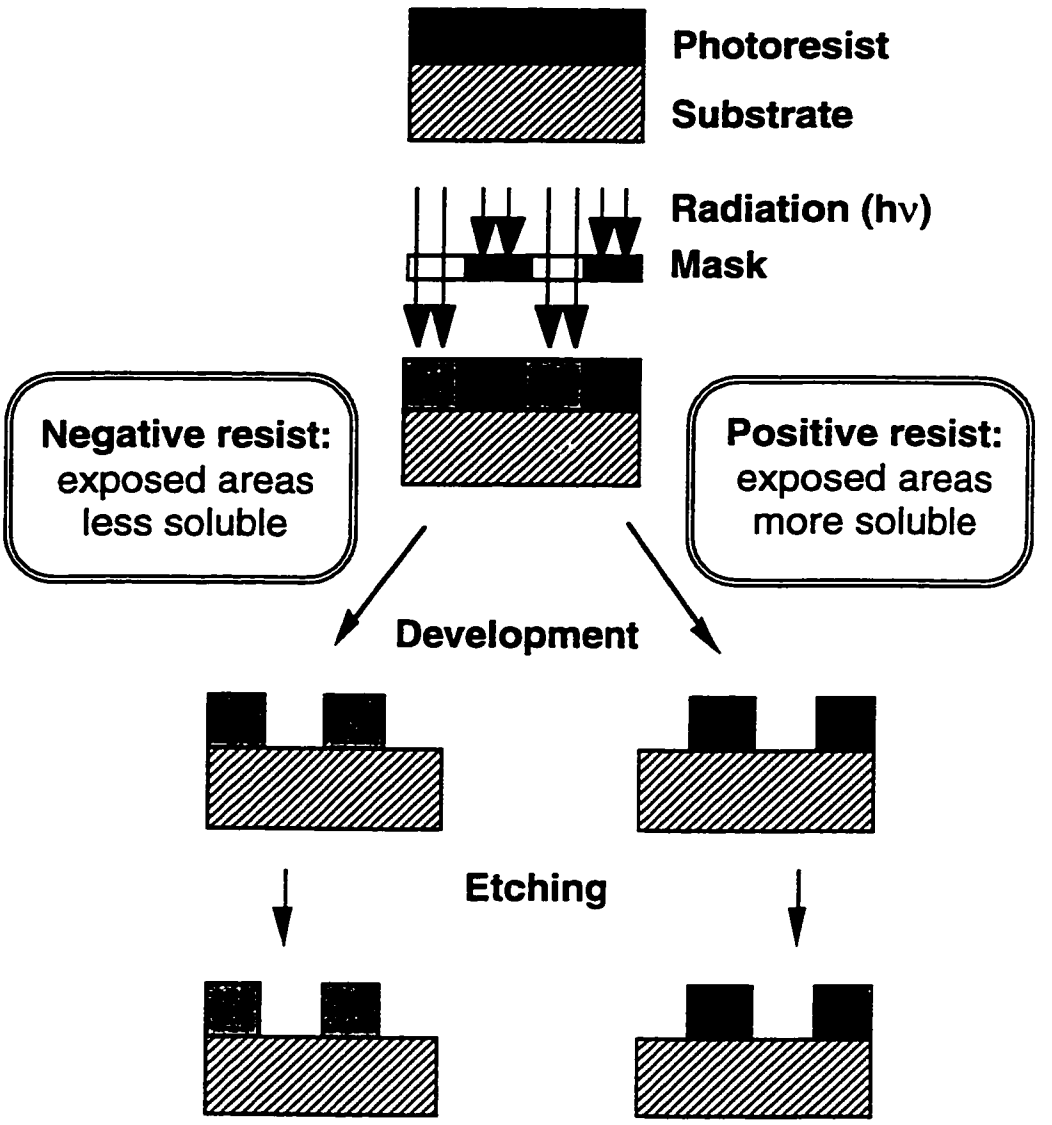

Figure 1.1: Schematic representation of the photolithographic process sequence outlying the difference between positive and negative photoresists.

generally involves immersion in an appropriate solvent. Depending on the chemical nature of the resist material, the exposed areas may become more soluble in the developing solvent than the unexposed areas, thereby producing a positive-tone image of the mask, or conversely the exposed areas may become less soluble, producing a negative-tone image of the mask[1,21,22].

The areas of most solubility are usually removed by treatment with an appropriate solvent. The two families of photoactive materials are termed either negative or positive resists depending on the solubility behavior described above. The overall effect in either case is to produce a three-dimensional relief image in the resist material that is a replication of the opaque and transparent areas on the mask.

For a resist to be useful in semiconductor manufacturing, it must not only have high sensitivity and the ability to resolve such small features but also must be capable of being spin-coated into thin and continuous films that will adhere to a variety of substrates ranging from metals to semiconductors to insulators. It must also be able to withstand exposure to extremely high temperature and exceedingly corrosive etching environments such as strong acids and plasmas without loss of adhesion or line definition.

1.5. Diffusion of Acid

To delineate exposed from unexposed areas in the film, chemically amplified resists use thermally activated acid catalytic reactions to change the local solubility of the resist's polymer. During exposure of the resist, an acid is photo-generated. At temperatures that are sufficient to activate the catalytic reaction, the acid diffuses within the resist. A little diffusion may improve the resist's lithographic capability because acid movement into the standing wave nodes, allows the regions to deprotect and develop[23]. However, acid diffusion into areas of low exposure, results in a size bias between the developed pattern and the image from the imaging tool and causes problems when designing processes for imaging many different types of features simultaneously. Also, excessive diffusion into the unexposed areas of the resist may also degrade the overall quality of the resist image.

It has been shown that the initial acid concentration is a factor in defining the final image, but the initial acid concentration is also subjected to the effects of acid diffusion, and all factors that effect the acid concentration will effect the final resist image[24]. The diffusion of

acid in chemically amplified resist will follow Fick's laws. The acid will tend to move from an area of relatively high concentration to an area of relatively low concentration. Thus, the initial acid distribution in the resist will change due to diffusion in time interval between exposure and the post exposure bake and also during the post exposure bake. Diffusion of the photoacid has been identified as the most important mechanisms responsible for image loss during the post-exposure bake (PEB)[25]. The diffusion mechanism has been shown to change as the post-exposure bake time (PEB) is increased[26], and in relation to the glass transition temperature (Tg) of the polymer [27]. Furthermore, diffusion has been shown to decrease with increasing photoacid bulkiness[28], and with respect to the concentration of remaining solvent upon baking[29]. The change in acid concentration with time is the key to understanding how acid diffusion affects the acid concentration and the final resist image.

Although the diffusion range of the acid is a crucial parameter, up to now, only limited information about the diffusion range of the photogenerated acid could be obtained. There have been attempts to estimate the diffusion range from the catalytic volume, i.e., the volume occupied by the average number of inhibitor molecules deprotected by one acid molecule[16,30]. The diffusion ranges obtained from such estimations typically vary in the range of 5-20 nm. Thus the acid diffusion would not reduce the resolution capability to a marked degree. This estimation, however, relies on the idealistic assumption that only molecules within a sphere in the nearest vicinity of the acid molecule are affected. As this hypothesis is not confirmed, since in real systems acid would likely diffuse randomly and act as a catalyst within the resist. For this reason, the diffusion range of acid should preferably be determined directly by experiments.

Several methods have been applied for the measurement of acid diffusion and its influence on lithography. Fedynyshyn *et al.*[31] have used the threshold acid density model on 1.0 μm lines/spaces exposed by excimer laser radiation. Yoshimura *et al.*[32] used single line

patterning with SEM. Nakumura *et al.*[33,34] used a mask replication method based on X-Ray exposure and measuring the undercut beneath a X-Ray absorber layer. They investigated the diffusion acid molecules in polymer film by an acid transfer experiment between two polymer films and subsequent depth of acid measurement after developing the films. Similarly, Schlegel *et al.*[35,36] also used an acid transfer experiment between two polymer films and subsequent scanning electron micrograph (SEM) pictures were taken to monitor diffusion. This technique gives more accurate estimations of the diffusion range than those estimated from the catalytic volume. Methods for physicochemical measurement of acid diffusion coefficients, e.g. conductivity measurements[24,34] have also been developed. In another study, *Raptis et al.*[37,38] used a single pixel e-beam exposure method which is based on the measurement of the diameter of lithographic features (pillars for negative resists) after a wide range of doses and PEB times. All of these methods have led to some insight into the acid diffusion processes within resist sample. However, they lack in the sense that diffusion is monitored once the chemical event is over, and thus the dynamic range of acid diffusion cannot be observed. Zuniga *et al.*[39] have conducted a number of diffusion by monitoring the deprotection front of acid diffusion by monitoring the transmission of the patterned and unpatterned wafers by FTIR and then using SEM to obtain linewidth measurements. Furthermore, Zuniga *et al.*[40-42] have monitored diffusion through the quantitative modeling of resist top loss in unexposed samples due to acid diffusion from a top-to-top contact bake with an exposed sample. Another study by Watanabe *et al.*[43] was done to monitor acid diffusibility in a film using an acidic water-soluble overcoat film and monitoring acid diffusion by SEM.

A number of studies have aimed to suppress acid-diffusion within chemically amplified resists [23,42,44-46], but much research is still required to understand the processes of acid diffusion and whether the diffusion is significant enough to pose a problem for further decreases in circuit size. The method that is proposed in this research, is different from any

previous work on this subject and is more advantageous due to its simplicity and ability to dilineate between the areas of image and non-image using fluorescent sensors. With the proposed method, the diffusion of acid can be monitored within the polymer matrices. The only other work that employ acid-sensitive dyes were reported by Mckean *et al.*[47]. However, this method did not look at the *in situ* processes of acid diffusion and were based on a solution method of quantifying the acid. Furthermore, as discussed above this method was based on a acid diffusion model based on catalytic chain length and thus a correct representation of actual events may not be represented. Two other studies were done after the proposed method of this research had begun. The first was by Ohmori *et al.*[48]. They used propargyl alcohol, a compound that undergoes acid-catalyzed rearrangement to monitor the migration of acids in polymer films. Their method is similar in the sense that they use the prototopic changes of a compound to monitor acid diffusion. However, they look at the diffusion from one coated disk to another. Furthermore, they use absorption spectroscopy, whereas we propose to use fluorescence. The other study was by Zhang *et. al.*[49]. Their study, like ours used fluorescence intensity changes of a pH-sensitive fluorescent dye to monitor acid diffusion through polymer films. However, the technique of their measurement is quite different. They introduce acid-vapor to quench the fluorescence intensity of the pH sensor. They obtain diffusion coefficients, by covalently bonding the dye onto a quartz substrate and subsequently spin coating the dye layer with a polymer layer. By introducing an acid in a chamber with the spin coated films, they measure the diffusion constant of the vaporized acid in the polymer film. We believe the technique we propose is more direct, in the sense that, we are using the actual photogeneration of the system to obtain acid diffusion information, i.e. we do not introduce acid vapor to monitor the changes in fluorescence of the pH sensitive dyes.

1.6. Plan of Study

1.6.1. The Use of Acid-Sensitive Probes to Monitor Acid Diffusion

The continuing increase in the complexity of integrated circuits, coupled with the decreasing size of the individual circuit elements, are placing more stringent demands on the fabrication processes, particularly with respect to resolution and overlay accuracy. Hence, it is important to gain a thorough understanding of the lithographic processes that are key to the continuing evolution of integrated circuit technology.

Since the sizes of integrated circuits are continually decreasing the phenomenon of acid diffusion may become an increasing problem that would lead to degradation of the resist resolution and subsequent failure of the chip. With the minimum feature size expected to approach the 0.1 μm mark within the next decade, preserving the integrity of the latent image becomes more and more critical. Diffusion of the photogenerated acid during the period of time between exposure and development can cause contrast loss and ultimately loss of the latent image. This is especially relevant for chemically amplified photoresists that require a post-exposure baking step, which in turn facilitates the diffusion of the acid due to the high temperature normally employed. A schematic of the diffusion of acid is given in **Figure 1.2**. Due to the ever decreasing feature size, diffusion of the photogenerated acid within the photoresist material leading to the deterioration of the latent image has recently become a matter of great concern in microlithography. Thus, for the ability of microlithography to keep pace with the demand for higher resolution imposed by microelectronics, the need for detailed knowledge of acid generation and diffusion processes in photoresist systems will increase dramatically during the next few years. For this reason, it is important to develop techniques to easily monitor the generation of acids in thin (~1 μm) polymer films. We believe that fluorescence spectroscopy using the dyes characterized in this thesis is a suitable tool for this purpose.

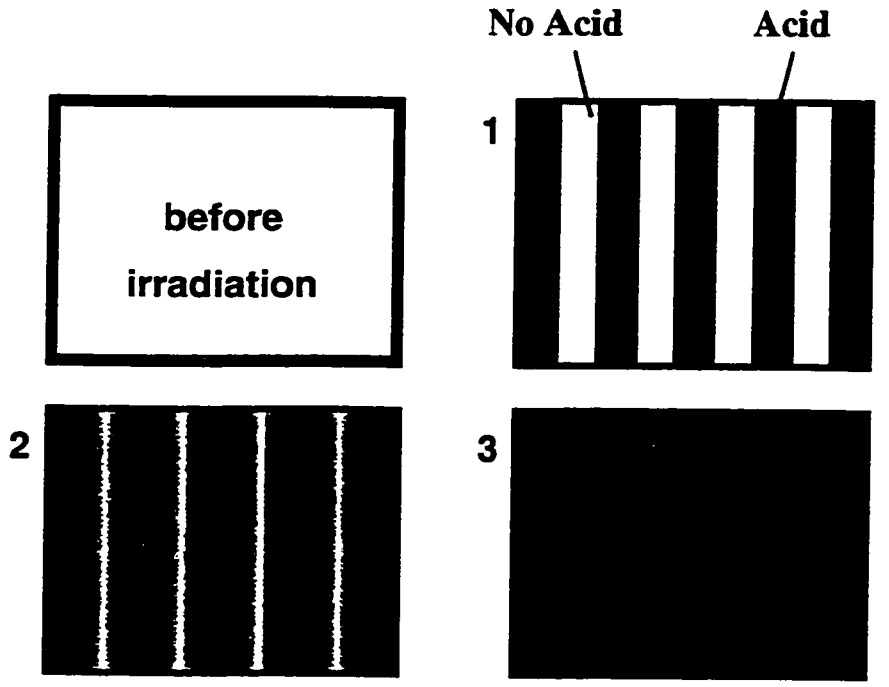

Figure 1.2: Representative drawing of the acid diffusion process within a photoresist sample.

With this technique the exact boundary between acid-containing domains and acid free regions can be observed. In accomplishing the proposed task, a number of steps are required in order to obtain such a generation of lines and spaces. Most importantly, the appropriate fluorescent sensors or dyes must be developed. In order to choose the most suitable dyes a number of factors must be considered, as will be discussed in **Chapter 2**. Specifically, it is necessary to identify molecules that have very different fluorescent properties in the presence and absence of acid. Once the dyes are developed or synthesized, they must be tested for their acid sensitivity by incorporating them into a polymer/photoacid generator (PAG) systems. This will give the changes in absorption or fluorescence spectra of these dyes in the presence of acid in the polymer system. This acid is generated from the photoacid generators upon UV exposure, and we hope to be able to present a method to be able to quantify the amounts of acid generated, as will be discussed in **Chapter 3**. The next major step, is to be able to generate an

image in these polymer samples with incorporated dye by irradiating the sample through a photomask (provided by Shipley, and manufactured by IBM). Images (specifically lines and spaces) as small as 1 μm in width are proposed to be generated.

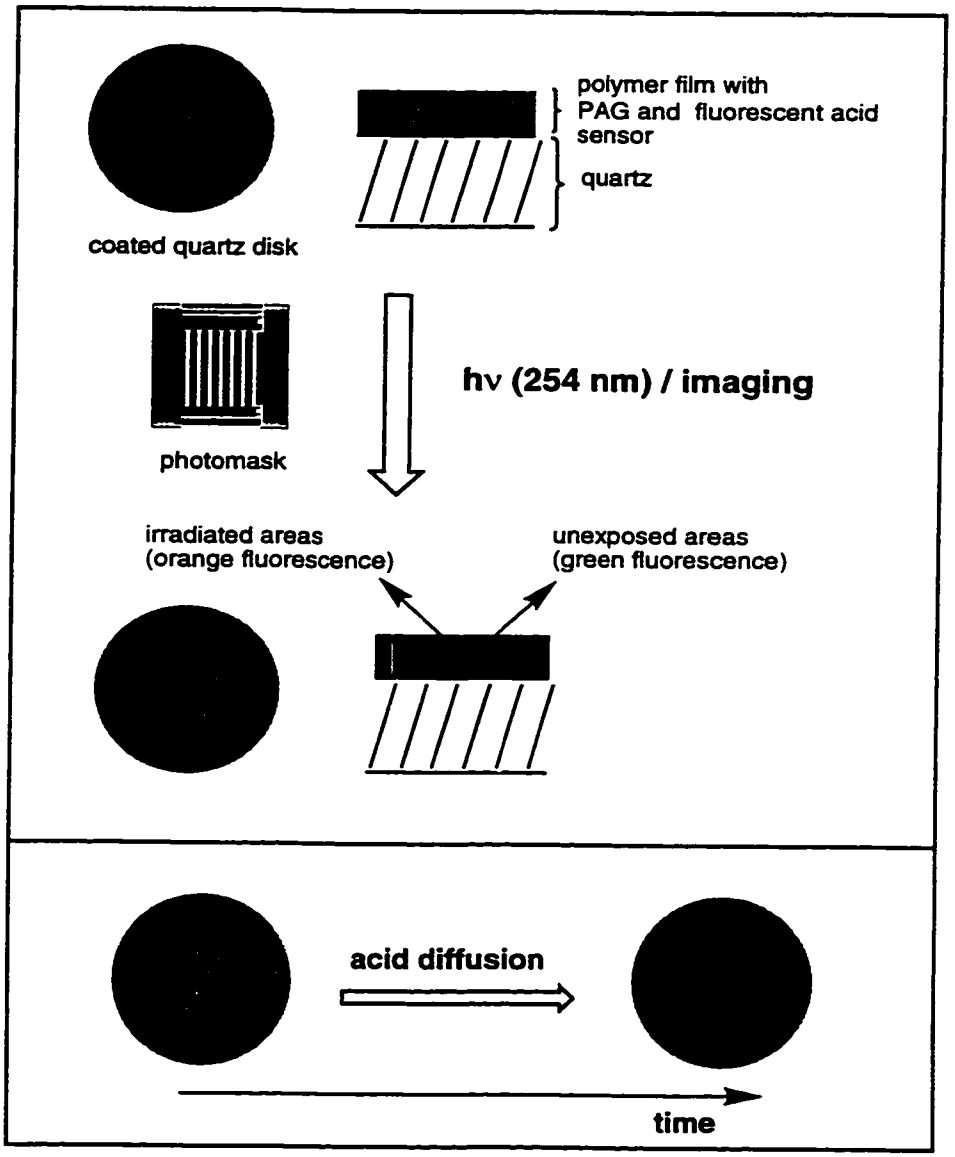

Figure 1.3: Experimental Method for Monitoring the Diffusion of Acid.

Once these images are generated, the diffusion of the acid front can be monitored. The experimental method for monitoring acid diffusion is outlined in **Figure 1.3**. For the

purposes of this work acid diffusion is proposed to be monitored using two main approaches. The first approach, is by investigating the fluorescence for both a patterned sample and a non-patterned sample (reference sample) and monitoring the changes in each as a function of time. The effect of acid diffusion would result in changes in fluorescence intensity of the patterned sample, such that it would reach that of the unpatterned sample (i.e. one). This result would happen if the protonated dye was monitored for its increase in fluorescence intensity. Subsequently, if the fluorescence of the unprotonated form was monitored, there would be a decrease in intensity until it approached zero. Thus, to monitor acid diffusion in this way either the protonated or unprotonated forms can be monitored for changes in fluorescence. The expected trends are outlined in **Figure 1.4**.

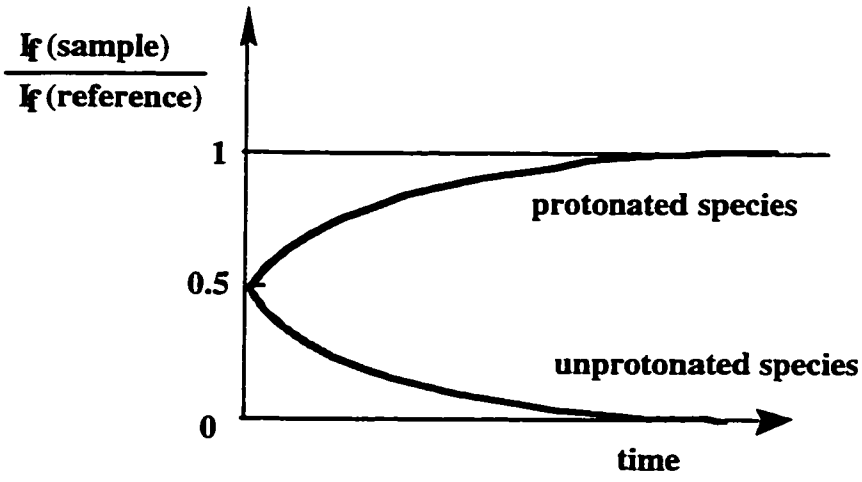

Figure 1.4: Trends that would occur when monitoring the ratio of fluorescence intensity (I_f) of the imaged sample to the non-imaged (reference) sample. Either the protonated or unprotonated species of the imaged sample can be monitored in comparison to the reference. The protonated species would eventually lead to a ratio approaching one, whereas the unprotonated species would eventually lead to a ratio approaching zero.

The second main approach to monitor acid diffusion is by directly observing the vanishing of the lines using a fluorescence microscope, as will be discussed in Section 1.9. Although, this method is only semi-quantitative, it works in conjunction with the first method to pictorially describe the events of acid diffusion within the polymer system.

In addition to lateral diffusion, an acid can also escape the film by vertical diffusion. For this reason acid loss experiments were also done. These experiments looked at the diffusion between two stacked polymer films, as depicted in **Figure 1.5**.

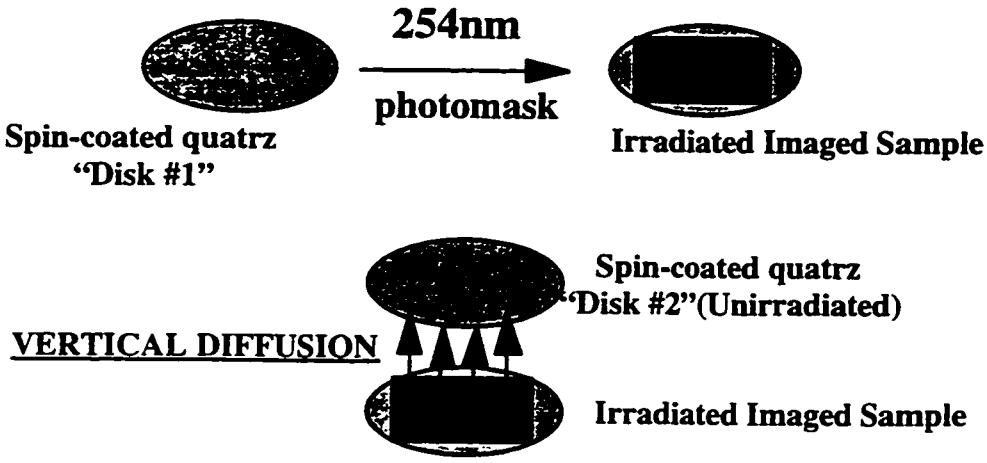

Figure 1.5: Illustration depicting the set-up of a vertical diffusion or "pancake" experiment.

The overall objective of the above research is to set-up the initial parameters (experiments) required to be able to obtain diffusion coefficients in photoresist samples. Overall, this research aims to prove the validity of the proposed technique. This will be done by testing various proposed dyes within polymer/PAG samples, testing the acid generating abilities of the PAGs, generating photoimages with UV irradiation, and subsequently monitoring the presence of the images. In future work, interpretation of diffusion data and modeling will be necessary.

1.6.2. The Use of Acid-Sensitive Probes to Quantify Photoacid Production in Thin Polymer Films

The second main objective of this research was to develop a method to quantify acid-generation in thin polymer films. Although, this work will be fully introduced in **Chapter 3** of this thesis, background is mentioned here. Up until now, there has not been an *in situ* technique of quantifying acid production from irradiated resist samples. Previous techniques have involved irradiating the samples in film and then dissolving the samples. Quantification would then be conducted by solution methods. The method proposed in this research utilizes the acid-sensitive probes characterized in this work to quantify the acid within the polymer sample. We propose this technique is more favorable since a more accurate representation of the acid quantification is achieved.

To conduct this research, suitable acid-sensitive probes must first be studied. These experiments are similar to those conducted for purposes of acid diffusion. These dye studies are reported in **Chapter 2**. Once the dyes have been studied for their acid-sensitive properties, absorption spectroscopy will be used to quantify the amounts of acid produced. This will be done by quantifying the changes in intensity at the wavelength of the protonated form of dye. The results of the acid quantification studies will be reported in **Chapter 3**.

In order to understand the techniques used for the acid diffusion and acid-quantification studies, some background information is required, as will be discussed in Sections 1.7-1.10.

1.7. Interaction of Light

When a molecule absorbs a photon, the molecule is promoted to a more energetic excited state. Conversely, when a molecule emits a photon, the energy of the molecule necessarily drops by an amount equal to the energy of a photon. When a molecule absorbs a photon, the energy of the molecule is increased. It can be said that the molecule is promoted to an excited state. If a molecule emits a photon, its energy is lowered. The lowest energy state

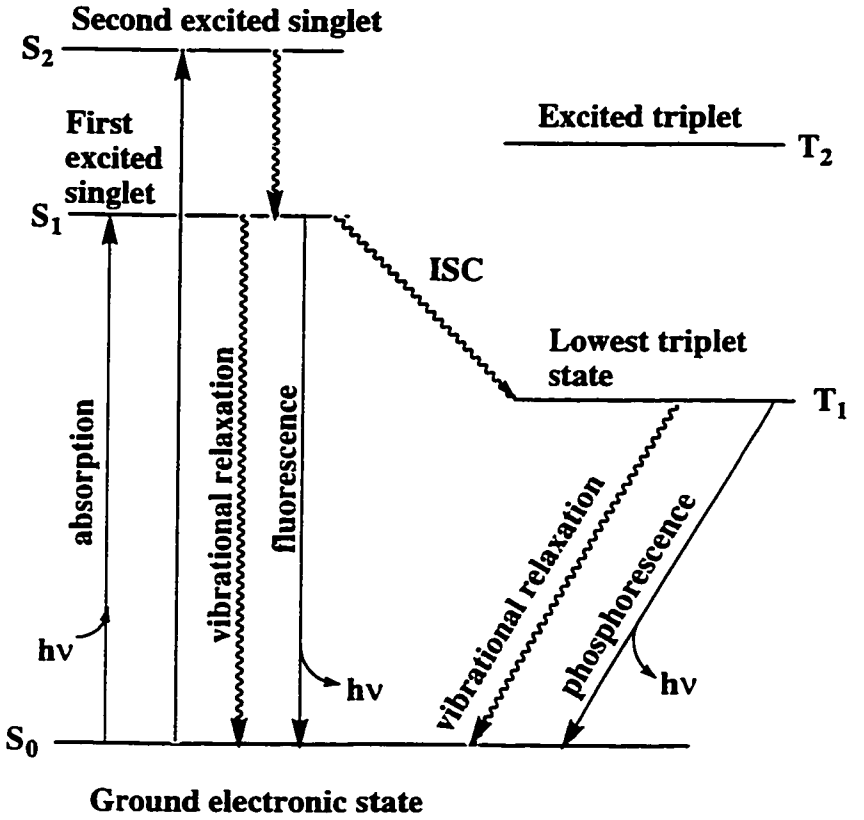

Figure 1.6: Jablonski diagram showing the absorption of light (hυ) and subsequent unimolecular deactivation processes. Radiative pathways are fluorescence and phosphorescence; nonradiative pathways are internal conversion (not shown), intersystem crossing and vibrational relaxation.

of a molecule is called the ground state. Absorption of light of an appropriate wavelength involves the promotion of an electron to an excited singlet state which relaxes back down to the ground state via radiative or nonradiative pathways. The unimolecular photophysical processes that can occur to deactivate the excited state of a molecule are depicted by the simplified Jablonski Diagram in **Figure 1.6**.

When a quantum of light impinges on a molecule, it is absorbed in about 10^{-15} sec, and a transition to a higher electronic state takes place. This absorption of radiation is highly specific, and radiation of a particular energy is absorbed only by a characteristic structure. The electron is raised to an upper excited singlet (S_1, S_2, etc.) via ground-to-singlet state transitions, which are responsible for the visible and ultraviolet absorption. Absorption transitions usually originate in the lowest vibrational level of the ground state electronic state.

During the time the molecule can spend in the excited state (10^{-1} sec), some energy in excess of the lowest vibrational energy level is rapidly dissipated The lowest vibrational level of the excited singlet state is attained. If all the excess energy is not further dissipated by collisions with other molecules, the electron returns to the ground electronic state, with the emission of energy. This process can be termed fluorescence. Since some energy is lost in the brief period before emission can occur, the emitted energy (fluorescence) is of longer wavelength than the energy that was absorbed.

The process of phosphorescence involves an intersystem crossing, or transition, usually from the excited singlet to the triplet state. A triplet state results when the spin of one electron changes so that the spins are the same, or unpaired. The transition from the ground state to the triplet excited state is a forbidden (highly improbable) transition. Internal conversion from the singlet to the triplet (electron-spin reversal) is more probable, since the energy of the lowest vibrational level T* is lower than that of S*. Molecules in T* can then

return to the ground state directly, since a return via S* can result only by acquiring energy from the environment (delayed fluorescence).

The processes of absorption and fluorescence are important with regards to the work done in this thesis. These processes will be outlined and discussed in terms of the techniques that were used.

1.8. The Use of Absorption Spectroscopy to Monitor Acid Generation:

In this work, absorption spectroscopy was used to monitor the amounts of acid generated upon UV irradiation. In order to understand the method, it is helpful to review the fundamental background of the technique.

When light is absorbed by a sample, the radiant power of the beam of light is decreased. Radiant power, P, refers to the energy per second per unit area of the light beam. A schematic of a typical spectrophotometric set-up is illustrated in **Figure 1.7**.

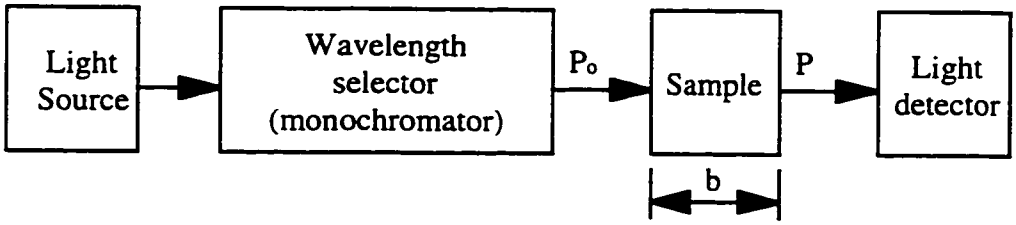

Figure 1.7: Schematic diagram of a spectrophotometric set-up.

Light is passed through a monochromator (a prism, grating, or even a filter) to select one wavelength. Light of this wavelength, with radiant power P_o strikes a sample of length b. The radiant power of the beam emerging from the other side of the sample is P. Some of the light may be absorbed by the sample so $P \leq P_o$.

The transmittance, T, is defined as the fraction of the original light that passes through the sample ($T = (P_o/P)$). Therefore, T has the range zero to one. The percent transmittance is simply 100 x T and ranges from 0 to 100%. More usefully, the other quantity that can be defined is absorbance or OD:

$$\boxed{A = \log 10\left(\frac{P_o}{P}\right) = -\log T}$$

When no light is absorbed, $P = P_o$ and $A = 0$. If 0% of the light is absorbed, 10% is transmitted and $P = P_o/10$. This gives $A = 1$. If only 1% of the light is transmitted, $A = 2$.

Absorbance is important because it is directly proportional to the concentration of the light-absorbing species in the sample by the Beer-Lambert law, or simple Beer's law:

$$\mathbf{A = \varepsilon b c}$$

The absorbance, A, is dimensionless. The concentration of the sample, c, is usually given in units of moles per liter (M). The pathlength, b, is commonly expressed in centimeters. The quantity ε (epsilon) is the molar absorptivity (or extinction coefficient) and has the units $M^{-1}\ cm^{-1}$. This quantity is the characteristic of the sample that tells how much light is absorbed at a particular wavelength. Basically, it is a coefficient of proportionality between absorbance and the product bc. The larger the value of ε, the greater is A. We will be using this relationship to quantify the amounts of acid generated from different photoacid generators upon irradiation with UV exposure. This can be done since the quantity of acid generated is a function of the light intensity, how many photons are absorbed by the PAG and the photochemical efficiency of the acid generation. To be able to quantify the amounts, we propose to use acid-sensitive probes that exhibit shifts in their absorption spectra upon protonation. In some cases this may involve a color change.

The part of a molecule responsible for light absorption is called a chromophore. Any substance that absorbs visible light will appear colored when white light is transmitted through it or reflected from it. The substance absorbs certain wavelengths of the white light, and our eyes detect the wavelengths that are not absorbed. The observed color is said to be the complement of the color of light that it absorbs. A rough guide of the colors observed upon absorption at different wavelengths is given in **Table 1.2.**

Wavelength of maximum absorption (nm)	Color absorbed	Color observed
380-420	Violet	Green-yellow
420-440	Violet-blue	Yellow
440-470	Blue	Orange
470-500	Blue-green	Red
500-520	Green	Purple
520-550	Yellow-green	Violet
550-580	Yellow	Violet-blue
580-620	Orange	Blue
620-680	Red	Blue-green
680-780	Purple	Green

Table 1.2: Table of observed colors at specific wavelengths.

In part of this work, acid-sensitive probes will be used to monitor and quantify acid generation in photoresist samples. The acid sensitivity of these probes results in a shift of the absorption bands upon protonation. This results in a shift in color of the observed dye and

subsequently a change in absorption spectra. Upon generating increasing amounts of acid the dye becomes proportionally protonated and thus the amounts of generated acid can be quantified. This will be discussed more in **Chapter 3**.

1.9. The Use of Fluorescence Spectroscopy to Monitor Acid Diffusion:

Although absorption measurements account for the majority of analytical spectrophotometric methods at present, luminescence measurements are being used for more and more applications. Luminescence refers to any emission of radiation, including fluorescence (singlet → singlet emission) and phosphorescence (triplet → singlet emission) as seen in **Figure 1.6**. Luminescence measurements are increasingly being used because they are inherently more sensitive than absorption measurements. However, luminescence measurements are not universally applicable because many molecules only produce weak or negligible emission when they are irradiated and this is where the choice of fluorescent dyes becomes difficult as will be discussed in **Chapter 2**.

Fluorescence is the aspect of luminescence that we will be using for purposes of this work. Fluorescence is an important emission process in which atoms or molecules are excited by the absorption of electromagnetic radiation. The excited species then relax to the ground state, giving up their excess energy as photons. In general, molecular fluorescence or phosphorescence is observed at a lower energy than that of the absorbed radiation (the excitation energy).

The advantages of molecular emission (fluorescence and phosphorescence) are excellent sensitivity, good specificity, and a large linear range of analysis[50]. Fluorimetric methods can detect concentrations of substances as low as one part in 10 billion, a sensitivity 1000 times greater than that of most spectrophotometric methods. This increased sensitivity is

because in fluorescence the emitted radiation is measured directly and can be increased or decreased by altering the intensity of the exciting radiant energy. With other spectrophotometric methods the analogous quantity, absorbed radiation, is measured indirectly as the difference between the incident and transmitted beams. This small decrease in the intensity of a very large signal is measured with a correspondingly large loss in sensitivity. Although the net fluorescence signal might be the same as in absorbance spectroscopy, the emission can be amplified many times to give great sensitivity of analysis. Overall, fluorescence measures emitted light, while absorption measures a change in light intensity, therefore the sensitivity of fluorescence measurements is usually higher[51].

The specificity of fluorescence is the result of two main factors. The first factor is that there are fewer fluorescent compounds than absorbing ones because all fluorescent compounds must necessarily absorb radiation but not all compounds that absorb radiation emit. Only about 10% of all absorbing compounds will emit radiation via luminescence. The other factor, is that in fluorescence analysis there are two variables (excitation and emission wavelengths), as opposed to only one in the case of absorption, thus making fluorescence a better diagnostic method. Furthermore, fluorescence has a linear range of about six orders of magnitude; that of absorption, however, is only 2-3 orders of magnitude. This means in fluorescence the error curve is almost flat, and measurements can be made over a larger linear range than for absorption spectroscopy.

There are a few possible ways to study fluorescence properties. The most common is the measurement of the emission intensity upon excitation with a monochromatic light. The spectrum that one obtains in this way is called an emission spectrum. Emission spectra give information about the characteristics of the excited states of a molecule as well as its interaction with the solvent. Measuring the dependence of emission intensity while changing the excitation wavelength produces the excitation spectrum. Excitation spectra should be identical

to the absorption spectrum since both measure the S_0-S_1 transition. However, due to instrumental artifacts they show some differences.

The basic equation defining the relationship of fluorescence to concentration is:

$$F = \Phi I_o(1 - e^{-\epsilon bc})$$

where Φ is the quantum efficiency, I_o is the incident radiant power, ε is the molar absorptivity, **b** is the path length of the cell, and **c** is the molar concentration. The basic fluorescence intensity-concentration equation indicates that these three major factors (other than concentration) affect the fluorescence intensity. It is seen that the greater the value of Φ, the greater will be the fluorescence. Furthermore, the more intense incident source (I_o) will yield the greater fluorescence, however, a very intense source can cause photodecomposition. of the sample. Mercury or xenon lamps are frequently used since they are of moderate intensity. And finally, the higher the molar absorptivity of a compound (ε), the better will be the fluorescence intensity. Furthermore, all these factors are important when choosing the fluorescent probes to conduct the experiments for purposes of this work.

In this work, we propose to use fluorescence spectroscopy due to its higher sensitivity, to monitor the diffusion of acid in 1 μm imaged photoresist samples. Since the quantities of acid that will be diffusing will be very small, a technique sensitive to detect the acid movement is needed. Specifically, the use of fluorescence emission spectroscopy will allow us to monitor the changes in fluorescence due to the diffusion of acid into the non-imaged areas of the irradiated photoresist samples. This will be done with the use of fluorescent acid-sensitive probes as will be discussed in **Chapter 2.**

1.10. The Use of Fluorescence Microscopy to Monitor Image Formation and Subsequent Acid Diffusion:

As a tool in microscopy, fluorescence provides a number of possibilities in addition to absorption methods. Fluorescence probes can, for instance, be selectively excited and detected in a complex mixture of molecular species. It is also possible to observe a very small number of fluorescent molecules, in a small unit area of space[52]. Furthermore, fluorescence microscopy offers excellent temporal resolution, since events that occur slower than about 10^{-8}s can be detected and measured with appropriate instrumentation[52].

In this work, fluorescence microscopy was used fundamentally used to establish the image quality obtained by irradiating a PAG sample through a photomask at 254 nm. In terms of acid diffusion, fluorescence microscopy will be used to monitor acid diffusion as well. This can be done by monitoring the diffusion of acid from imaged areas (regions of acid production upon UV exposure through a patterned mask) to non-imaged or dark areas (regions that were covered by the mask and thus no acid was produced). Specifically, fluorescence microscopy will be used to view the actual movement (diffusion) of imaged area into the area that was dark. This can be done by observing the broadening of the imaged band with time.

To be able to view such images, a method of distinguishing the imaged area from the non-imaged is required. We propose that the use of acid-sensitive probes will facilitate the ability to do such experiments. These probes will ideally show a fluorescence shift in the presence of acid and thus will exhibit a different color of fluorescence when protonated. The use of these dyes in a photoresist sample should, therefore, be able to detect the presence of acid upon UV irradiation. And thus, the use of these acid-sensitive probes should enable the distinction between the area of image and non-image, ideally resulting in a fluorescent photopattern of the lined mask. And, thus, the diffusion of acid can be monitored by taking a series of pictures to record the movement of the lines, resulting in an area of blurred lines.

1.11. Toxicology Component

As a requirement to qualify for a Specialization in Environmental Chemistry and Toxicology, a toxicology component must be included with this thesis. In order fulfill such requirements, **Chapter 4** was written to outline the toxicological properties of some of the components that are used to manufacture the photoresist compounds. Furthermore, the toxicological properties of the dyes that are proposed to be used in this thesis, for purposes of monitoring acid quantification and acid diffusion, will be reviewed.

References:

(1) Thompson, L. F.; Wilson, C. G.; Bowden, M. J. *Introduction to Microlithography, 2nd Edition*; American Chemical Society: Washington, DC, 1994.

(2) Moore, G. E. *Proc. IEEE* **1976**, *64*, 307.

(3) Bruning, J. J. *J. Vac. Sci. Technol.* **1980**, *17*, 1147.

(4) Buckley, J. D.; Karatzas, C. *Proc. SPIE Opt.-Laser Microlithogr.* **1989**, 1088.

(5) Feder, R.; Spiller, E.; Topalion, J. *J. Vac. Sci. Technol.* **1975**, *12*, 1332.

(6) Ito, H. *IBM J. Res. Develop.* **1997**, *41*, 69.

(7) Dammel, R.; Doessel, K. F.; Lignau, J.; Theis, J.; Huber, H. L.; Oertel, H. *Microelectron. Eng.* **1986**, *5*, 97.

(8) Feely, W. E.; Imhof, J.; Stein, C. *Polym. Eng. Sci.* **1986**, *26*, 1101.

(9) Frechet, J. M. J.; Eichler, E.; Ito, H.; Willson, C. G. *Polymer* **1983**, *24*, 995.

(10) Frechet, J. M. J.; Matuszczak, S.; Reck, B.; Stoever, H. D.; Willson, C. G. *Macromolecules* **1991**, *24*, 1746.

(11) Ito, H.; Willson, C. G. *Polym. Eng. Sci.* **1983**, *23*, 1012.

(12) Thackeray, J. W.; Orsula, G. W.; Canistro, D.; Berry, A. K. *J. Photopolym. Sci. Technol.* **1989**, *2*, 429.

(13) Delzenne, G. A. *Adv. Photochem.* **1979**, *11*, 1.

(14) Iwayanagi, T.; Ueno, T.; Nonogaki, S.; Ito, H.; Willson, C. G. *Electronic and Photonic Applications of Polymers* Washington, DC, 1988.

(15) Mckean, D. R.; Schaedeli, U. P.; Kasai, P. H.; MacDonald, S. A. *J. Polym. Sci. Polym. Chem. Ed.* **1991**, *29*, 309.

(16) Mckean, D. R.; Schaedeli, U. P.; MacDonald, S. A. *J. Polym. Sci. Polym. Chem. Ed.* **1989**, *27*, 3927.

(17) Frechet, M. J.; Iizawa, T.; Bouchard, F.; Stanciulescu, M.; Willson, C. G.; Clecak, N. *Proc. ACS Div. Polym. Mater. Sci. Eng.* **1986**, *55*, 299.

(18) Crivello, J. V. In *ACS Symposium Series*; American Chemical Society: Washington, DC, 1984; Vol. 242; pp 3.

(19) Allen, R. D.; MacDonald, S. A.; Willson, C. G. *Proc. ACS Div. Polym. Mater. Sci. Eng.* **1986**, *55*, 299.

(20) Shirai, M.; Tsunooka, M. *Prog. Polym. Sci.* **1996**, *21*, 1.

(21) Reiser, A. *Photoreactive Polymers: the Science and Technology of Resists*; John Wiley and Sons: New York, 1989, pp 409.

(22) Pappas, S. P. *J. Imaging Tech.* **1985**, *11*, 146.

(23) Petersen, J. S.; Byers, J. D.; Carpio, R. A. *Microelectron. Eng.* **1997**, *35*, 169.

(24) Fedynyshyn, T. H.; Thackeray, J. W.; Georger, J. H.; Denison, M. D. *J. Vac. Sci. Technol. B* **1994**, *12*, 3888.

(25) Szmanda, C. R.; Fedynyshyn, T. H.; Houck, W. E.; Root, J.; Blacksmith, R. F. *Proc. SPIE 2195*, 269.

(26) Itani, T.; Yoshino, H.; Hashimoto, S.; Yamana, M.; Samoto, N.; Kasama, K. *J. Vac. Sci. Technol. B* **1996**, *14*, 4226.

(27) Zuniga, M. A.; Neurether, A. R. *J. Vac. Sci. Technol. B* **1996**, *14*, 4221.

(28) Itani, T.; Yoshino, H.; Fujimoto, M.; Kasama, K. *J. Vac. Sci. Technol. B* **1995**, *13*, 3026.

(29) Itani, T.; Yoshino, H.; Hashimoto, S.; Yamana, M.; Samoto, N.; Kasama, K. *Jpn. J. Appl. Phys.* **1996**, *35, Part 1*, 6501.

(30) Mckean, D. R.; Schaedeli, U.; MacDonald, S. A. *Polymers in Microlithography*, Washington, DC, 1989.

(31) Fedynyshyn, T. H.; Thackeray, J. W.; Mori, J. M. *Microelect. Eng.* **1994**, *23*, 315.

(32) Yoshimura, T. Y.; Nakayama, Y.; Okazaki, S. *J. Vac. Sci. Technol.* **1992**, *B10*, 2615.

(33) Nakamura, J.; Ban, H.; Tanaka, A. *Proc. ACS Div. PMSE* **1995**, *72*, 153.

(34) Nakumura, J.; Ban, H.; Deguchi, K.; Tanaka, A. *Jpn. J. App. Phys.* **1991**, *30*, 2619.

(35) Schlegel, L.; Ueno, T.; Hayashi, N.; Iwayanagi, T. *J. Vac. Sci. Technol. B* **1991**, *9*, 278.

(36) Schlegel, L.; Ueno, T.; hayashi, N.; Iwayanagi, T. *Jpn. J. App. Phys.* **1991**, *30*, 3132.

(37) Glezos, N.; Oatsis, G. P.; Raptis, I.; Argitis, P.; Gentilli, M.; Grella, L. *J. Vac. Sci. Technol. B* **1996**, *14*, 4252.

(38) Raptis, I.; Grella, L.; Argitis, P.; Glezos, N.; Petrocco, G. *Microelect. Eng.* **1996**, *30*, 295.

(39) Zuniga, M.; Wallraff, G.; Tomacruz, E.; Smith, B.; Larson, C.; Hinsburg, D.; Neurether, A. R. *?* **1993**, 2862.

(40) Zuniga, M.; Neurether, A. R. *SPIE Adv. Res. Tech. & Proc.* **1996**, *2724*, 110.

(41) Zuniga, M.; Walraff, G.; Neurether, A. R. *SPIE Adv. Res. tech & Proc.* **1995**, *2438*, 113.

(42) Yoshimura, T.; Shiraishi, H.; Okazaki, S. *Jpn. J. Appl. Phys.* **1995**, *34*, 6786.

(43) Watanabe, H.; Sumitani, H.; Kumada, T.; Inoue, M.; Marumoto, K.; Matsui, Y. *Jpn. J. Appl. Phys.* **1995**, *34*, 6780.

(44) Yoshimura, T.; Shirashi, H.; Teresawa, T.; Okazaki, S. *J. Vac. Sci. Technol. B* **1996**, *14*, 4216.

(45) Itani, T.; Yoshino, H.; Hashimoto, S.; Yamana, M.; Samoto, N.; Kasama, K. *Microelect. Eng.* **1997**, *35*, 149.

(46) Asakawa, K.; Ushirogouchi, T.; Nakase, M. *SPIE Adv. Res. Tech. & Proc.* **1995**, *2438*, 363.

(47) Mckean, D. R.; Allen, R. D.; Kasai, P. H.; Schaedeli, U. P.; MacDonald, S., A. *SPIE Adv. Res. Tech & Proc.* **1992**, *1672*, 94.

(48) Ohmori, H.; Arimitsu, K.; Kudo, Y.; Ichimura, K. *J. Photopolym. Sci. and Tech.* **1996**, *9*, 25.

(49) Zhang, P. L.; Eckert, A. R.; Willson, C. G.; Webber, S. E.; Byers, J. *SPIE Adv. Res. Tech. & Proc.* **1997**, *3049*, 898.

(50) Guilbault, G. G. *Practical Fluorescence, 2nd Ed.*; Marcel Dekker, Inc.: New York, NY, 1990.

(51) Skoog, D. A.; West, D. M.; Holler, J. F. *Analytical Chemistry, An Introduction, 6th Ed.*; Saunders College Publishing: Orlando, Fl., 1994.

(52) Mason, W. T. *Fluorescent and Luminescent Probes for Biological Activity*; Academic Press Inc.: San Diego, CA, 1993.

Chapter 2

The Use of Acid-Sensitive Probes to Monitor Acid Diffusion in Thin Polymer Films-Experimental and Results

2.0. Background:

This chapter is separated into three main sections. As discussed in the introduction, pH sensitive dyes are proposed to be used for monitoring acid diffusion in polymer/PAG systems. In order to do such diffusion analysis, a number of other experiments must first be conducted. The chapter is separated by categories in terms of the dyes that were studied. These dyes include; the aromatic monoazines (2-phenylpyridine, 2-phenylquinoline and acridine), the xanthene dyes (rhodamine B base and fluorescein), and some benzothiazole derivatives. The three main objectives of this chapter consist of 1) choice of the appropriate sensors; 2) observation of generated Images through fluorescence microscopy; and 3) to monitor diffusion through fluorescence spectroscopy. With each set of dyes that were used, the experiments vary to some degree and for this reason they have been separated.

2.1. Criteria for Choice of Acid-Sensitive Probes:

The proposed method of monitoring acid generation and diffusion in photoresist compounds requires the use of an acid-sensitive probe that must incorporate a number of different properties. These include increase in quantum yield or significant bathochromic shift of fluorescence upon protonation, high fluorescence quantum yield, emission in the visible range of the spectrum ($\lambda > 450$ nm), thermal stability up to 120°C, good photostability, good solubility in the solvents used, high extinction coefficient at $\lambda > 300$ nm, high molecular weight, and high sensitivity (high pKb value).

To explain these parameters, the following can be stated. An ideal sensor should increase in quantum yield and/or show significant change in spectral range of fluorescence upon protonation. A large spectral shift upon protonation is required because it allows for selective excitation of only the protonated form of the dye. Another ideal criterion is emission in the visible range. Emission in the visible range allows the use of the fluorescence microscope to directly study acid diffusion within the polymer film.

A high extinction coefficient at the excitation wavelength is needed to get a good signal-to-noise ratio in the thin polymer film. This problem cannot be solved by just increasing the sensor concentration since the acid consumption by the sensor cannot exceed a certain limit without influencing the effectiveness of any subsequent chemical process (i.e. crosslinking). Furthermore, solubility problems may come into play. For these reasons, a high extinction coefficient at the excitation wavelength, i.e., in the region > 300 nm, is ideal. Another criterion, is that the extinction coefficient at 254 nm should be small. This is required since the polymer/PAG samples are irradiated at this wavelength or at 248 nm in industry. Thus, a smaller extinction coefficient at 254 nm would minimize photodegradation.

An important criterion in choosing the ideal sensor is that it should have a high molecular weight. This need stems from the fact that we are observing the mobility of molecules within the polymer/PAG system. If the sensor, has a low molecular weight it would likely move as well. Thus, the criterion for a high molecular weight compound, partly ensures that diffusion of the sensor will be minimal or none. For similar reasons, the sensor should be of moderate polarity to ensure its minimal diffusion.

While many molecules with pH dependent fluorescence properties are known, most of these find applications in fluorimetric titrations or as probes for intracellular pH determinations, i.e. they are used in aqueous media. For resist applications it is more important to develop sensors that are soluble in organic solvents of moderate polarity and that are used in

microelectronic applications[1,2]. For this reason, it is essential that these have relatively good solubility in the solvents used for resist manufacture. Most commonly used solvents for photoresist manufacture are ethyl cellosolve acetate, 2-methoxyethyl ether (or diglyme), propylene glycol monomethylether acetate, and ethyl lactate. The two solvents used for the purposes of this work are mainly diglyme and ethyl lactate. For this reason, the ideal sensor must exhibit a moderate solubility (> 0.001 M) in these solvents. This criterion would exclude highly polar or charged molecules.

Since the lithographic process involves a baking step, the ideal sensor should have thermal stability in the polymer matrix up to 90°C. This is essential since the preparation of these materials, requires the solvent to be evaporated once the film is spin coated onto the disk. The ideal sensor should also be thermally stable up to 120°C and maybe even up to 150°C. The stability up to 120°C and 150°C is ideal when doing temperature related diffusion studies.

For the purpose of this work, a number of fluorescent sensors were analyzed. In order to choose ideal sensors and understand how such compounds work in polymer/PAG systems, various compounds were tested for acid-sensitive capabilities. In doing this research, we first started with a group of aromatic monoazines. These included acridine, 2-phenylquinoline and 2-phenylpyridine. A paper was written on this work by us, titled "Aromatic Monoazines as Fluorescent sensors for Photoacid generation in Thin Polymer Films"[3] in 1995. It soon became evident that some of these dyes were not suitable for use with phenolic polymers, which are widely used in microlithography. The fluorescence bands of 2-phenylpyridine and 2-phenylquinoline overlap with the fluorescence of these polymers and thus are not suitable. A number of other dyes proved to be more favorable in terms of the criteria factors discussed above. The first set of dyes are xanthene dyes, which included fluorescein and rhodamine B Base. Finally, another set of dyes which were analyzed, consisted of benzothiazole derivatives and a few other similar dyes that were synthesized by Gerd Pohlers, a Post-Doc in our lab.

These last set of dyes and the aromatic monoazines were used for actual diffusion monitoring experiments by fluorescence spectroscopy. Only the benzothiazole derivatives (i.e. DSB, DMBB, Coumarin-6) were used for diffusion studies by fluorescence microscopy analysis. Furthermore, one of these benzothiazole dyes, DSB, was used for the vertical diffusion experiment. Rhodamine B Base was also used for some vertical diffusion experiments. Rhodamine B base, fluorescein, DSBS, DMBB, and Coumarin-6 were also used to quantify acid generation in thin films, as discussed in **Chapter 3**. Other dyes are still in the testing phase and have not been used for diffusion yet.

2.1.1. Acridine, 2-Phenylquinoline and 2-Phenylpyridine

It has been known for a long time that aromatic monoazines such as acridine and quinoline are essentially non-fluorescent in non-hydrogen bonding solvents, whereas the protonated forms of these molecules were found to be highly fluorescent, at least in aqueous solutions[4-8].

These findings make this class of molecules an interesting candidate for potential acid sensors. Thus, we employed 2-phenylpyridine (**1**), 2-phenylquinoline (**2**) and acridine (**3**) for our study. The structures of these dyes are shown in **Figure 2.1**.

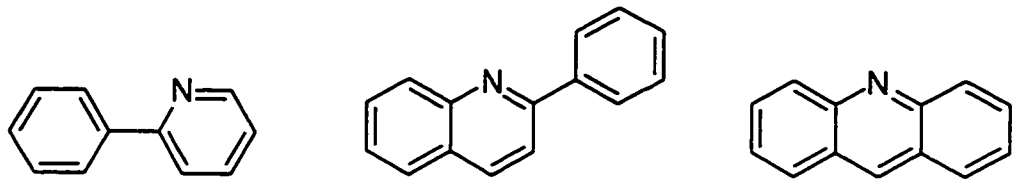

1 **2** **3**

Figure 2.1: The molecular structures of **1**) 2-phenylpyridine, **2**) 2-phenylquinoline, and **3**) acridine.

The phenyl derivatives provide a bathochromic spectral shift compared to the unsubstituted molecules. The long wavelength emission characteristic of the sensor is required to avoid overlap with the fluorescence of the phenolic polymers that are widely used in microlithography. We preferred the 2-isomers over the 3- and 4-isomers since a recent study of phenylpyridines by Testa *et al.*[9] indicated that these provide the most desirable combination of properties with respect to our application, i.e., both the highest absolute fluorescence quantum yield and the most pronounced increase in fluorescence quantum yield upon protonation.

The only other study that deals with the protonated forms of these substrates in non-aqueous solution, is a seminal study done by Mataga[4]. For purposes of this thesis, we have investigated the effect of acid on the absorption and fluorescence properties in diglyme solution, employing both direct addition of p-toluenesulfonic acid and photoacid generation using 1,2,3-tris(toluenesulfonyloxy)benzene,[10] a PAG yielding p-toluenesulfonic acid. Diglyme was the solvent of choice since it is a good coating solvent for the materials used. In a second step we extended our studies to thin polymer films using poly(methyl methacrylate) (PMMA) as a model polymer. Although PMMA is not frequently used as a polymer in photoresist formulations we preferred it over polymers like poly(p-hydroxystyrene) (PHS) or novolac because it is both transparent and exhibits no background fluorescence in the spectral region of interest, in the case of these dyes. These dyes are found to absorb close to the absorption of PHS and thus PHS could not be utilized.

2.1.2. Xanthene Dyes (Rhodamine B Base and Fluorescein)

Two different xanthene dyes, rhodamine B base and fluorescein were utilized because of their known properties of exhibiting a significant change in absorption characteristics upon protonation. Rhodamine dyes are well known for their high fluorescence yield. Fluorescein also has a high fluorescence quantum yield and high photostability.

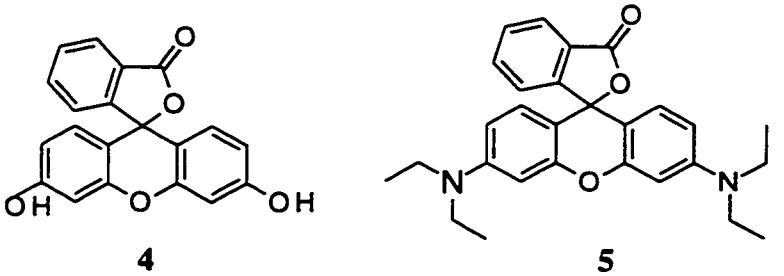

4 5

Figure 2.2: Structures of **4)** Fluorescein and **5)** Rhodamine B Base.

Both dyes are interesting because of these properties, when looking at film applications. The structures of rhodamine B base and fluorescein are shown in **Figure 2.2**. Furthermore, it is seen that fluorescein has various protolytic forms as shown in **Figure 2.3**.

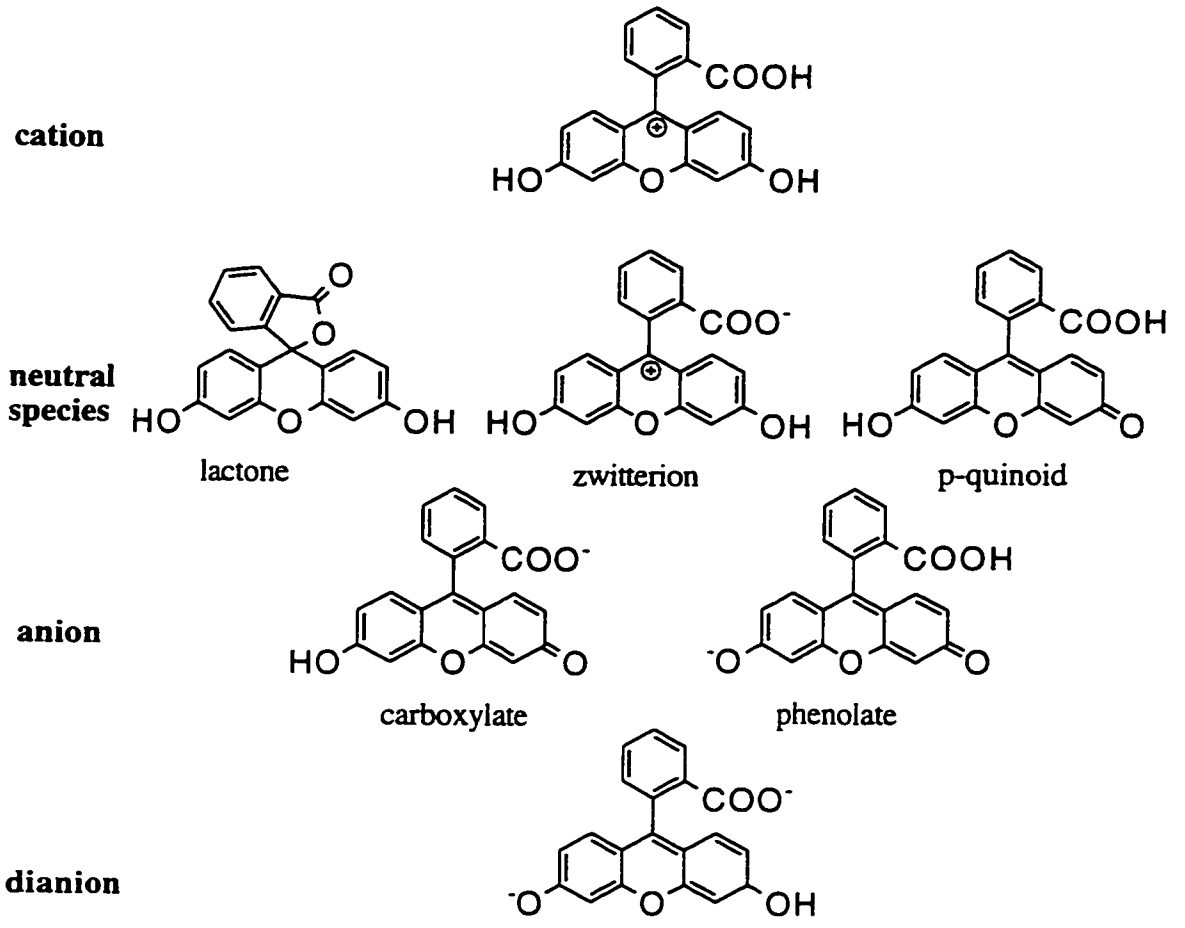

Figure 2.3: Chemical structures of fluorescein.

Fluorescein in aqueous solution occurs in cationic, neutral, anionic and dianionic forms[11] making its absorption and fluorescence properties strongly pH dependent. It is seen that there are various protolytic forms of fluorescein, as shown above[12]. The cation and dianion are expected to occur in only one chemical form. The neutral species can be obtained

as a solid; as a colorless lactone, yellow zwitterion or red p-quinoid[13]. In this work, the two forms that were used were the yellow and red forms of fluorescein.

Rhodamine B Base and fluorescein dyes exist in a colorless lactone form in aprotic solvents but undergo opening of the lactone ring upon protonation or in protic solvents. The opening of the lactone ring can be observed in **Figure 2.4**.

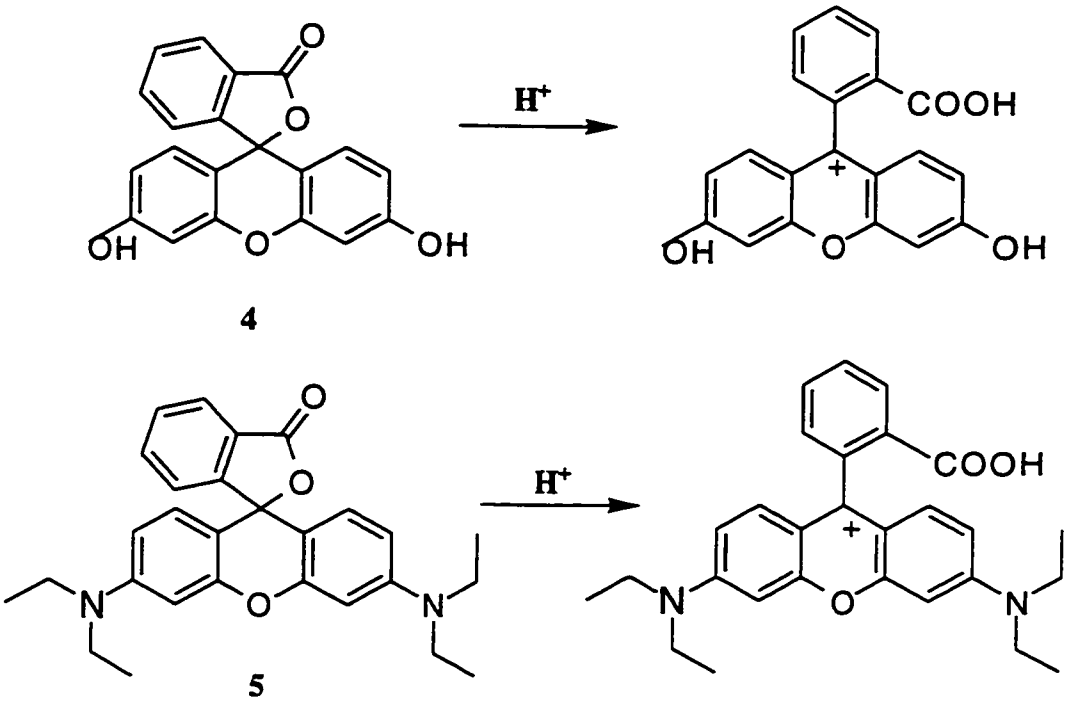

Figure 2.4: Opening of the lactone forms of dye for **4)** Fluorescein and **5)** Rhodamine B base upon protonation.

The absorption spectra of the cations of rhodamine B base and fluorescein are markedly different from the lactone forms as will be seen in the results section. A large bathochromic shift occurs upon protonation which makes these compounds ideal acid sensors for the polymers used in microlithography. In this work, the effects of protonation on these dyes will be studied in some of the polymers used in the photoresist industry. Both dyes were studied in

PHS and PMMA to test the compatibility with the polymers. Furthermore, a vertical diffusion experiment was conducted with rhodamine B base due to its high extinction coefficient and sensitivity to acid.

2.1.3. Benzothiazole Dyes

With the exception of DSB and Coumarin-6, all the dyes were synthesized and characterized in solution in our lab. The first of these dyes is *trans*-2-[4-(dimethylamino) styryl]benzothiazole (DSB) (**Figure 2.5**). Although, not too much is known about the physical properties of this dye, the work conducted in this thesis and the solution work done in this laboratory, helps understand its acid-base properties.

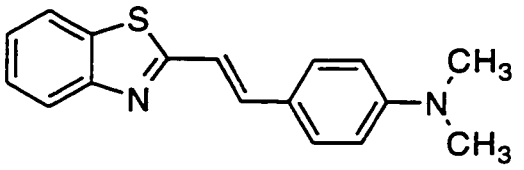

Figure 2.5: Structure of the dye DSB.

This compound is likely to be the most successful candidate as a potential acid sensor for the technique proposed in this work. The reasoning behind this is that the fluorescence of this compound increases in quantum yield and/or has a significant change in spectral range of fluorescence upon protonation. A large spectral shift upon protonation is required because it allows for selective excitation of only the protonated form of the dye. Unlike, any of the dyes proposed before this, DSB was the only one that has a large spectral shift upon protonation. DSB is a dye that has three prototopic species, neutral form, monocation and dication, as seen in **Figure 2.6**.

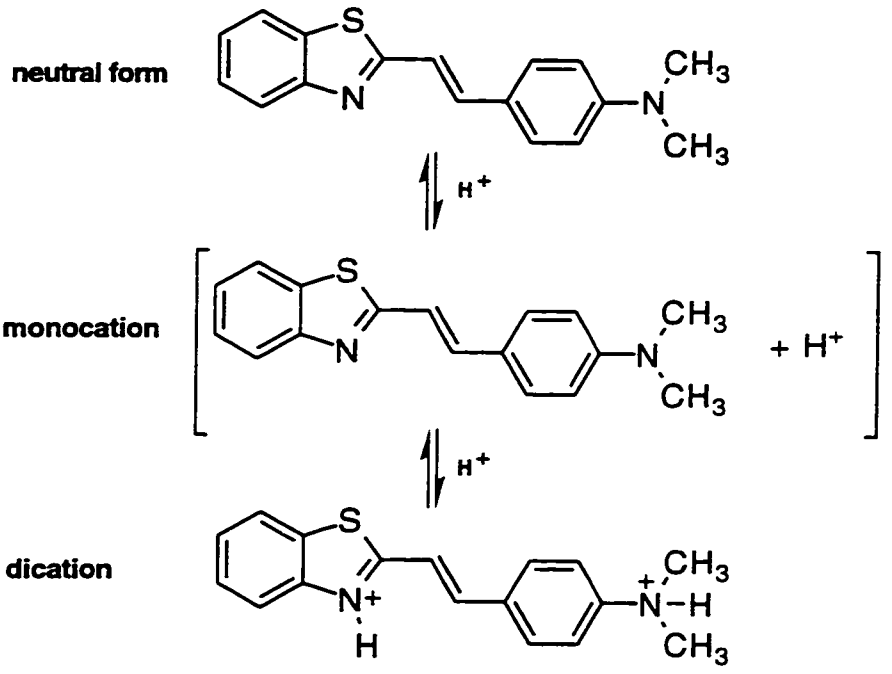

Figure 2.6: Three prototopic forms of DSB.

In solution, the protonated (or monocation) form of the dye has been found to absorb at 506 nm and 328 nm, whereas the neutral form has an absorption at 396 nm. Similarly, the fluorescence of the neutral form has a band at 531 nm. In accordance with the absorption spectra, fluorescence spectra of the protonated form occur at 413 nm and 590 nm. Furthermore, formation of the dication occurs upon higher acid concentration.

An interesting aspect of DSB is that it has two basic centers, the heterocyclic nitrogen and the terminal amino-nitrogen. In our lab, work is being done on the protonation of these sites, and in what order these processes occur. Pohlers *et al.* have proposed that the two bands that occur upon protonation are due to the two monocations, that have been found to have similar pKa values. Furthermore, they have concluded that the red-shifted band arises from the ring-protonated monocation, whereas the second band is due to the protonation of the amino group.

A similar compound that will be studied is Coumarin-6, a commonly employed laser dye. This compound was also studied by Pohlers et al. as a comparison to the protonation of DSB. Since this compound has a second electron acceptor, a carbonyl group that is connected to the electron donor via a π - system, it would be expected to be favorably protonated at the ring nitrogen. From their work, it was concluded that Coumarin-6 protonates exclusively at the ring nitrogen. This dye as well as some other related dyes are shown in **Figure 2.7** .

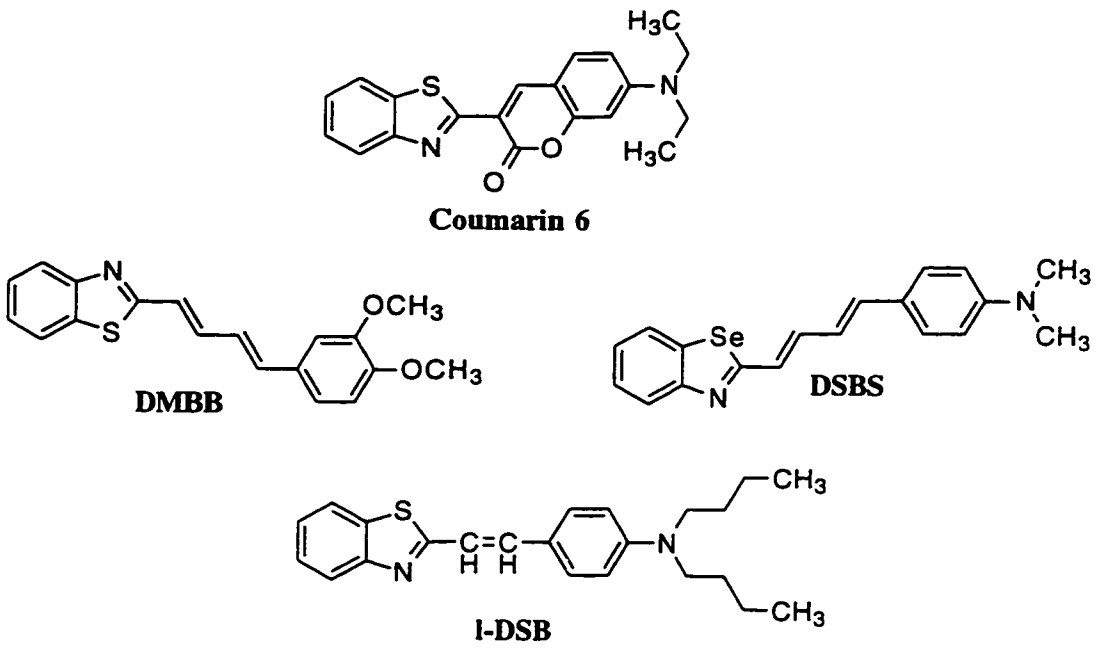

Figure 2.7: Structures of DMBB, Coumarin-6, DSBS, and l-DSB.

Other dyes that are similar to DSB and Coumarin-6 were also used. These included DMBB, l-DSB, DSBS. In most of the cases these dyes were synthesized and studied in hopes of improving the physical properties of the dyes, such that a more ideal dye would be obtained. These all behave in a similar fashion, differing only in wavelength maxima. However, the new dyes were made either to increase the molecular weight or improve the photostability, fluorescence or other properties of the dye. Furthermore, the absorption and fluorescence

properties of some other potential dyes were recorded in PHS films. These dyes included HSB, MBB, TSB, and MSB. The structures of these compounds are in **Figure 2.8.**

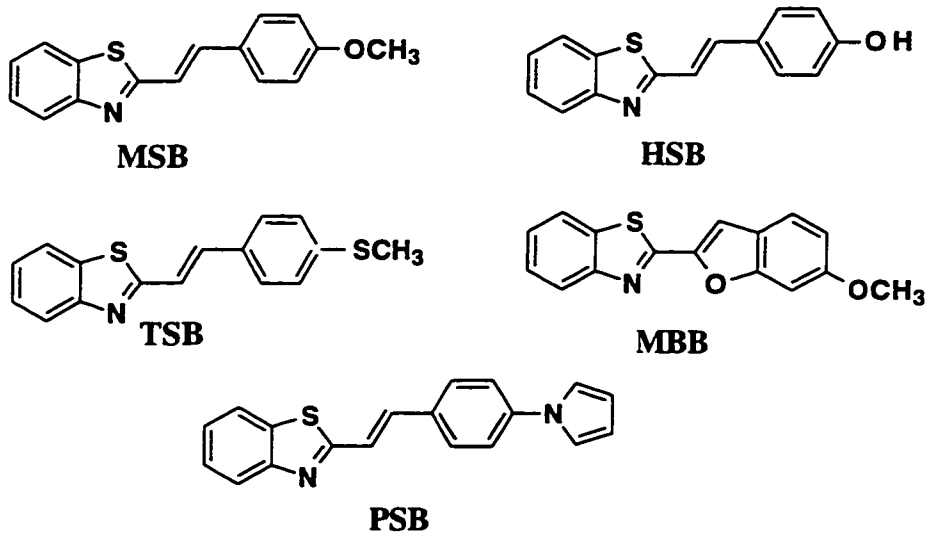

Figure 2.8: Structures of some benzothiazole derivative dyes.

In this work, photoacid generation was tested with DSB, l-DSB, DSBS, DMBB and Coumarin-6. However, diffusion work was manly done with DSB, modified DSB (l-DSB) and some with Coumarin-6 and DMBB. Exploratory diffusion experiments were conducted by the two proposed techniques of fluorescence spectroscopy and fluorescence microscopy.

2.2. Experimental Section:

2.2.1. General Techniques Applicable to all Dyes

2.2.1.1. Spin Coating of Polymer Films

Thin polymer films were spin coated at 3000 rpm (20 seconds) from 25% w/v diglyme solutions, onto 1 inch quartz disks using an Integrated Technologies Inc. P-6000 spin coater. Typical film thickness was ~1 μm. The thicknesses were determined at Shipley Co. in Marlboro, Massachusetts. An uncontaminated oven was used to bake the samples upon spin-coating. The samples were placed on an aluminum plate within the oven to ensure consistent heating.

2.2.1.2. Steady-State Irradiation

Most UV irradiation was performed at room temperature in a photoreactor equipped with four RPR-254 nm lamps from the Southern New England Ultraviolet Co. However, towards the end of this work, a HTG imaging unit equipped with a mercury arc lamp was provided by Shipley Co. (Marlboro, Massachusetts). This unit is made by the Hybrid Technology Group, Inc. Images were produced by placing a IBM chrome plated photomask on top of the polymer film, within a iron quartz plate holder.

2.2.1.3. UV-Visible Spectra

Absorption spectra were recorded using a Varian Cary 1E spectrophotometer. All data were converted into ASCII files and then plotted using Kaleidagraph software.

2.2.1.4. Fluorescence Spectroscopy

Fluorescence spectroscopy was carried out using a Perkin-Elmer LS-50 luminescence spectrometer. To obtain the fluorescence spectra in thin polymer films a front face attachment was employed. The excitation source was a Xenon discharge lamp which had an equivalent to 20 kW for an 8 μs pulse duration. Pulse width at half-peak height was <10 μs. The detector

was a gated photomultiplier. Excitation and emission slits were generally 5 nm. The scanning speed was 240 nm/min.

Instrumental parameters were controlled by the Fluorescence Data Manager software. The processor was an Epson PC AX2. The spectra collected were transferred as ASCII files to a Macintosh computer, and Kaleidagraph 3.0 software was used to plot the data.

2.2.1.5. Fluorescence Microscopy

To observe the generated lines upon photoimaging the polymer samples, we used an Zeiss Axiophot Fluorescence microscope equipped with epifluorescence, that is located in the Biology Department of University of Ottawa. Epi-illumination makes use of a vertical illuminator allowing an illuminating light path according to the Koehler principle. The microscope had three excitation filters in which red, blue, or green fluorescence could be monitored. The filters consisted of FITC, Rhodamine and DAPI combinations.

The microscope had a built in camera so that pictures could be taken. In all cases, Kodak or Black's brand 200 ASA film was used to take color photographs. The timing of the photographs could be controlled in automatic or manual mode. The exposure time usually varied from 5 sec to 25 sec depending on the sample .The objective magnification was usually 20X or 40X.

2.2.2. Acridine, 2-Phenyquinoline and 2-Phenylpyridine

2.2.2.1. Materials

Diglyme (bis(2-methoxyethyl) ether, spectrophotometric grade), poly(methyl methacrylate) (average M. W. 120,000), p-toluenesulfonic acid monohydrate (190.22 g/mol), 2-phenylpyridine, 2-(4-biphenylyl)-5-phenyl-1,3,4-oxadiazole and 1,1,4,4-tetraphenyl-1,3-butadiene were purchased from Aldrich and used as received. Acridine (Aldrich) was

recrystallized from hexane and ethanol followed by treatment with activated charcoal and then sublimed. The 2-phenylquinoline (Aldrich) was first sublimed and then recrystallized several times from methanol and 2-(1-naphthyl)-5-phenyloxazole (Fluka) was used without further purification. The PAG 1,2,3-tris-(toluenesulfonyloxy)benzene (**6**) was prepared according to literature procedures[10] and the structure is shown in **Figure 2.9**.

6

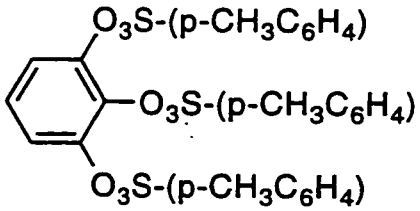

Figure 2.9: Structure of the PAG 1,2,3-tris-(toluenesulfonyloxy)benzene (**6**).

2.2.2.2. Experiments in Solution

Solutions of the three fluorescent sensors in diglyme were prepared to give an absorbance of 0.1–0.2 at the excitation wavelength. From these solutions, two sets of samples were made, one in which p-toluenesulfonic acid (0.05 M) was added directly and one with PAG added (0.01 M). The latter set of samples was irradiated at 254 nm in a photoreactor for various time intervals and fluorescence spectra were taken after each period of irradiation.

The fluorescence quantum yields of **1-3** in diglyme were measured relative to 2-(4-biphenylyl)-5-phenyl-1,3,4-oxadiazole (PBD, $\Phi_f = 0.69$)[14], 2-(1-naphthyl)-5-phenyloxazole (α–NPO, $\Phi_f = 0.78$)[14], and 1,1,4,4-tetraphenyl-1,3-butadiene ($\Phi_f = 0.52$)[15] in cyclohexane, respectively. These fluorescence quantum yields were measured by Gerd Pohlers. In these experiments, the absorbance of all samples at the excitation wavelength did not exceed 0.1, and the emission spectra were corrected for photomultiplier response between 380 and 650 nm. All

experiments in solution were carried out with deaerated samples using sealed 1 cm x 1 cm Suprasil quartz cells.

2.2.2.3. Experiments in PMMA Films

Samples of **1-3** were prepared in a 25% w/v solution of PMMA in diglyme to give an absorbance between 0.1 and 0.4 at the excitation wavelength. Again, two sets of samples were prepared as described above and spin-coated onto quartz disks. After being baked at 90° C for 10 minutes, the samples containing PAG (0.2 M in the coating solution) were irradiated at 254 nm for various time intervals and fluorescence spectra were taken.

2.2.3. Xanthene Dyes (Rhodamine B Base and Fluorescein)

2.2.3.1. Materials

Diglyme (bis(2-methoxyethyl) ether, spectrophotometric grade), ethyl lactate, 98%, poly(methyl methacrylate) (average M. W. 120,000), polyhydroxystyrene (average M.W. 5000, p-toluenesulfonic acid monohydrate (190.22 g/mol), camphorsulfonic acid (500.13 g/mol), perfluorooctane sulfonic acid, rhodamine B base (442.56 g/mol) were purchased from Aldrich and used as received. The fluorescein (332.31 g/mol) (Aldrich) was purified by dissolving it in NaOH and then reprecipitating with HCL. The positive resist formulation (XP9549Q) and the photoacid generators (see **Figure 2.10** for structure) were supplied by Shipley Co.

2.2.3.2. Experiments in PMMA and PHS Films

Samples of rhodamine B base and fluorescein were prepared in 25% w/v solutions of PMMA or PHS in diglyme. These polymer solutions were made to have a dye concentration of 0.02 M. To study the effects of added acid, two sets of samples were prepared one without and one with added acid. In samples with added acid, p-toluenesulfonic acid was added to a concentration of 0.08 M. All samples were spin-coated onto quartz disks and baked at 90°C

for 10 minutes. Absorption and fluorescence spectra were taken of each dye in each polymer, with and without added acid.

The effects of adding subsequent increments of acid (both a strong and weak acid were used) were studied in rhodamine B base and fluorescein incorporated films. The weak acid was camphorsulfonic acid and the strong one was perfluorooctane sulfonic acid. Polymer solutions of each were made with varying amounts of added acid. Samples were spin coated, baked and absorption spectra taken. In the case of fluorescein, three PAGs (**Figure 2.10**) were also utilized to monitor the effects of acid generation as compared to added acid. These samples were prepared in ethyl lactate instead of diglyme, due to the toxicity of the latter solvent. In most cases, the concentration of added PAG was 0.022 M due to the lower solubility in ethyl lactate.

Furthermore, spectra have been recorded using polymer solutions of both PHS and PMMA with incorporated fluorescein. The concentration of fluorescein in PMMA films had to be decreased to 0.01 M due to its lower solubility (Note: red fluorescein was used in this work but when yellow was used it would be soluble at concentrations of 0.02 M). Spectral differences between using diglyme or ethyl lactate as the solvent have also been recorded. For rhodamine B base only PMMA samples were prepared. The rhodamine B base samples were made only in diglyme.

2.2.3.3. Vertical Diffusion Experiment with Rhodamine B Base

A polymer solution of 0.02 M rhodamine B base in 25% w/v PMMA film was spin coated onto a quartz wafer. Another quartz disk was spin coated with a sample of a positive resist formulation (XP9549Q) which consists of a PAG, a phenolic polymer and other components. Both samples were baked at 90°C and the absorption spectra of the dyed sample was recorded. The resist sample was irradiated for 5 minutes at 254 nm to produce acid from the photoacid generator. The two disks were placed on top of one another with a 2.5 mm metal spacer in between. The resist sample was on the bottom, with the dye sample (polymer face-down) was placed on top. The sample "sandwich" was taped together and stored overnight in a beaker closed off with parafilm and wrapped in foil. After approximately 24 hours of exposure, the absorption spectra of the dyed sample was taken to monitor for acid migration and thus protonation of the dye.

2.2.4. Benzothiazole Dyes

2.2.4.1 Materials

Diglyme (bis(2-methoxyethyl) ether, spectrophotometric grade), ethyl lactate, poly(methyl methacrylate) (average M.W. 120,000), polyhydroxystyrene (average M.W. 5000), p-toluenesulfonic acid monohydrate (190.22 g/mol), camphorsulfonic acid, the dye DSB (364.55 g/mol), Coumarin-6 were purchased from Aldrich. The positive resist formulation (XP9549Q) and the photoacid generators were supplied by Shipley, Co. All other dyes were synthesized by Gerd Pohlers. The structures of the PAGs used are in **Figure 2.10**.

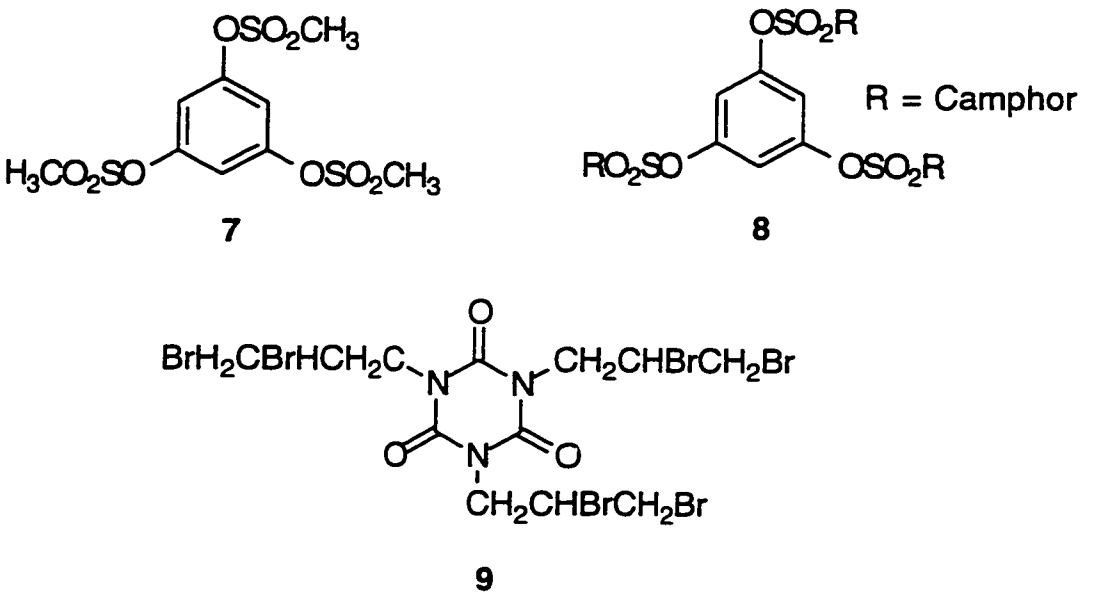

Figure 2.10: Structures of three main photoacid generators (PAGs) that were used: **7**) 1,3,5-tris(methylsulfonyloxy) benzene (357.34 g/mol) generates methane sulfonic acid upon irradiation, **8**) 1,3,5-tris(camphorsulfonyloxy) benzene (772.10 g/mol) generates camphorsulfonic acid upon irradiation, and **9**) tris 2,3-dibromopropyl 1,3,5-isocyanurate (728.73g/mol) generates hydrogen bromide (HBr) upon irradiation. All the PAGs were irradiated at 254 nm.

2.2.4.2. Experiments in Solution

A solution of DSB in diglyme was prepared to give an absorbance of 0.1–0.2 at the excitation wavelength. p-Toluenesulfonic acid (0.05 M) was added such that the monocation and dication prototopic forms would be obtained. Both absorption and fluorescence spectra were recorded for each species such that a comparison to experiments in films could be made.

The pKa of the monocation of DSB was also calculated. To do this DSB was dissolved in a 50/50 methanol/deionized water solution due to DSB's insolubility in water. Solutions of pH ranging from pH 1.21 to 6.17 were prepared using buffer solutions. For

pH's between 1-2.2, 0.2 M KCl and 0.2 M HCl were used. For pH's between 2.2-4.0, 0.1 M potassium hydrogen phthalate and 0.1 M HCl, and for pH's greater than 4.10, 0.1 M potassium hydrogen phthalate and 0.1 M NaOH. An absorption spectra of each solution of varying pH was recorded.

2.2.4.3. Experiments in Films

To test the effects of protonation of the dyes in a polymer matrix, samples of 0.02 M dye in a 25% w/v PHS matrix were prepared. The dyes for which such calibration curves were prepared were DSB, Coumarin-6, DSBS, and DMBB. The DSB samples were made with increasing amounts of p-toluenesulfonic acid. The molarity of the solution refers to the molarity in the polymer solution before spin coating. All samples were spin coated onto quartz disks, baked for 10 minutes at 90°C, cooled to RT and analyzed by absorption spectroscopy.

The next step in understanding the protonation effects of the dyes in polymer matrices was to determine whether the use of PAGs resulted in the same general trend as did added acid for each dye. For DSB and l-DSBS, this was tested using all three PAGs. In both cases 0.02 M dye was used, however, for the DSB samples 0.002 M dye concentrations were also used. The PAG concentration used was approximately 0.062 M for each PAG. DMBB and Coumarin-6 were also used to obtain such photoacid generation absorption and fluorescence spectra. Fluorescence spectra are important because they will be used to conduct the diffusion analysis. For DMBB, 0.002 M dye was used with 0.022 M concentration of all three PAGs. For Coumarin-6, 0.02 M dye was used with 0.062 M gyro in a PHS matrix. All PAG samples were irradiated at 254 nm in a photoreactor or a HTG unit for various time intervals and absorption and fluorescence spectra were taken after each period of irradiation.

To determine whether the dyes would be able to detect the photoacid generation of an actual photoresist, DSB and DMBB were used. Using DSB, a concentration of 0.005 M was

added to a positive photoresist (XP9549Q). For DMBB, a 0.02 M dye concentration was used.

For the dyes: HSB, MSB, TSB and MBB, only the change in spectra upon addition of acid was studied. In each case a 0.02 M solution of the dye was made in a 25% PHS solution (in diglyme). Two sets of samples were made for each dye: one with and one without acid. The concentration of acid (p-toluenesulfonic acid) used was 0.08 M in each case. Both absorption and fluorescence spectra were obtained for each dye.

2.2.4.4. Vertical Diffusion "Pancake" Experiment

For this experiment, two spin coated polymer disks are required. The polymer sample consisted of 0.02 M DSB in a 25% (w/v) PHS matrix with 0.062 M 7 (see **Figure 2.10**). Two quartz disks were spin coated, and baked. The initial absorption and fluorescence spectra of each disk was recorded. One of the disks was irradiated at 254 nm for 7 minutes in a photoreactor. The irradiation time was determined by irradiating a sample for increasing amounts of time and determining where maximum acid production had occurred. The absorption and fluorescence spectra of this disk was recorded. The two disks were stored in a sample sandwich (or pancake), with a metal spacer between and a lead weight placed on top, overnight. This experiment was done both by storing the sample at room temperature and at 130°C overnight. Absorption and fluorescence spectra were recorded for both samples.

2.2.4.5. Diffusion by Fluorescence Spectroscopy

Diffusion experiments were conducted using the dyes: 0.02 M and 0.002 M DSB, 0.002 M Coumarin-6 and 0.002 M DMBB. In a typical experiment the dye solution was made in a 25% PHS made in diglyme, with a 0.062 M concentration of PAG. A sample was spin coated onto a quartz disk and irradiated at 254 nm for increasing amounts of time. At each irradiation dose the absorption and fluorescence spectra would be recorded to determine the

change in spectra. The spectra yielding the maximum intensity at the wavelength of the protonated form would be chosen as the optimum irradiation time.

For purposes of the diffusion analysis, two disks were spin coated. One disk would serve as a blank whereas the other disk was imaged. However, both disks were irradiated with the mask on top. The mask consisted of 9 windows, which ranged from 55 μm lines down to 1 μm lines and also had a window in which there were no lines. The "blank or reference" sample was imaged with this blank window. The "patterned" sample was usually imaged with the window that had 1 μm or 3 μm line spaces. Both samples were irradiated for the same period of time. Since the position of where the lamp strikes the sample is critical, the samples were irradiated one at a time making sure that each was placed in the same position. Upon irradiation, the initial fluorescence spectra were recorded for each sample. The samples were then stored for various intervals of time. Between each interval, the fluorescence spectra of both samples were recorded. This experiment was done by storing the samples at room temperature and by storing the samples at 120-130°C.

Furthermore, the time-drive application of the fluorimeter was used to keep a sample stationary within the instrument. With this technique, the instrument scanned the sample automatically at intervals of time but only recorded the intensity at the excitation wavelength. The sample had to be covered with foil paper between the intervals of measurement to minimize any effects of photodegradation from the lamp. Furthermore, the disadvantage of this technique is that only one sample can be analyzed. Thus, a comparison to the reference cannot be made.

2.2.4.6. Observation of Imaged Lines by Fluorescence Microscopy

A sample of 0.02 M DSB with 0.062 M **7** & **9** (see **Figure 2.10** for structures) in 25% PHS was prepared. Samples were spin coated onto disks and irradiated for 7 or 10 minutes (again according to the PAG) at 254 nm in a photoreactor. Each sample was made

using the various windows of the mask and thus, different sizes of lines were generated. The samples were then monitored under a fluorescence microscope to observe whether the lines were actually generated. Photographs were also taken of samples made using 0.002 M DSB, 0.02 M l-DSB, 0.002 M DMBB and 0.002 M Coumarin-6.

2.3. Results and Discussion:

2.3.1. Acridine, 2-Phenyquinoline and 2-Phenylpyridine

2.3.1.1. Experiments in Solution

Figure 2.11 (**A-C**) shows the effect of 0.05 M p-toluenesulfonic acid on the absorption / fluorescence spectra of **1-3** in diglyme. The absorption spectra of each of the three compounds show both a bathochromic shift of the protonated form relative to the samples without acid. The fluorescence spectrum of acridine exhibits the same bathochromic shift that is observed in the absorption spectrum. No fluorescence due to the unprotonated species could be detected for **1** and **2** with our instrument, indicating that the fluorescence quantum yield of these molecules in diglyme must be very low (< 0.0001). These findings are in accordance with Testa's results, who was unable to detect any fluorescence for (**1**) in several organic solvents. The fluorescence quantum yields of all three compounds are listed in **Table 2.1**.

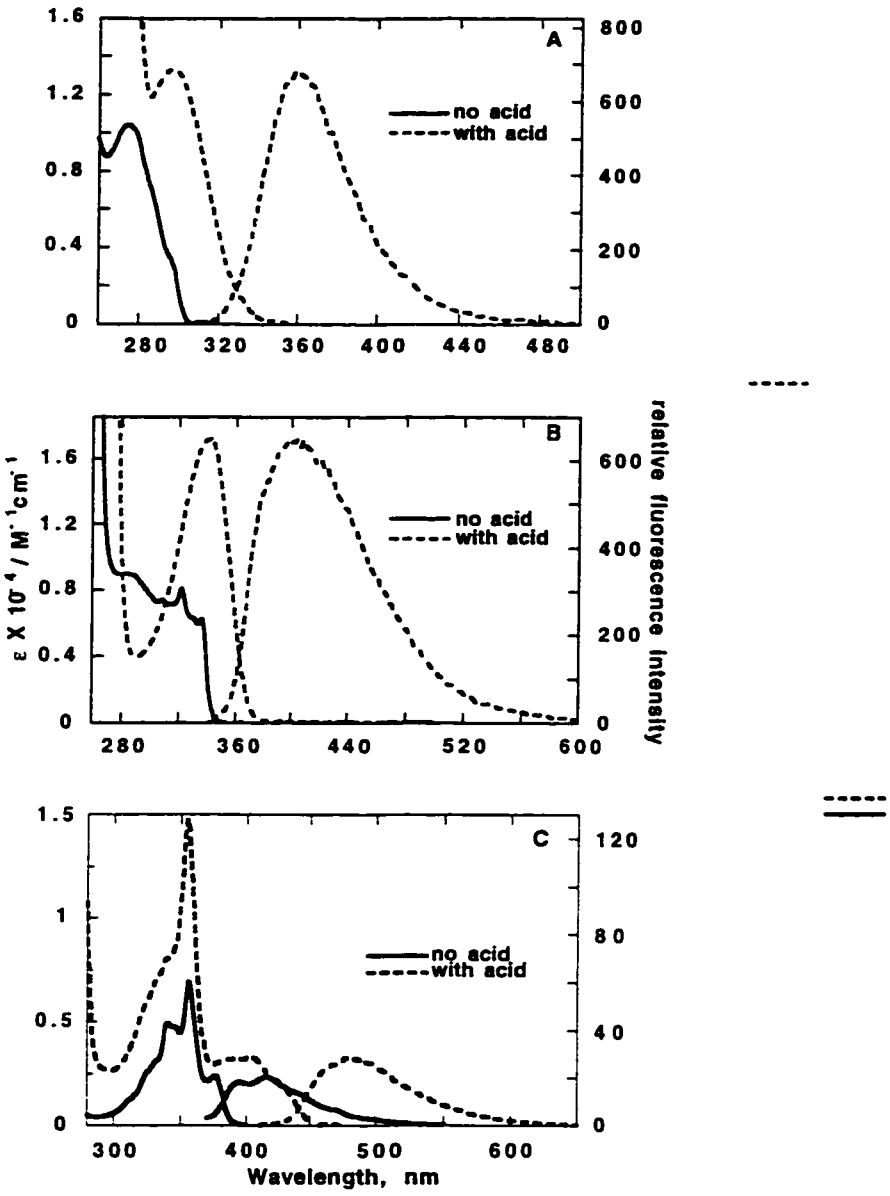

Figure 2.11. **(A):** Absorption and fluorescence (normalized to the longest wavelength absorption band) spectra of 2-phenylpyridine with and without p-toluenesulfonic acid in diglyme at room temperature. **(B):** Absorption and fluorescence spectra for 2-phenylquinoline with and without p-toluenesulfonic acid. **(C):** Absorption and fluorescence spectra for acridine with and without p-toluenesulfonic acid in diglyme at room temperature.

SENSOR MOLECULE	Fluorescence ($\lambda_{max.}$ / nm)	Φ_f	Excitation Wavelength / nm
2-phenylpyridine[a]	-	< 0.0001	-
2-phenylpyridinium cation	359	0.031	300
2-phenylquinoline[a]	-	< 0.0001	-
2-phenylquinolinium cation	409	0.016	340
acridine	414	< 0.001	365
acridinium cation	480	0.31	415

[a] No fluorescence could be detected with our instrument (see text).

Table 2.1: Fluorescence band maxima (λ_{max}), quantum yields (Φ_f) and excitation wavelengths used for the fluorescence spectra in **Figure 2.11**. All data in diglyme at room temperature.

Since a very similar behavior has been found to be characteristic for monoazines upon protonation in aqueous solution[5,7], we conclude that the observed changes are due to the protonation of these molecules caused by the p-toluenesulfonic acid. Thus, it should be possible to monitor the photogeneration of acid in diglyme by simply monitoring the change in fluorescence intensity. To check whether this is correct, we employed 1,2,3-tris(toluenesulfonyloxy)benzene (**6**), a PAG yielding p-toluenesulfonic acid, to monitor the photoacid generation upon irradiation at 254 nm. **Figure 2.12** shows the fluorescence spectra of 2-phenylquinoline and acridine in the presence of PAG in diglyme taken upon subsequent intervals of irradiation time. The increase in fluorescence intensity upon irradiation observed for both compounds indicates acid production.

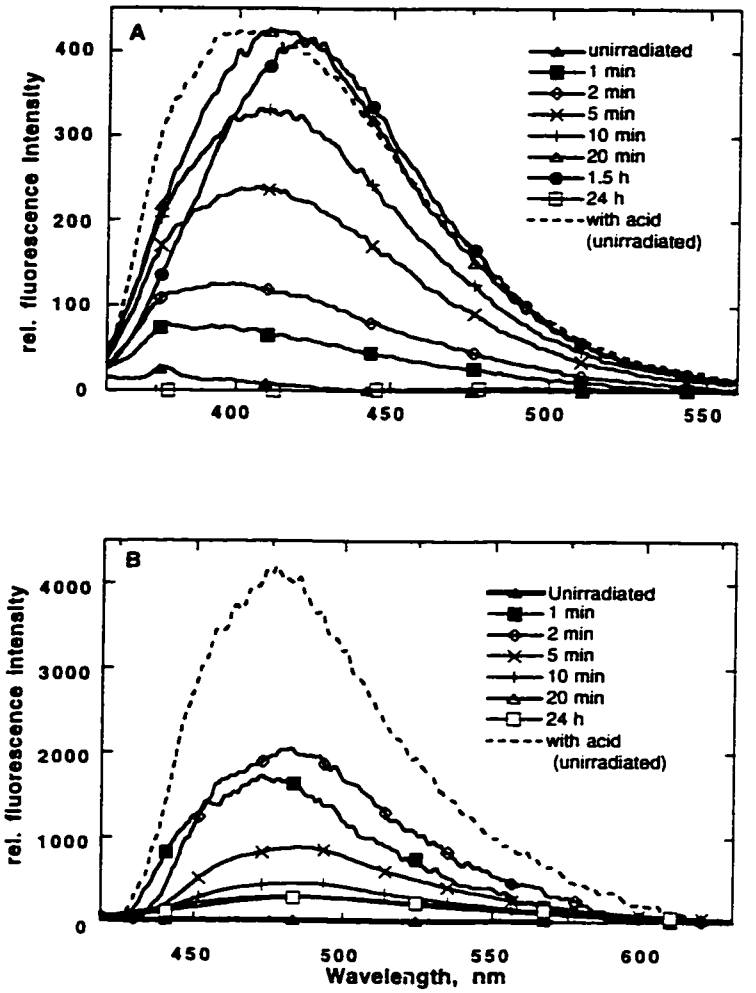

Figure 2.12. **(A):** Changes in fluorescence spectra of 2-phenylquinoline in diglyme (room temperature) in the presence of PAG upon irradiation at 254 nm for various irradiation time intervals. Also depicted is the fluorescence spectrum of **2** (same concentration) with p-toluenesulfonic acid added. The excitation wavelength was λ_{ex} = 340 nm. **(B):** Changes in fluorescence spectra of acridine in the presence of PAG upon irradiation at 254 nm for varying time intervals, instead λ_{ex} = 415 nm.

Due to the relatively small spectral shift upon protonation observed for **2**, the 2-phenylquinolinium cation could not be excited selectively. The weak fluorescence observed for

the unirradiated sample is probably due to trace impurities.

In the case of 2-phenylquinoline, no further increase in fluorescence intensity was observed for irradiation times longer than 20 min., indicating that all sensor molecules had been protonated at this time. This is supported by the finding that the fluorescence intensity observed after 20 min. and in the experiment where the acid was added directly to the same solution are essentially the same. The small spectra shift is observed because of the presence of PAG. The same shift could be induced in the sample of sensor and acid by adding PAG. Furthermore, this implies that photodegradation of the sensor due to irradiation is negligible at this point, and even the spectrum recorded after 1.5 hr. of irradiation shows only a slight decrease in fluorescence intensity accompanied by a bathochromic shift. This is at least partially due to the high concentration of PAG (which acts as an UV screen at 254 nm) rather than to the photostability of **2**, since in an irradiation experiment without PAG the 2-phenylquinoline was found to photodegrade much faster. After 24 hr. irradiation the photodegradation of the sensor is nearly complete, and the observed weak fluorescence maximizing around 480 nm is probably due to a photoproduct. However, in terms of using this sensor in such PAG experiments, this photodegradation should not be a problem. Irradiation times for most experiments will be carried out at shorter irradiation for use in microlithographic applications. And thus, the worry of photodegradation is lessened.

In contrast to **2**, under the same conditions acridine was found to photodegrade very quickly in diglyme solution (**Fig 2.12B**). After 5 minutes, the fluorescence intensity is already decreasing, maximizing between 2 and 5 minutes irradiation time. Although we did not monitor the exact maximum in fluorescence intensity, the value corresponding to complete protonation of all sensor molecules without photodegradation (broken line) is not reached. This is inferred from the analog experiment with 2-phenylquinoline where it was shown that it takes at least 20 minutes to achieve complete protonation. However, the acridine sample was four

times the concentration used in the experiment with 2-phenylquinoline. Taking into account the difference in both optical density and the spectral power distribution of the xenon lamp at the excitation wavelengths, the higher fluorescence intensity observed for **3** relative to **2** in these experiments roughly reflects the difference in fluorescence quantum yields of both sensors.

2.3.1.2. Experiments in Films

Since fluorescence properties can be strongly dependent on the environment, it was important to determine whether these results could be reproduced in a thin polymer film. Again, first the effect of directly added p-toluenesulfonic on the absorption and fluorescence spectra was examined. **Figure 2.13** shows that both the change in intensity and spectral shifts are essentially identical to those observed for the absorption spectra in solution, indicating that it is possible to protonate these monoazines in a PMMA film using p-toluenesulfonic acid.

Although we did not determine the exact values of the fluorescence quantum yield in films, the qualitative changes in the fluorescence spectra parallel those observed in solution. The poor signal-to-noise ratio observed for the fluorescence spectra in film compared to the spectra in solution is due to the fact that a front face setup had to be used in these experiments.

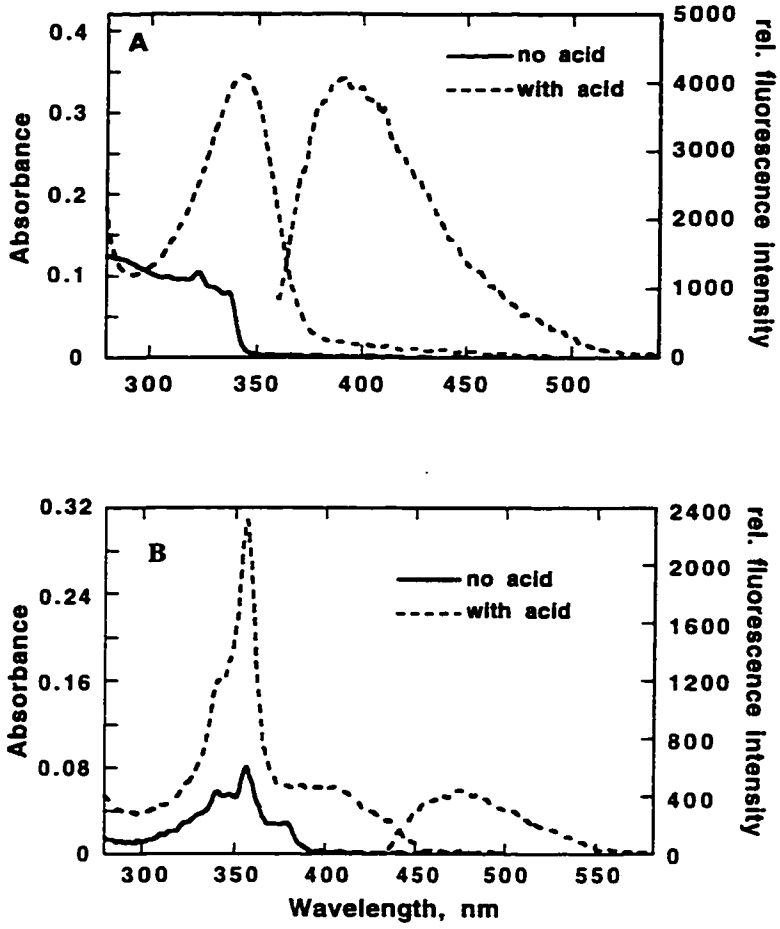

Figure 2.13. (A): Absorption and fluorescence (normalized to the longest wavelength absorption band) spectra of 2-phenylquinoline with and without 0.01 M p-toluenesulfonic acid in PMMA film at room temperature. No fluorescence signal due to **2** was observed in the absence of acid. (B): Same as (A) for acridine.

Finally, the photogeneration of acid in PMMA films was employed to test the suitability of the investigated sensors under conditions which come close to real photoresist applications. Again, the results (**Figures 2.14 and 2.15**) show close resemblance with those obtained in solution, clearly indicating the buildup in acid concentration in the film upon irradiation.

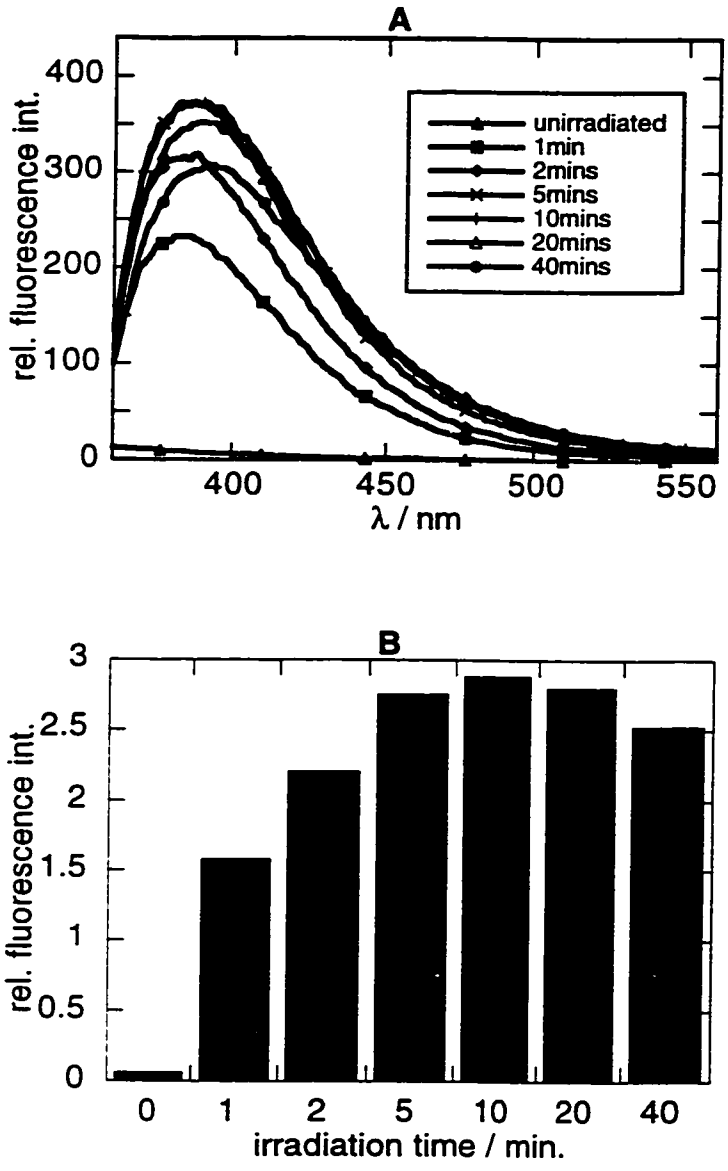

Figure 2.14: **A):** Changes in fluorescence spectra of 2-phenylquinoline in PMMA film (room temperature) in the presence of PAG **6** upon irradiation at 254 nm for various irradiation time intervals; λ_{ex} = 340 nm. **B)** Bar graph of the changes in fluorescence intensity of 2-phenylquinoline in PMMA film (room temperature) in the presence of PAG upon irradiation at 254 nm for various irradiation time intervals. The bars represent the area under the respective fluorescence spectrum between 360 and 520 nm.

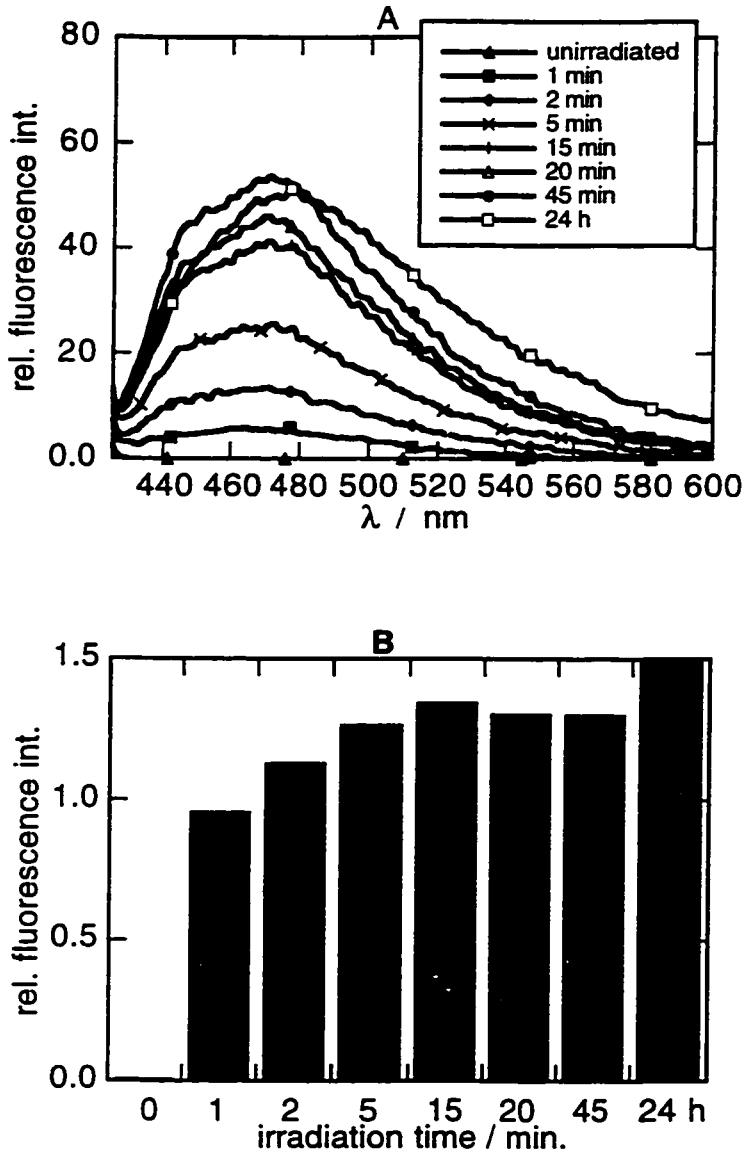

Figure 2.15: **A)** Changes in fluorescence spectra of acridine in PMMA film (room temperature) in the presence of PAG **6** upon irradiation at 254 nm for various irradiation time intervals. **B)** Bar graph of the changes in fluorescence intensity of acridine in PMMA film (room temperature) in the presence of PAG upon irradiation at 254 nm for various irradiation time intervals; λ_{ex} = 415 nm. The bars represent the area under the respective fluorescence spectrum between 430 nm and 600 nm.

In contrast to the experiments in solution the peak value of fluorescence intensity for *both* sensors is reached before significant photodegradation takes place. Furthermore, the fluorescence intensity observed for the acridine sample is lower than for the 2-phenylquinoline. This is unexpected since the greater extinction coefficient at the excitation wavelength (ε_{340}(**2**) = 17,100 $M^{-1}cm^{-1}$, ε_{415}(**3**) = 2,600 $M^{-1}cm^{-1}$) of **2** should not even compensate for its lower fluorescence quantum yield (taking into account the difference in both optical density and the spectral power distribution of the xenon lamp at the excitation wavelengths). Apparently, the ratio of the fluorescence quantum yields of **2** and **3** changes going from diglyme solution to PMMA film, thereby indicating that the results obtained in solution might be of only limited use for predicting the behavior in polymer films.

The results show that within the group of molecules studied here acridine is the most promising sensor with respect to applications in phenolic polymers like polyvinyl phenol (PHS) or novolac. This is mainly due to the spectral range of the acridinium ion fluorescence which, in contrast to the fluorescence of the 2-phenylquinolinium and especially the 2-phenylpyridinium cation, does not overlap with the fluorescence emission of these polymers containing phenolic groups. The absorption and fluorescence spectra of a 25% PHS film are shown in **Figure 2.16**.

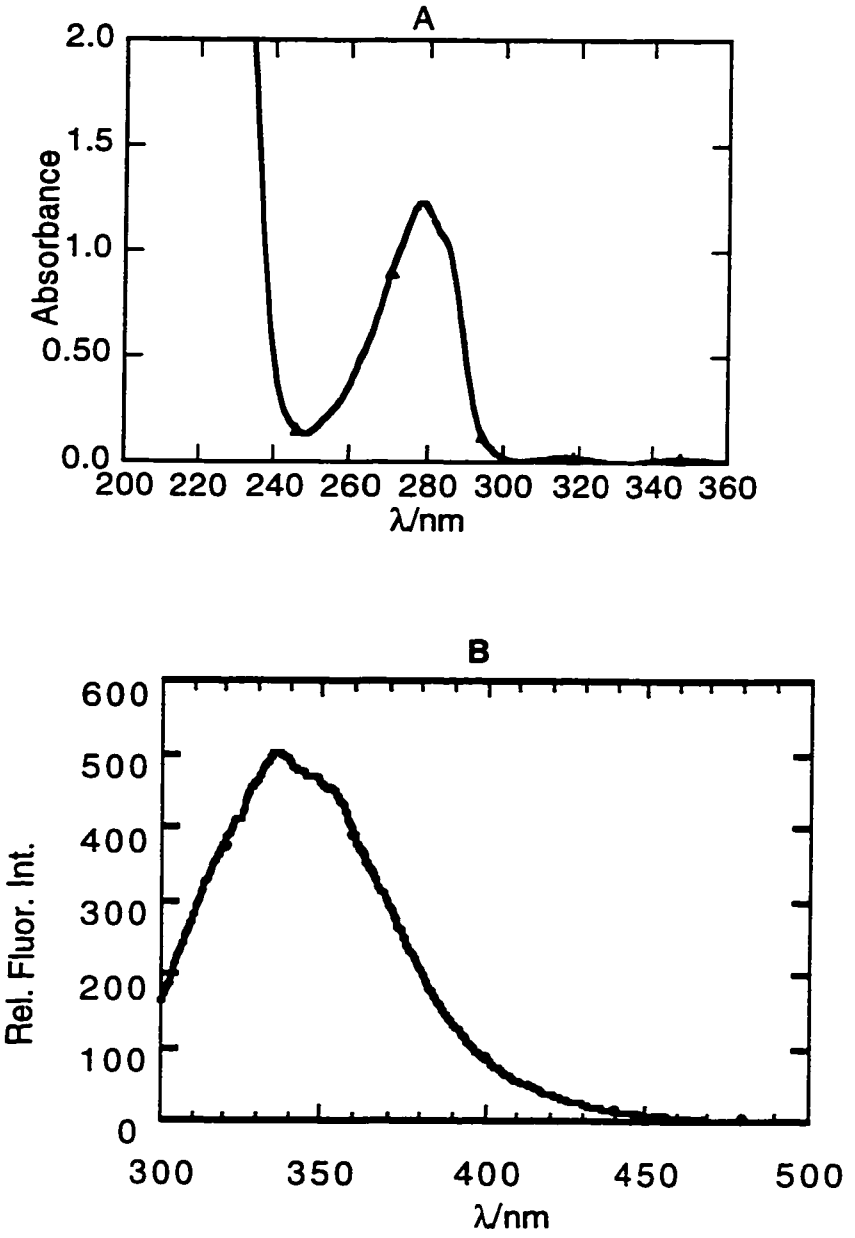

Figure 2.16: **A)** Absorption and **B)** fluorescence spectra of a 25% PHS film spin coated from diglyme.

Moreover, the emission in the visible range also allows the use of a fluorescence microscope to study the acid diffusion in the polymer film directly. Furthermore, the large spectral shift upon protonation observed for acridine allows the selective excitation of only the

protonated form. However, in terms of extinction coefficient at the excitation wavelength the 2-phenylquinoline proved to be superior to acridine. As mentioned above, a high excitation coefficient (i.e., a high absorbance) at the excitation wavelength is needed to get a good signal to noise ratio even in a thin polymer film.

2.3.2. Xanthene Dyes (Rhodamine B Base and Fluorescein)

2.3.2.1. Protonation Effects in PHS and PMMA

The absorption of fluorescein in a PHS film with and without p-toluenesulfonic acid are shown in **Figure 2.17A**. Upon the addition of acid, the protonated and ring opened form of fluorescein is seen to absorb at 445 nm both in PHS and PMMA films. In terms of the unprotonated forms of fluorescein there is a minor difference in the spectra between the two polymers. Fluorescein in PHS films exhibits some absorption at wavelengths > 300 nm where the lactone form does not absorb as was discussed by Pohlers *et al.* This absorption is due to the zwitterion and quinone forms. However, in a PMMA film the spectrum does not differ markedly from that observed in solution, as seen in **Figure 2.17B**. From these observations, it can be concluded that the lactone ring is opened in PHS and that this is due to the protic nature of the PHS matrix where protonation can lead to the cation.

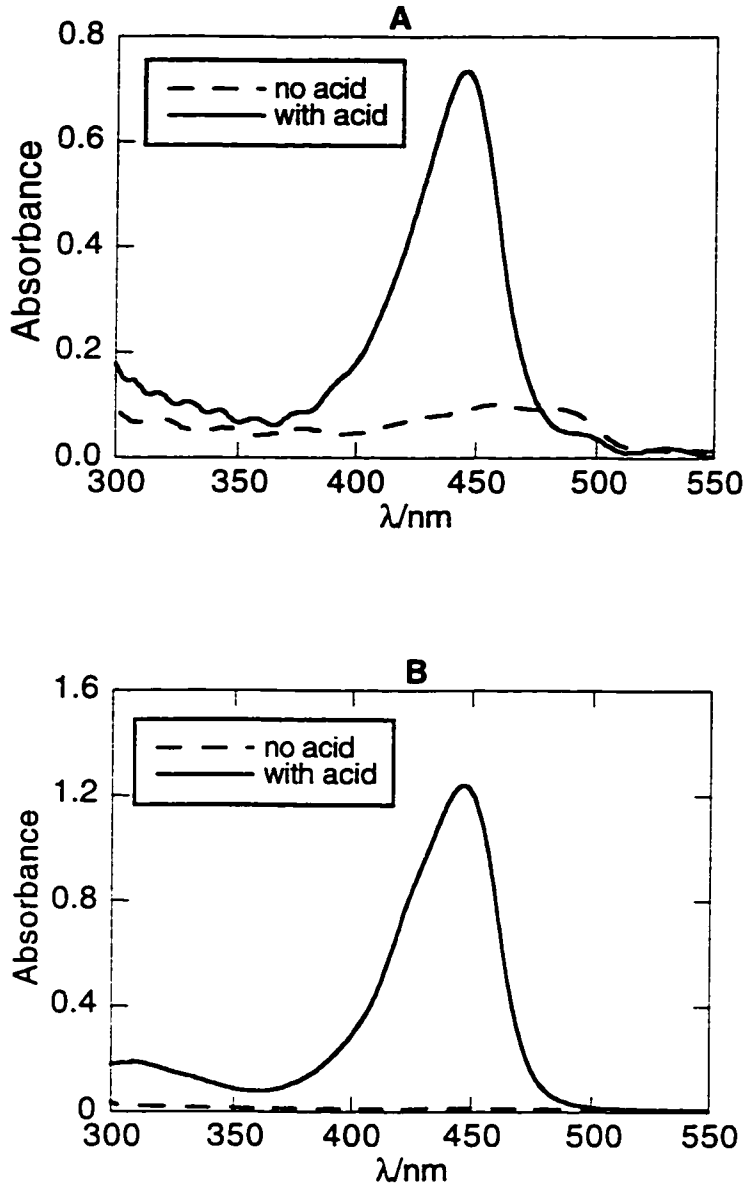

Figure 2.17: Absorption spectra 0.02 M fluorescein in **A**) PHS and **B**) PMMA films, with and without added 0.08 M p-toluenesulfonic acid.

In the case of rhodamine B base in PHS, it is seen that there is not a very big difference between samples with acid and those without. In both polymers, the protonated form of rhodamine B base has an absorption at 560 nm and this absorption has the same intensity, as

seen in **Figure 2.18A**. The spectra of rhodamine B base in a PMMA film is seen in **Figure 2.18B**. In this case, there is a difference in spectra of the sample with and without acid.

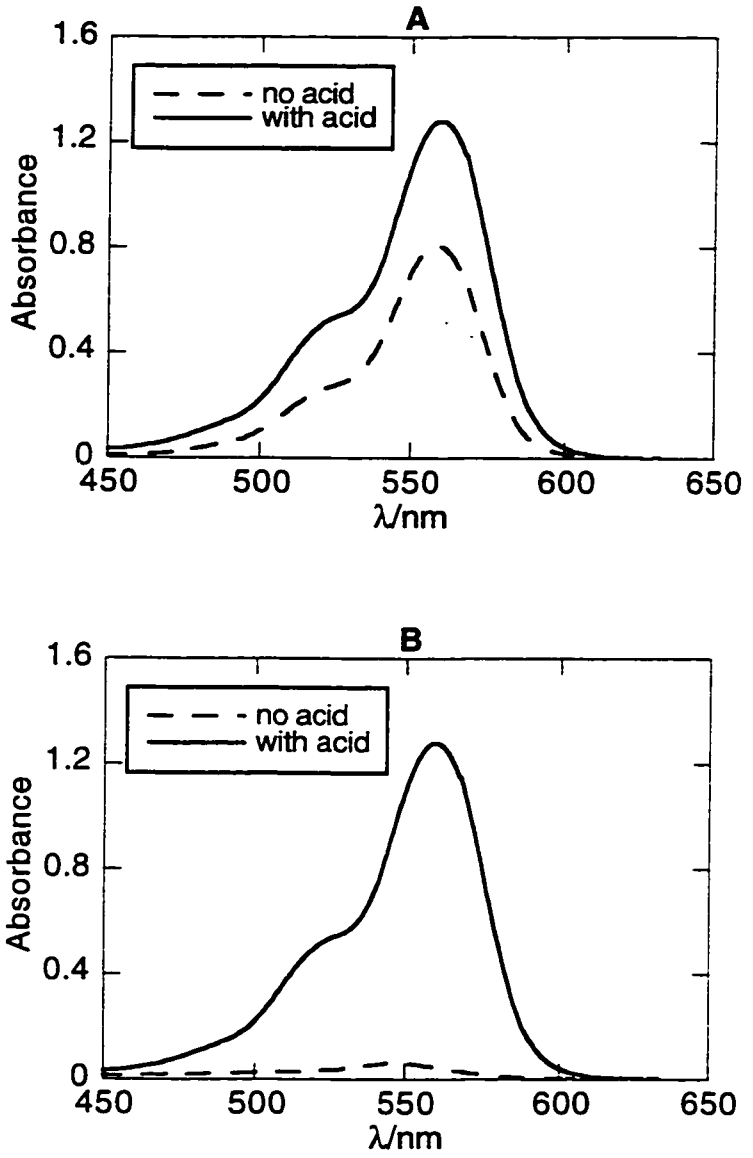

Figure 2.18: Absorption spectra 0.02 M rhodamine B base in **A**) PHS and **B**) PMMA films, with and without added 0.08 M p-toluenesulfonic acid.

The phenomenon observed in PHS, can be attributed to the instability of the lactone form. This instability would be due to the presence of phenolic groups in PHS, and thus the lactone

ring would open as was the case in fluorescein. However, from the essentially identical spectra observed with and without acid it can be inferred that in the case of rhodamine B base the ring opening seems to be induced by protonation leading directly to the cation rather than the zwitterionic form[16]. This is consistent with the higher sensitivity of rhodamine B base towards acid. Furthermore, the zwitterionic form of rhodamine B base is reported to have a significantly smaller extinction coefficient at the long wavelength band, but the presence of acid does not affect the intensity. This also means that there is no residual lactone form present in PHS since this would have lead to an increase in intensity for the acid sample due to complete ring opening induced by the acid.

In terms of the fluorescence spectra, it was seen that fluorescein does not undergo fluorescence in a PHS film, however in a PMMA film the spectra is complementary to the absorption spectra, as seen in **Figure 2.19**.

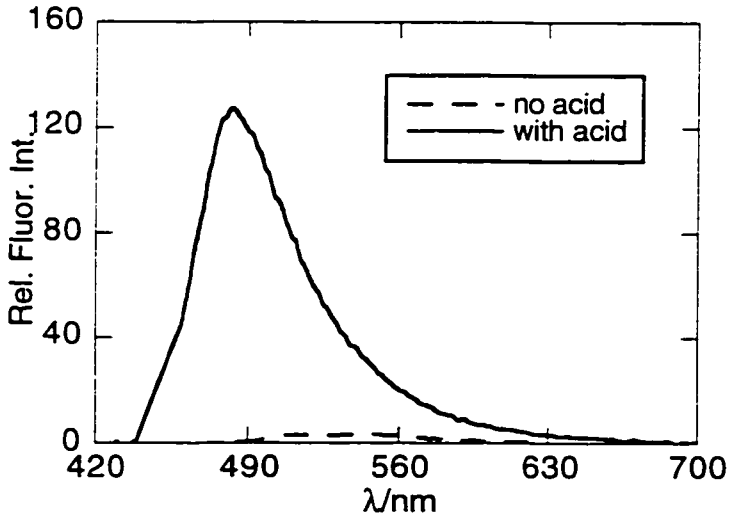

Figure 2.19: Fluorescence spectra of 0.02 M fluorescein in a PMMA film, with and without 0.08 M p-toluenesulfonic acid.

The fluorescence spectra of rhodamine B base in PHS was not taken because of the reasoning discussed above. This dye opens to the lactone form in PHS, and thus is not a suitable dye

when using this polymer. In PMMA, there is an initial fluorescence of the unprotonated form of rhodamine B base, thus absorption spectroscopy may be better when using this dye.

Figure 2.20 and Figure 2.21 show the effects on the absorption spectra of adding increasing amounts of acid to polymer samples (PHS and PMMA) containing fluorescein.

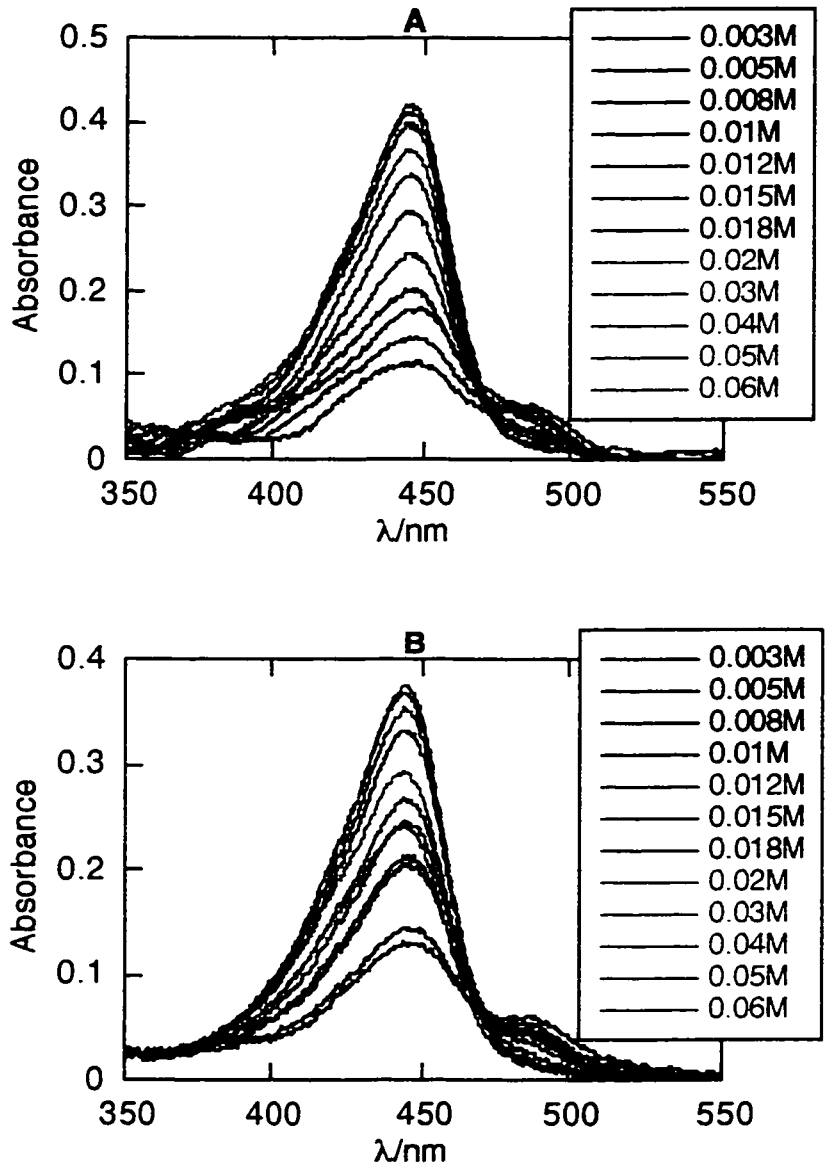

Figure 2.20: Absorption spectra of 0.02 M fluorescein in a PHS film with increasing amounts of **A**) camphorsulfonic acid and **B**) perfluorooctane sulfonic acid.

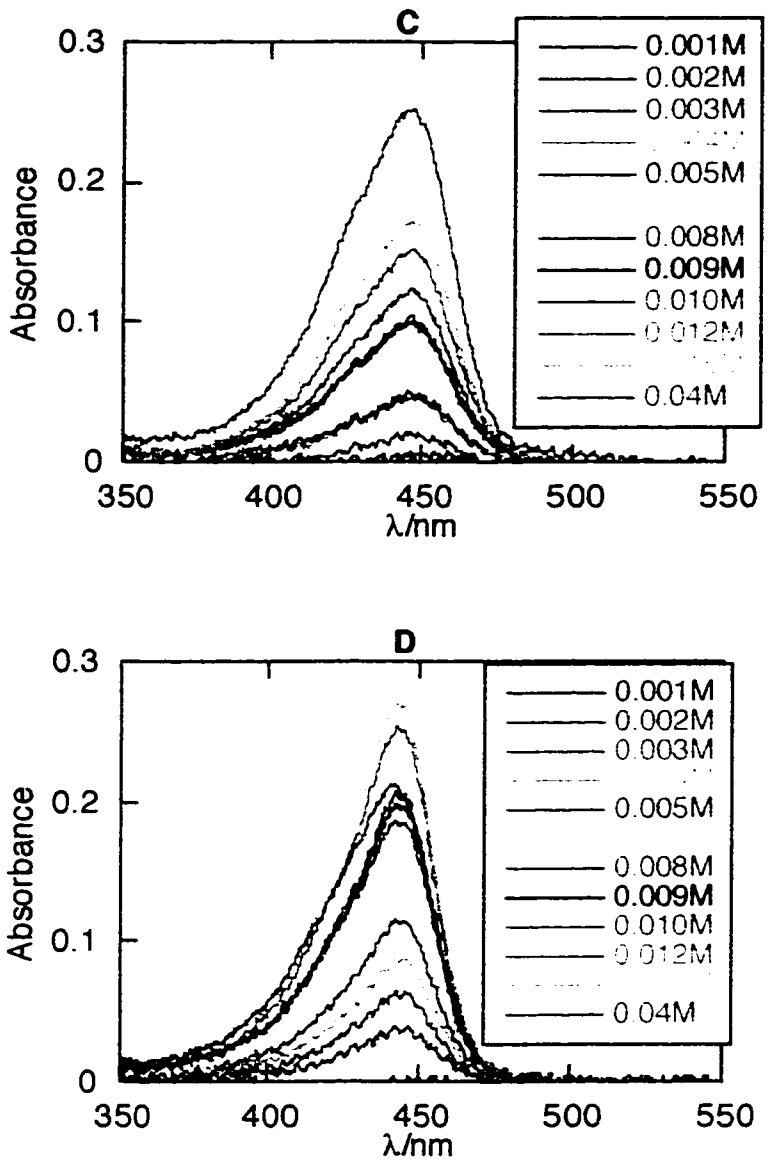

Figure 2.21: Absorption spectra of 0.01 M fluorescein in a PMMA film with increasing amounts of **C**) camphorsulfonic acid and **D**) perfluorooctane sulfonic acid.

Similarly, the effect of adding increasing amounts of acid to 0.02 M rhodamine B base in a PMMA film can be seen in **Figure 2.22.**

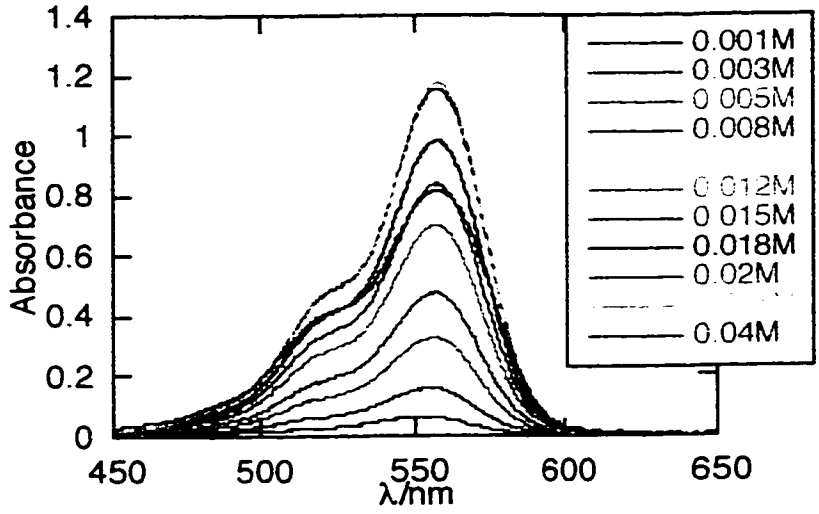

Figure 2.22: Absorption spectra of 0.02 M rhodamine B base in a PMMA film with increasing amounts of perfluorooctane sulfonic acid. Note: samples were also prepared with increasing amounts of camphorsulfonic acid but samples deteriorated such that absorption spectra could not be taken.

Furthermore, to test whether photoacid generation yields similar results to those with added acid, experiments were done with PAGs. **Figure 2.23** shows the changes in absorption spectra of fluorescein with **9** upon increasing the irradiation time. As the time of irradiation increases at 254 nm, greater amounts of acid is generated and thus the protonated form of fluorescein also increases, as was observed with the samples with added acid. Although, many PAGs in this work have been studied for the acid generation efficiencies by using fluorescein (as discussed in **Chapter 3**), the general trends in changes in fluorescence upon acid generation are the same for all the PAGs differing only in the rate of acid generation. Although, the spectra of fluorescein with added PAGs have been recorded for all the PAGs discussed in this chapter and in **Chapter 3**, these have not been shown due to the similarity of all trends in spectra. The PAGs used were **9** (a HBr generator), a camphorsulfonic acid generator, and a methanesulfonic acid generator (see **Figure 2.10**), plus all the PAGs

discussed in **Chapter 3**. Although, only the spectra of the acid generation with the PAG, **9**, is shown, similar trends in spectra are observed with all the PAGs.

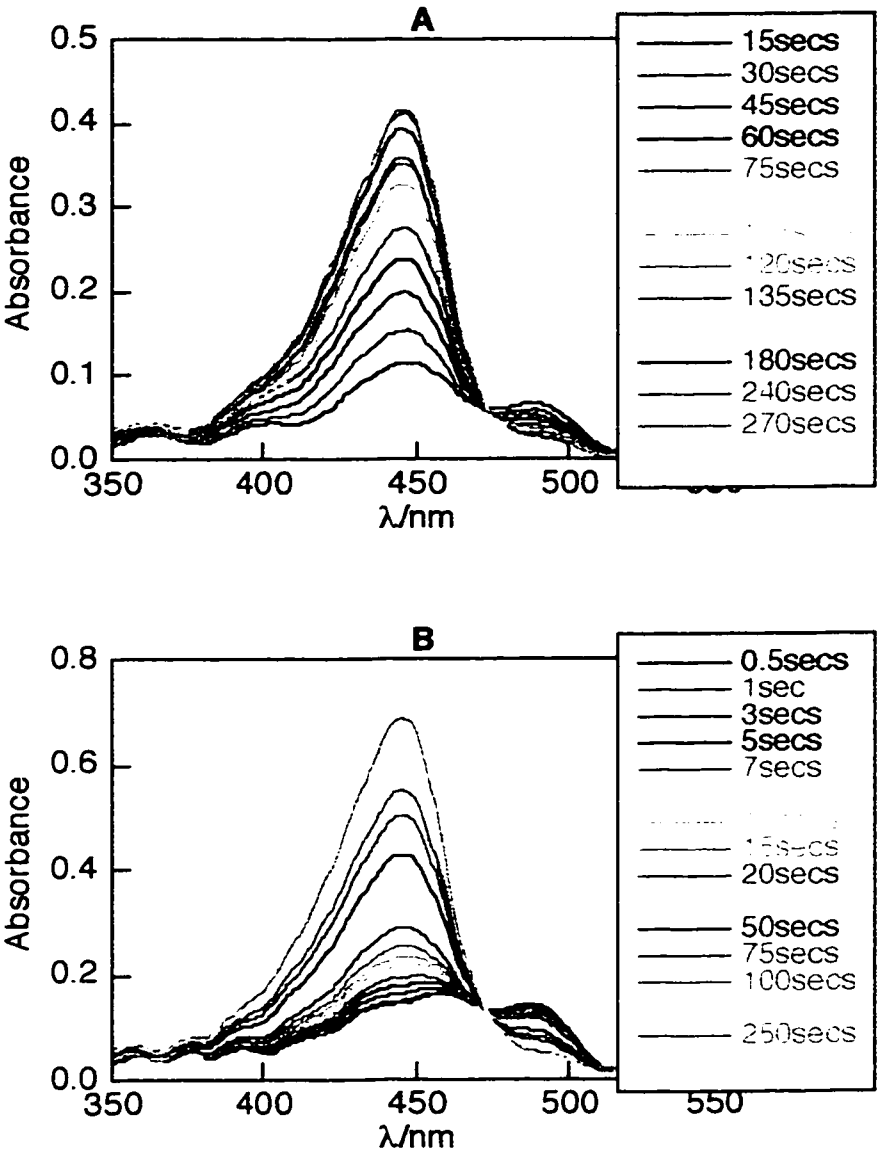

Figure 2.23: Changes in absorption spectra of 0.02 M fluorescein in 25% w/v PHS films made in **A**) diglyme and **B**) ethyl lactate. The concentration of **9** was 0.022 M for the samples made in ethyl lactate and diglyme.

It is seen that all three PAGs absorb relatively at the same wavelengths in **Figure 2.24**. These differ only in the intensity of absorption. This is due to the fact that it is very hard to match absorbances in films.

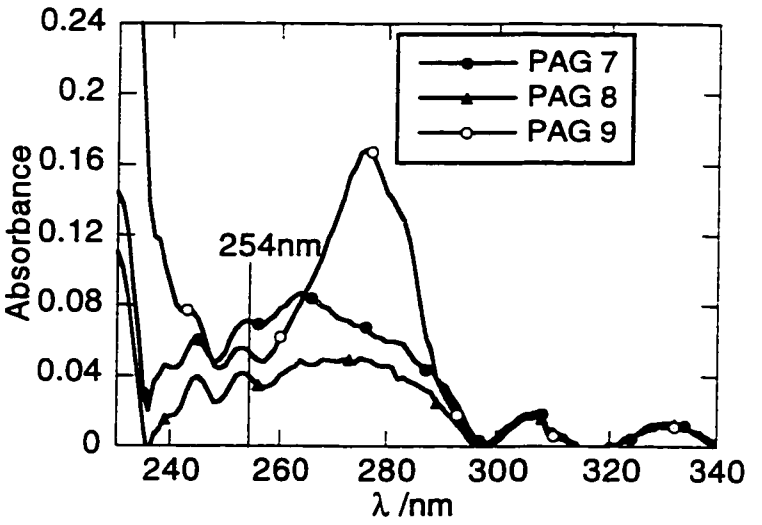

Figure 2.24: Absorption spectra of 0.062 M of PAGs that generate methanesulfonic acid (**7**), camphorsulfonic acid (**8**) and HBr (**9**).

The photoacid generator, **9**, produces HBr upon irradiation, whereas the other PAGs produce various other acids. Upon acid generation, fluorescein is protonated in the same way by generation of photoacid by these PAGs, in polymer films. It is seen that the absorbances of the photoacid generators do not interfere with the absorbance of the dye.

2.3.2.2. Vertical Diffusion Monitoring by Rhodamine B base

To monitor the effects of acid loss from an irradiated sample of PAG/polymer, a vertical diffusion experiment was conducted. The results of this experiment can be seen in **Figure 2.25**.

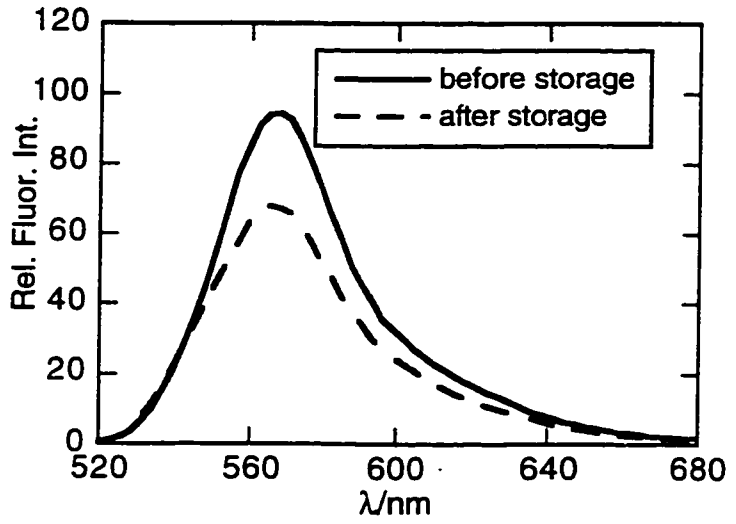

Figure 2.25: Fluorescence spectra of rhodamine B base before and after dark storage with an acid containing positive photoresist (XP9549Q) sample.

The above experiment was also repeated but stored at 130°C for 1 hour. Similar results were obtained. The spectra indicate that upon storage of the dye i.e., 'catching layer" sample with the irradiated resist "acid layer", the fluorescence of the protonated form increases. However, the problem with doing experiments at higher temperatures with rhodamine B base, is that it exhibits a temperature-dependent fluorescence quantum yield[17,18]which has been attributed to the flexibility of the diethylamino groups[19,20]. The result from the vertical diffusion experiment indicates that there is a movement of acid from the resist to the dye layer such that rhodamine B base converts to its protonated form. Although the quantities of acid that may migrate across the 2.5 mm barrier are quite small, rhodamine B Base has a high enough extinction coefficient to detect the presence of the acid. Since the system was sealed, the change in absorption cannot be the result of contamination in the air.

Although, this result is quite interesting it is better to have indicator molecules that do not have initial fluorescence. In the case of rhodamine B base, it has an background fluorescence signal and thus a change in intensity can only be measured. Fluorescein does not have this initial fluorescence, however, experiments that we conducted showed that fluorescein was not sensitive enough to monitor the acid production in the resist samples, and thus could not be used. The actual resist has very small quantities of PAG unlike the model polymer/PAG systems that we use for purposes of these experiments. Our experiments usually involve 0.062-0.08 M PAG but the quantities in a real resist are actually quite less, and thus we needed to use the most sensitive dye for this experiment.

Overall, the results of these experiments describe the behavior of these dyes in polymer films. Previous work has been done in solution on the prototopic forms and photophysics of fluorescein[12,13,21-23] and rhodamine B base [24-29]. However, not as many studies have been done in films[3,17,30]. Zhang *et al.*[30] studied fluorescein and fluoresceinamine, a derivative of fluorescein but which behaves similarly to fluorescein in film. Although, they used an acid vapor technique of protonating the dye, they observed similar protonation effects on fluorescein in a polymer film. The results reported here, indicate that rhodamine B base and fluorescein are just as sensitive in PHS and PMMA polymer matrices as in solution. However, these results indicate that rhodamine B base can only be used in PMMA matrices. Although phenolic polymers are preferred in the photoresist industry, rhodamine B base can still be used in PMMA for purposes of studying the acid-generating abilities (or efficiencies) of PAGs. It is seen that fluorescein can be used in either polymer when doing absorption studies. However, the more sensitive technique of fluorescence spectroscopy can only be done in PMMA samples incorporated with fluorescein. In this work these dyes were not used for acid diffusion studies because of the background absorption in PHS. However, these could still be used in PMMA. Acid diffusion studies of these dyes in PMMA may be a favorable study to be able to compare results to those done in PHS.

2.3.3. Benzothiazole Dyes

2.3.3.1. Experiments in Solution

As Pohlers *et al.*[31] have observed, there are three prototopic species of DSB in solution; the neutral, monocation and dication species. Each has a distinctive absorption and fluorescence spectra. The absorption and fluorescence spectra of DSB in diglyme are shown in **Figure 2.26 (A-B)**. It can be seen that the neutral form has a maximum absorption at approximately 400 nm, the monocation species, have a absorption maximum at 320 nm and 500 nm, and the dication has an absorption maximum at 340 nm. The excitation wavelengths that were used for the fluorescence spectra were 400 nm, 500 nm, and 340 nm for the neutral, monocation, and dication species, respectively.

Figure 2.27 shows the spectra of DSB in 50% methanol/distilled water solutions of varying pH. The change in spectra as a function of protonation of DSB can be clearly observed. The pH of 1.21 was low enough to form a small amount of the dication. The pKa value calculated for the monocation was 2.7. This experiment was done twice. The second pKa calculation resulted in a value of 2.9.

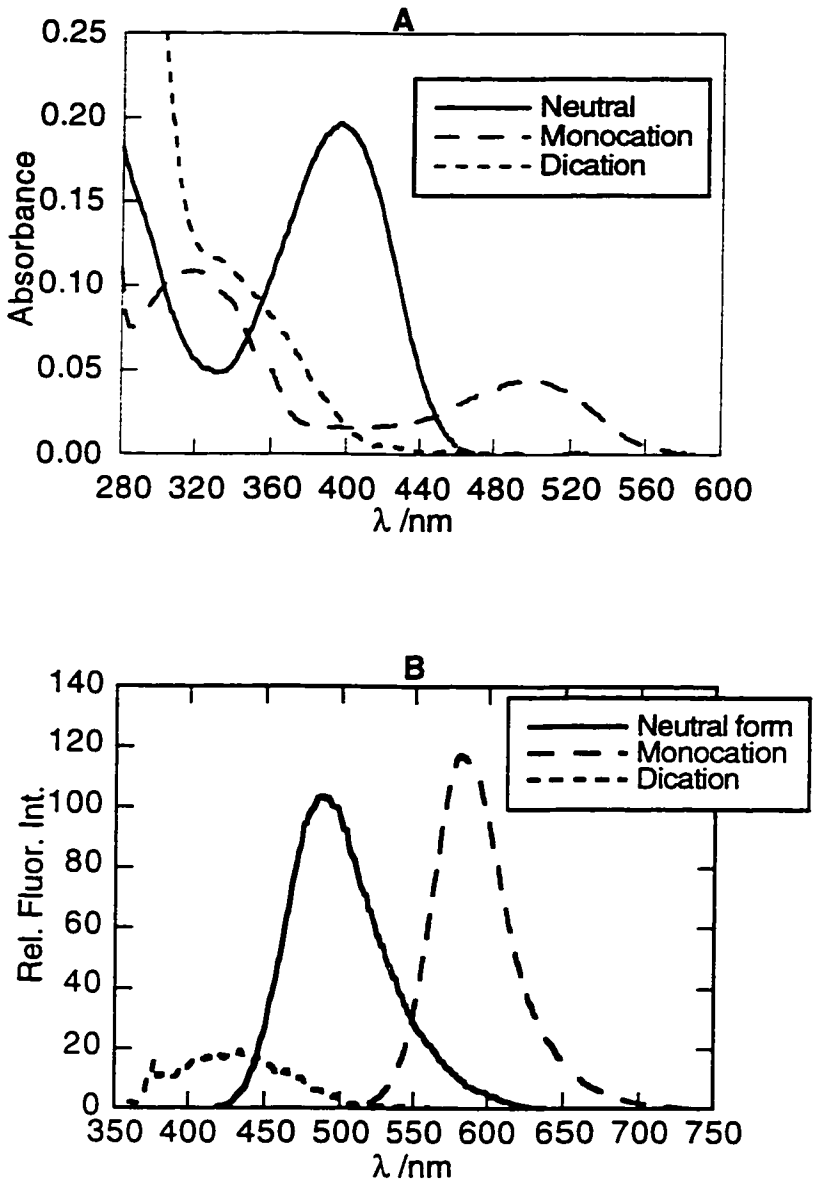

Figure 2.26: **A)** Absorption and **B)** fluorescence spectra of the neutral, monocation, and dication species of DSB in diglyme. A concentration of 0.05 M of p-toluenesulfonic acid was used to obtain the monocation and 0.2 M to obtain the dication. The fluorescence spectra were recorded at excitation wavelengths of 340 nm for the dication species, 400 nm for the neutral species and 500 nm for the monocation species.

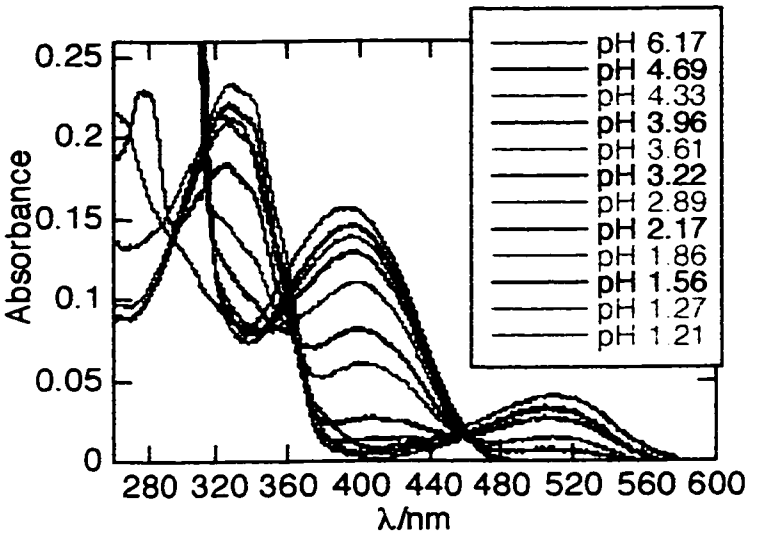

Figure 2.27: Plot of 0.02 M DSB absorption spectra in 50% MeOH/dH_20 as a function of pH.

2.3.3.2. Experiments in PHS and PMMA Films

The effects of adding acid in the dye/polymer systems were studied for DSB, DSBS, DMBB, and Coumarin-6. **Figure 2.28** shows the change in absorption spectra of DSB as a function of increasing amounts of p-toluenesulfonic acid.

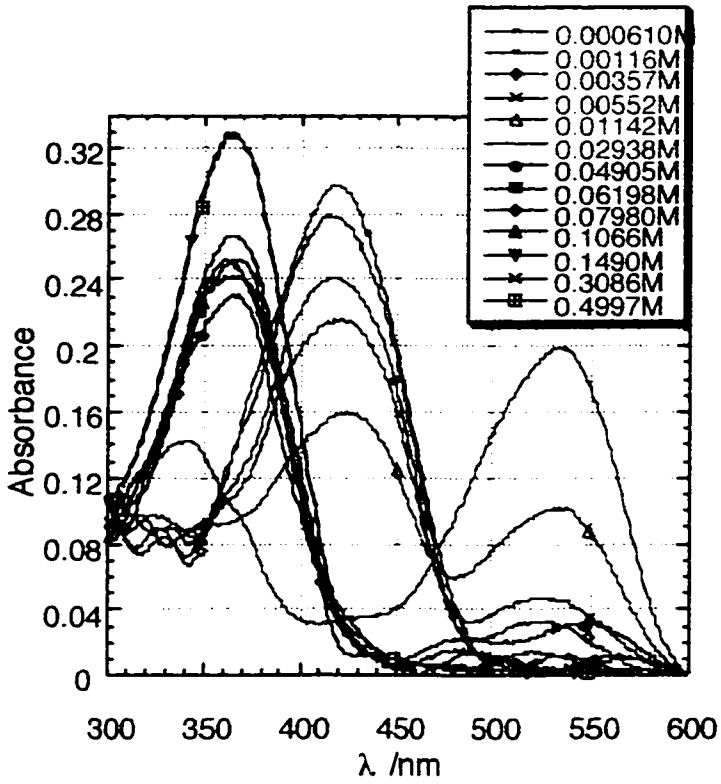

Figure 2.28: Calibration curve of 0.02 M DSB with increasing amounts of p-toluenesulfonic acid in a 25% PHS(diglyme) film.

From the plot above, it can be seen that the neutral form of DSB absorbs at 420 nm and the monocation species of interest absorbs at 540 nm. The monocation also has an absorption at 340 nm but for purposes of this work, only the 540 nm band was monitored. The band at 540 nm was used to monitor the absorption of the protonated form. Upon protonation, the peak at 420 nm decreases whereas the peak at 540 nm increases. In monitoring the fluorescence changes of DSB as a function of protonation, either the neutral or monocation form can be monitored.

The results of adding increasing amounts of acid to PHS polymer solutions of 0.02 M DMBB, Coumarin-6, and DSBS are shown in **Figure 2.29 (A-C)**. The results of such

spectra yield a calibration from which acid quantification of PAGs can be done. This type of acid quantification will be discussed in **Chapter 3**.

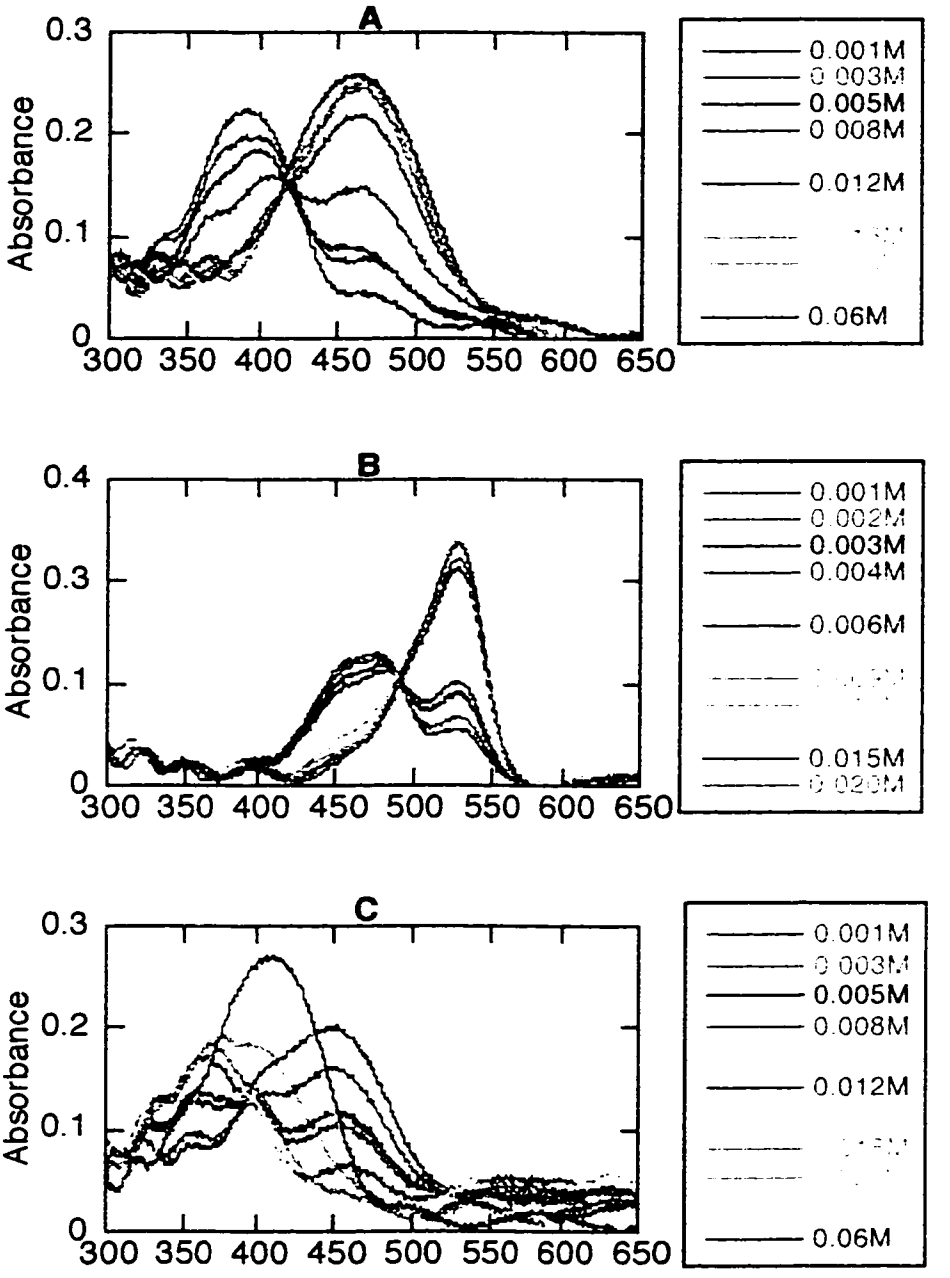

Figure 2.29: Calibration absorption curves of **A**) 0.02 M DMBB, **B**) 0.015 M Coumarin-6, and **C**) 0.0015 M DSBS with increasing amounts of added camphorsulfonic acid. Note: PFOS calibration curves yields similar spectra.

The calibration plots for DMBB, Coumarin-6, and DSBS all differ to some extent. Similarly to DSB, it is seen that in film, the absorption of the protonated form shifts to a higher wavelength. Furthermore, it is seen that Coumarin-6 and DSBS also have a dication form as did DSB. DMBB and Coumarin-6 only have one wavelength band for the protonated form, whereas DSBS has two. For DMBB, the λ_{max} of the neutral form is approximately at 390 nm and for the protonated form is 460 nm. For Coumarin-6, the neutral form is at 470 nm, the protonated form at 530 nm, and the dication at 370 nm. And for DSBS, the neutral form absorbs at 445 nm, two bands at 370 nm and 590 nm represent the protonated form, and the dication absorbs at 410 nm. For these dyes, calibration plots were also made using a strong acid. The acid used was PFOS. Both the CSA and PFOS calibration curves were used in the quantification of acid generation in **Chapter 3**.

The next step in the experiments was to verify that the photoacid generation from the PAG samples would follow the same trend in spectra as did with added acid. **Figure 2.30 (A-B)** and **2.31 (C-D)** show the absorption and fluorescence spectra of 0.02 M DSB in 25% PHS and PMMA films, with **8**.

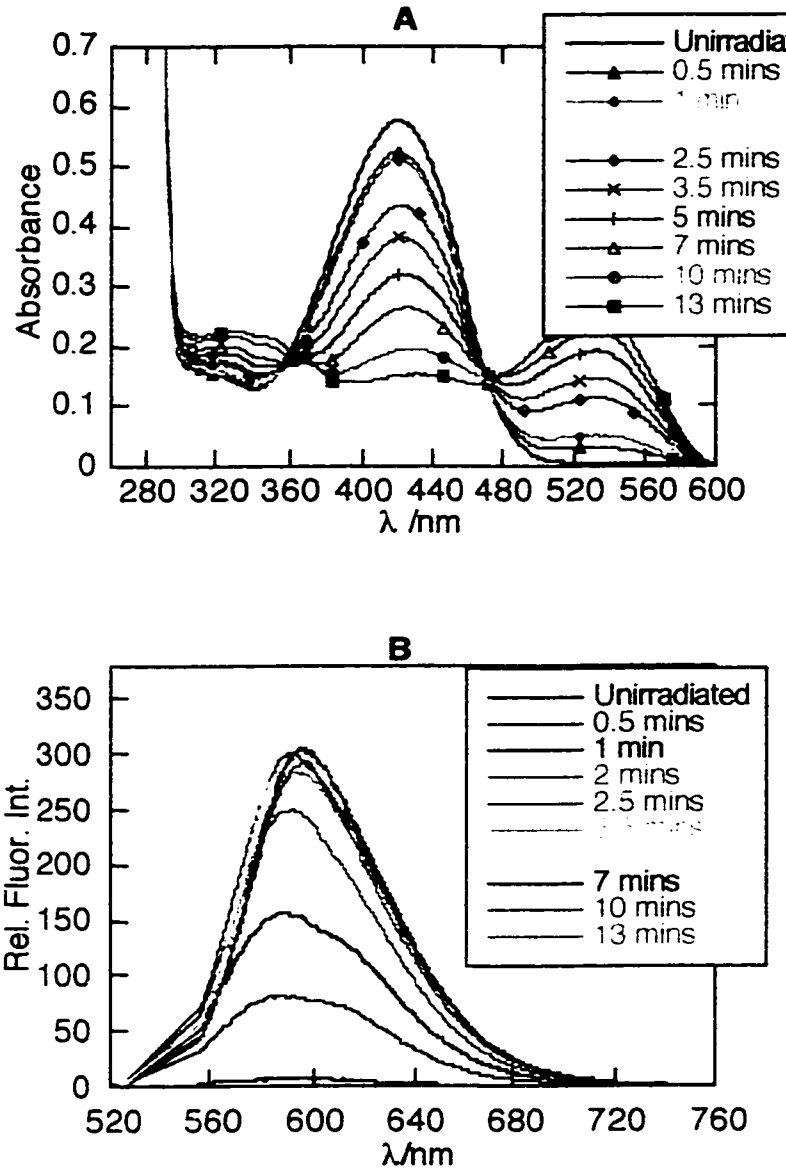

Figure 2.30: Plots **A**) & **B**) are absorption and fluorescence (λ_{ex} 540 nm) plots of 0.02 M DSB with 0.062 M **8** in 25% PHS (diglyme) as a function of irradiation time. Samples were irradiated at 254 nm and stored for varying amounts of time in a closed container between measurements.

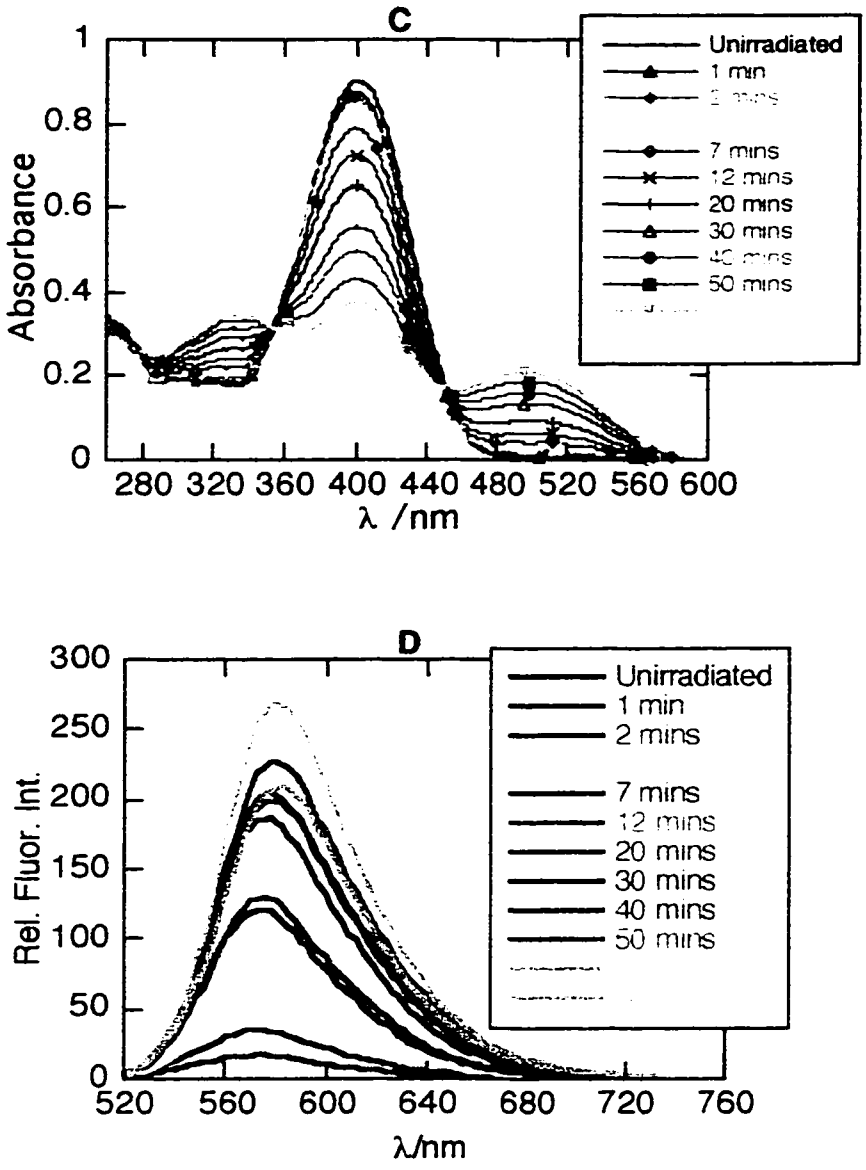

Figure 2.31: Plots C) & D) are absorption and fluorescence (λ_{ex} 540 nm) plots of 0.02 M DSB with 0.062 M **8** in 25% PMMA (diglyme) as a function of irradiation time. Samples were irradiated at 254 nm and stored for varying amounts of time in a closed container between measurements.

The above plots show how the absorption and fluorescence of DSB changes as a function of acid generation. The trends in spectra are similar between PHS samples and PMMA samples. The only difference is the irradiation times needed to get such changes. The times are so much longer in PMMA samples due to the higher viscosity of the polymer. To obtain comparable irradiation times, it will be necessary to decrease the PMMA solution from 25% to 15% (by weight).

Furthermore, similar spectra were also recorded for 0.002 M DSB in PHS polymer solutions. The only difference was that the irradiation times were much smaller, i.e. for 0.002 M DSB with **9**, the irradiation time was about 30 sec.

The spectra obtained when using l-DSB were very similar as those obtained for DSB. The only difference was that 0.02 M l-DSB samples yielded a smaller maximum fluorescence intensity at the λ_{max} of the protonated form.

Although, only plots for **8** are shown, similar spectra were recorded for all three PAGs. This was important to see how the spectra changed with different acids being generated. All PAGs generated similar spectra differing only in the irradiation time required to reach the optimum irradiation time. This optimum irradiation time was the irradiation time required to reach the maximum protonated sample (this was indicated by either a maximum intensity in absorption or fluorescence spectra at the λ_{max} of the protonated form. The irradiation times for 0.02 M DSB with **7** was 2.5 min., with **8** (from above) was 10 min. and for **9** was 2 min.. The irradiation times to depend on the size of the acid being generated. Furthermore, the irradiation times in PMMA were 80 min.. for **7**, 60 min.. for **8**, and 40 min.. for **9**.

Acid generation with PAGs was also studied with Coumarin-6 and DMBB. The absorption and fluorescence spectra of DMBB and Coumarin-6 in PHS, with a PAG are shown in **Figure 2.32 (A-B)** and **2.33 (A-B)**.

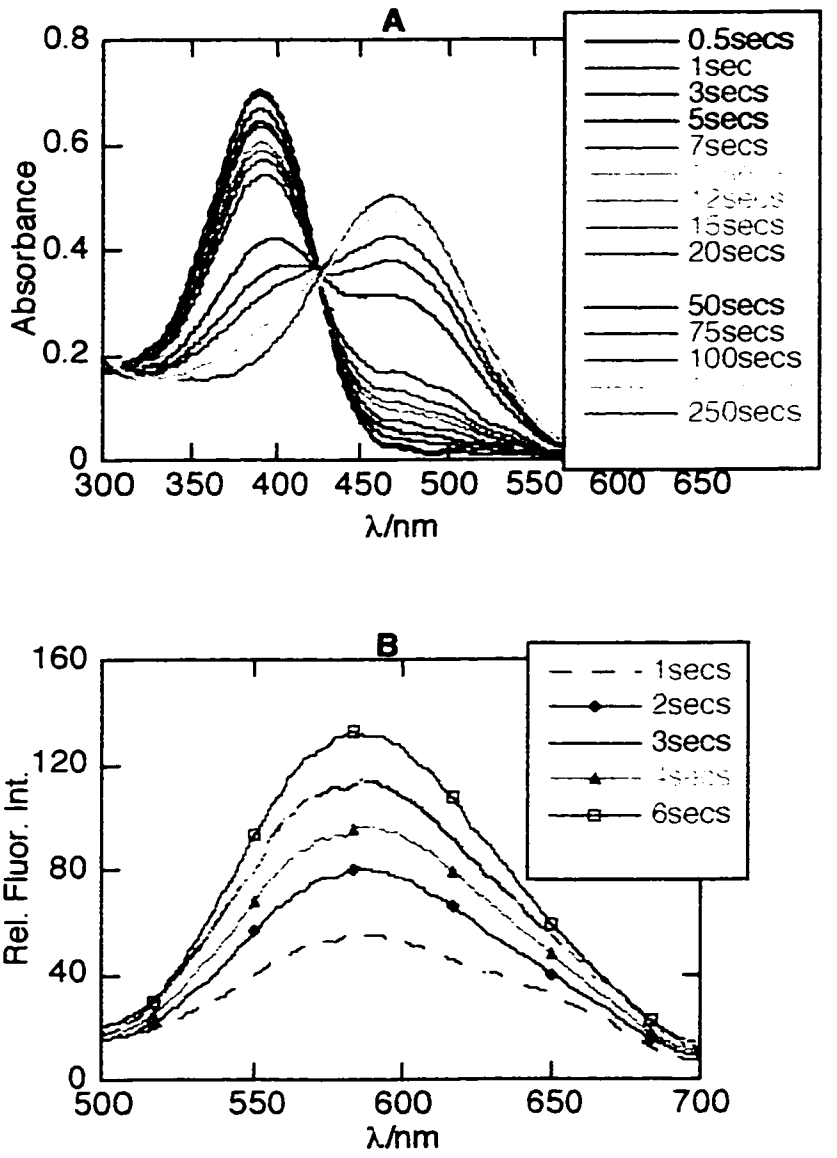

Figure 2.32: **A**) Absorption and **B**) fluorescence spectra of DMBB in a 25% PHS matrix. For plot **A**) 0.002 M DMBB was used with 0.022 M **9** in a 25% PHS/ethyl lactate polymer matrix. For plot **B**) 0.002 M DMBB with 0.062 M **9** in a 25% PHS/diglyme solution (λ_{ex} 450 nm).

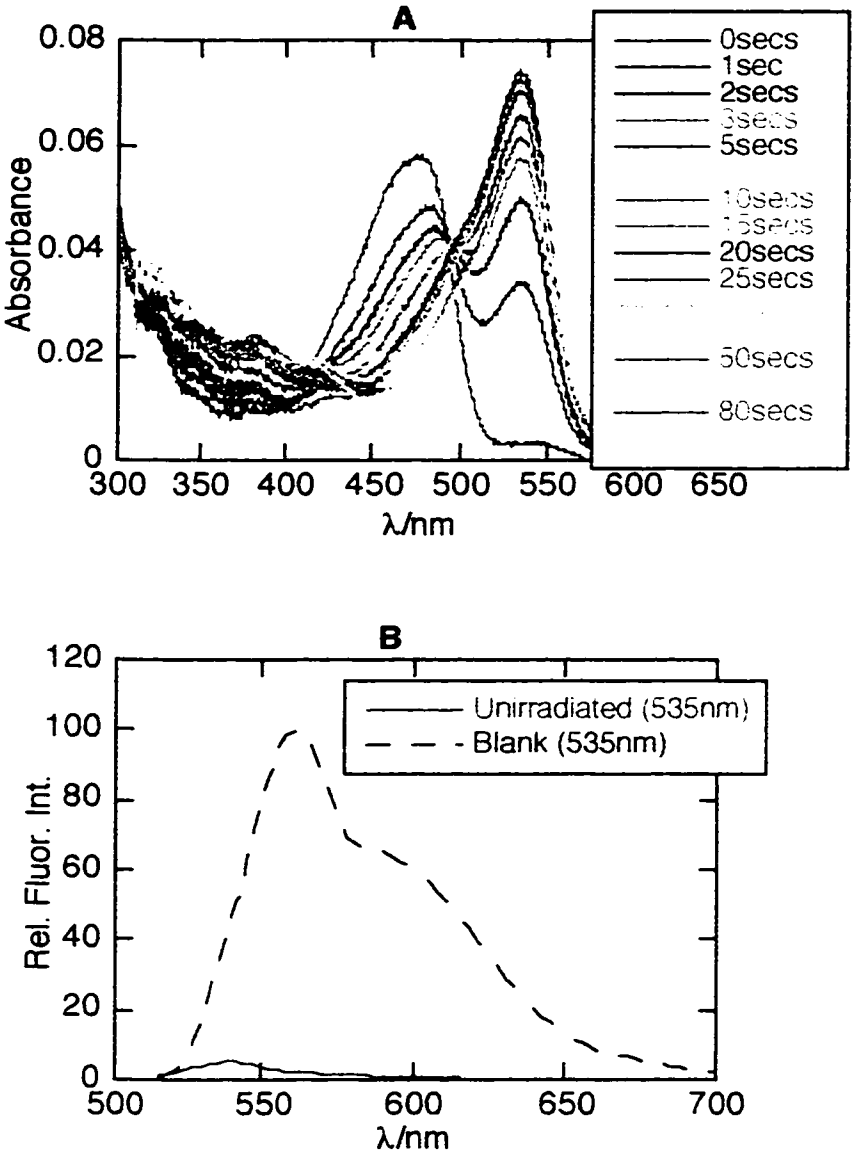

Figure 2.33: **A**) Absorption and **B**) fluorescence spectra of 0.002 M Coumarin-6 in a 25% PHS film with 0.062 M **9**. The irradiated samples were irradiated at 254 nm using the HTG Imaging Unit. Figure **B**) depicts the fluorescence of the protonated form (λ_{ex} 535 nm) before and after irradiation.

2.3.3.3 Photoacid Generation in a Positive Resist

To determine whether the dyes would be able to detect the photoacid generation of a real resist, DSB and DMBB were used. The absorption spectra of DMBB in a positive photoresist is shown in **Figure 2.34**.

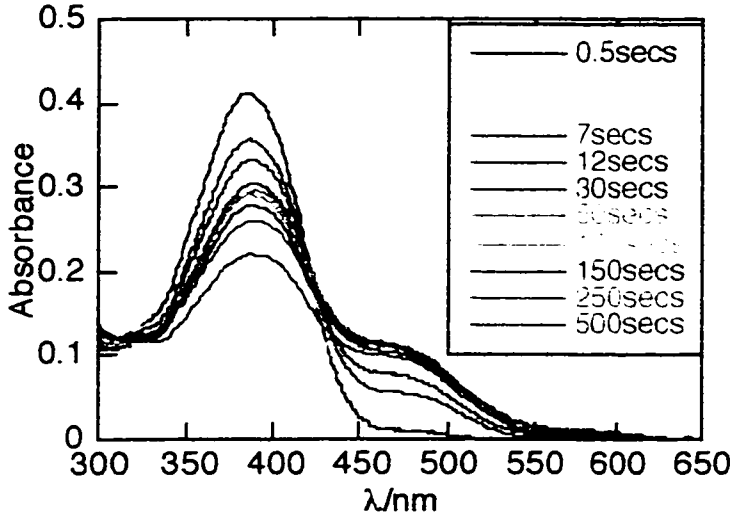

Figure 2.34: Absorption spectra of 0.02 M DMBB with a photoresist. The sample was irradiated at 254 nm for varying amounts of time.

The plot shows the same change in spectra as DMBB did in the polymer/ PAG solutions that were studied above. Because the concentration of PAG is much less in a real resist than the concentrations of PAG used above, enough acid was not generated to fully protonate the dye. For further experiments with photoresists, a lower concentration of dye was used. **Figure 2.35** shows the fluorescence spectra of 0.005 M DSB in a positive resist irradiated for varying amounts of time at 254 nm.

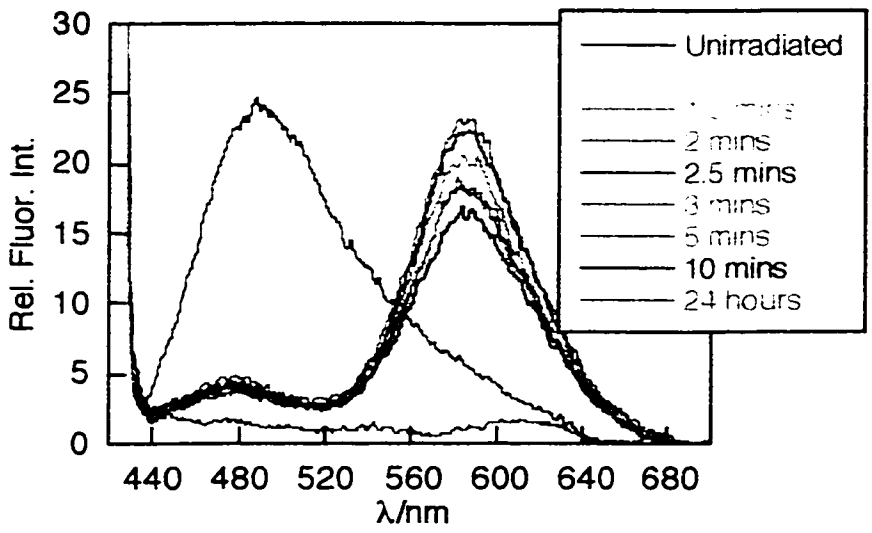

Figure 2.35: Fluorescence spectra (λ_{ex} 420 nm) of 0.005 M DSB in a positive resist. The sample was irradiated at 254 nm for varying amounts of time. Note: Fluorescence spectra were also obtained using a λ_{ex} 540 nm.

2.3.3.4. Other Dyes

The absorption and fluorescence spectra of HSB, PSB, TSB and MBB are shown in **Figure 2.36 (A-B)** and **2.37 (C-D)**. The spectra of MSB are not shown since it was found that this dye has an extremely low fluorescence, and thus is not ideal for diffusion analysis.

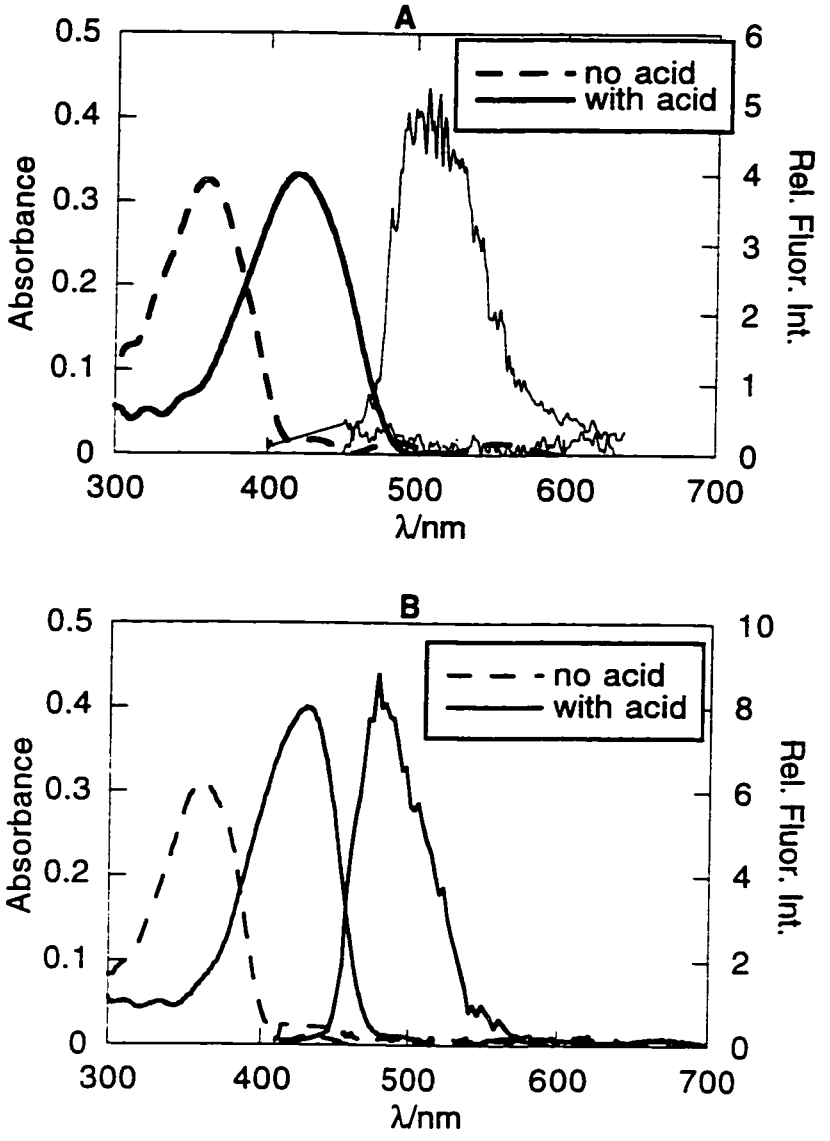

Figure 2.36: Absorption and fluorescence spectra of potential dyes: **A)** HSB (λ_{ex}: 420 nm), **B)** MBB (λ_{ex}: 420 nm) with and without added acid. The concentration of dye was 0.02 M and the concentration of p-toluenesulfonic acid was 0.08 M in each case.

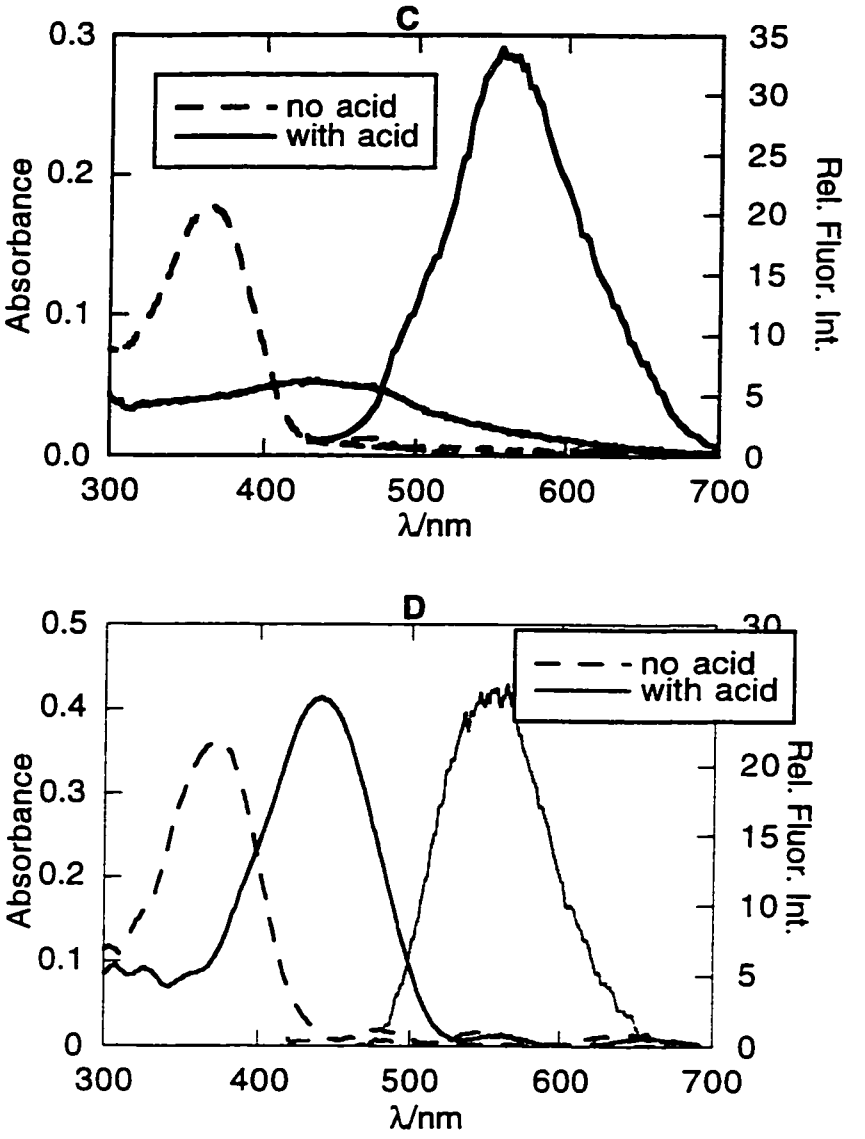

Figure 2.37: Absorption and fluorescence spectra of potential dyes: **C)** PSB (λ_{ex}: 420 nm), **D)** TSB (λ_{ex}: 420 nm). The concentration of dye was 0.02 M and the concentration of p-toluenesulfonic acid was 0.08 M in each case.

2.3.3.5. Vertical Diffusion "Pancake" Experiment

The results of this experiment confirm that to some degree acid loss occurs from photoirradiated PAG samples. **Figure 2.38 (A-B)** shows the absorption and fluorescence

spectra of the "blank" unirradiated sample. The changes in the spectra of the blank sample are important because information about acid loss is obtained.

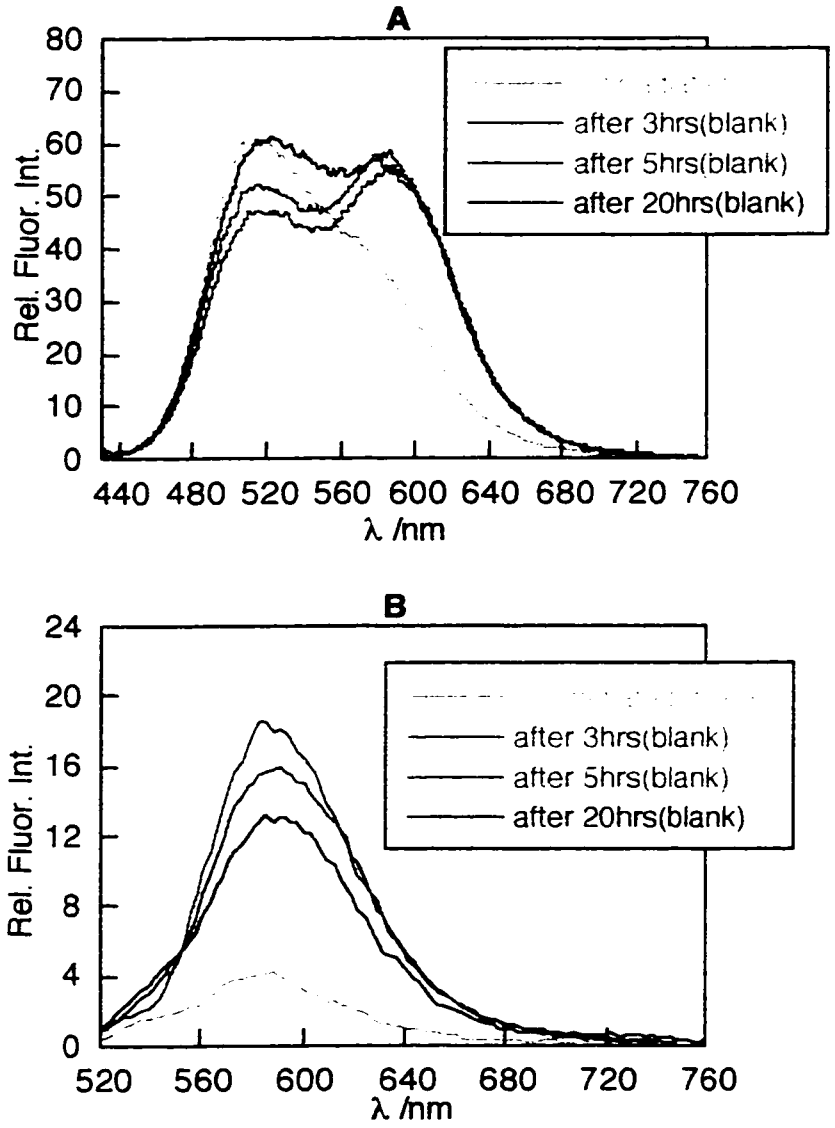

Figure 2.38: Plot of the "Pancake experiment". The above two plots represent the changes in fluorescence intensity of the blank sample upon being stored in a sandwich with a 254 nm irradiated sample. The blank sample was excited at the wavelengths of the unprotonated and

protonated forms of DSB : **A)** unprotonated form (λ_{ex} 420 nm) and **B)** protonated form at 540 nm.

By storage with the irradiated sample, there is a definite change in the fluorescence intensity of the blank (unirradiated sample). Because the sample has added dye, it is able to detect any capture of acid. This capture would be represented by changes in spectra. **Figure 2.38** above clearly shows that with longer storage times a shoulder in Plot A starts to develop. The fluorescence at 420 nm is due to the neutral form, but upon contact with acid a shoulder develops in the region of where the protonated monocation species emits (i.e. 560 nm). This change in absorption is observed more clearly when the excitation wavelength is set at 540 nm, as in Plot B.

2.3.3.6 Exploratory Diffusion Studies By Fluorescence Spectroscopy

A number of preliminary diffusion studies were done by the proposed method. Although many of the dyes under various conditions were used for these studies, only some of the spectra are shown. **Figure 2.39 (A-B)** shows the fluorescence spectra of 0.02 M l-DSB obtained from the reference and imaged sample as a function of storage time. Both samples were initially irradiated for the same amount of time, one with a blank mask, and the other with an imaged (1 μm lined mask). The samples were then stored in a closed container for the same amounts of time and compared for their changes in fluorescence spectra.

Although experiments were done with each PAG (**7-9**), only the results for **9** are shown. The use of this PAG was most favorable because it yields the smallest acid i.e., HBr and thus would be the easiest to diffuse within the polymer matrix. The other PAGs studied yield methanesulfonic and camphorsulfonic acid for **7** and **8** respectively.

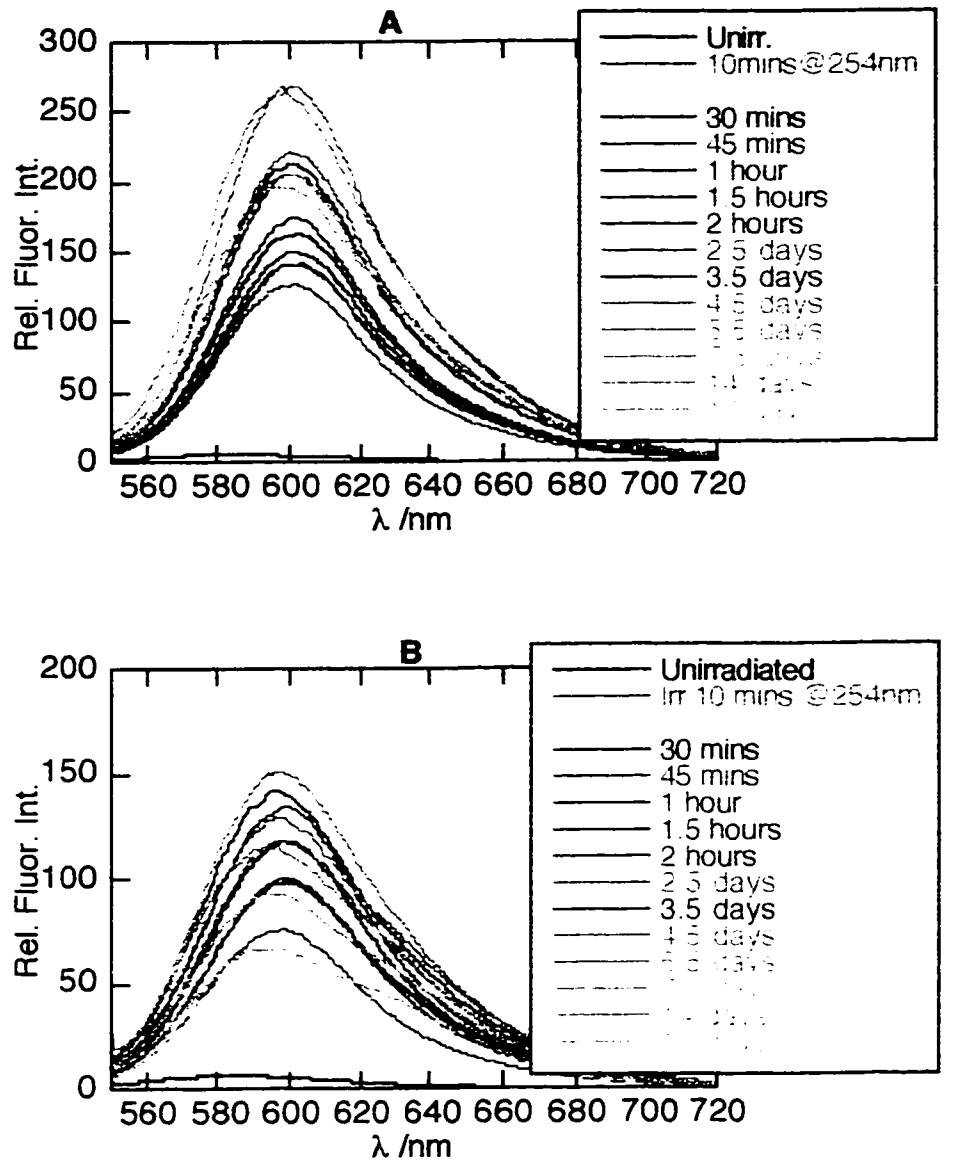

Figure 2.39: Diffusion experiment conducted at RT. The fluorescence spectra of **A**) the reference and **B**) the imaged sample were recorded at every storage interval to detect the change in fluorescence of the monocation (λ_{ex} 540 nm). Both consisted of 0.02 M I-DSB with 0.062 M **9** in 25% PHS (diglyme) films. The samples were irradiated with the blank and 1 μm mask windows when irradiated at 254 nm.

As expected, the results show that the imaged sample has approximately half the fluorescence intensity as that of the blank sample. This is expected because in the imaged sample only half the surface is being exposed as compared to the blank sample. Thus acid is only generated where the light has reached the sample, resulting in a fluorescence signal at 540 nm. Although, this initial result was good, there were some inherent problems that we came across. Both samples seemed to be fluctuating in their fluorescence intensity. This was observed by calculating the ratio of the intensity at the λ_{max} (540 nm) of the two samples. Although the ratio generally increased upon subsequent storage times, there was an erratic behavior of the trend. This was attributed to the sample not being placed in the fluorimeter exactly at the same position. Experiments at 120°C were also done but also resulted in such fluctuations. To remedy this problem, a time drive experiment was conducted to see how the fluorescence would change for a stationary sample. **Figure 2.40** shows the fluorescence intensity at 540 nm as a function of storage time.

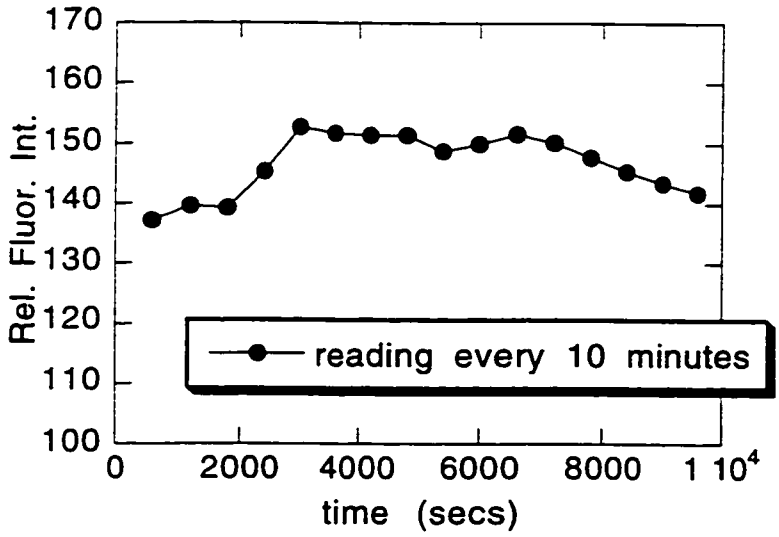

Figure 2.40: Plot obtained from the time drive experiment. The sample consisted of DSB with 0.062 M **9** in a 25% PHS/diglyme matrix. The sample was imaged with 1 μm lines with an irradiation time of 4 min. at 254 nm using the irradiation box.

This set-up seems favorable in the sense that the sample is not moved. However, by doing the experiment this way, a direct comparison to a reference sample cannot be made. The samples can be done one at a time, but the exact experimental conditions do not remain the same.

Furthermore, **Figure 2.40** shows that the fluorescence intensity of the sample initially increases, as expected, but then decreases. A number of experiments that were done with DSB and l-DSB showed that the sample seemed to undergo photodegradation or some other effect that led to the decrease in fluorescence intensity. Although, the samples were kept in closed containers, a noticeable decrease was observed. This effect was clearly seen in an experiment done with 0.002 M DSB with **9**. The sample was irradiated for 30 sec and spectra recorded. A continuous decrease in spectra was observed upon every measurement and the ratio of the fluorescence intensities did not follow the expected trends.

Initially experiments were done with 0.02 M dye but to ensure that the acid generated is in higher ratio than the amounts of dye present we had to lower the concentration of dye added. Although the lower concentrations led to noisier absorption spectra, fluorescence spectra with good signal-to noise were obtained.

Because of these results, other dyes were used for such diffusion experiments. **Figure 2.41** shows the results obtained by using Coumarin-6. Although DMBB was also used the results are not shown.

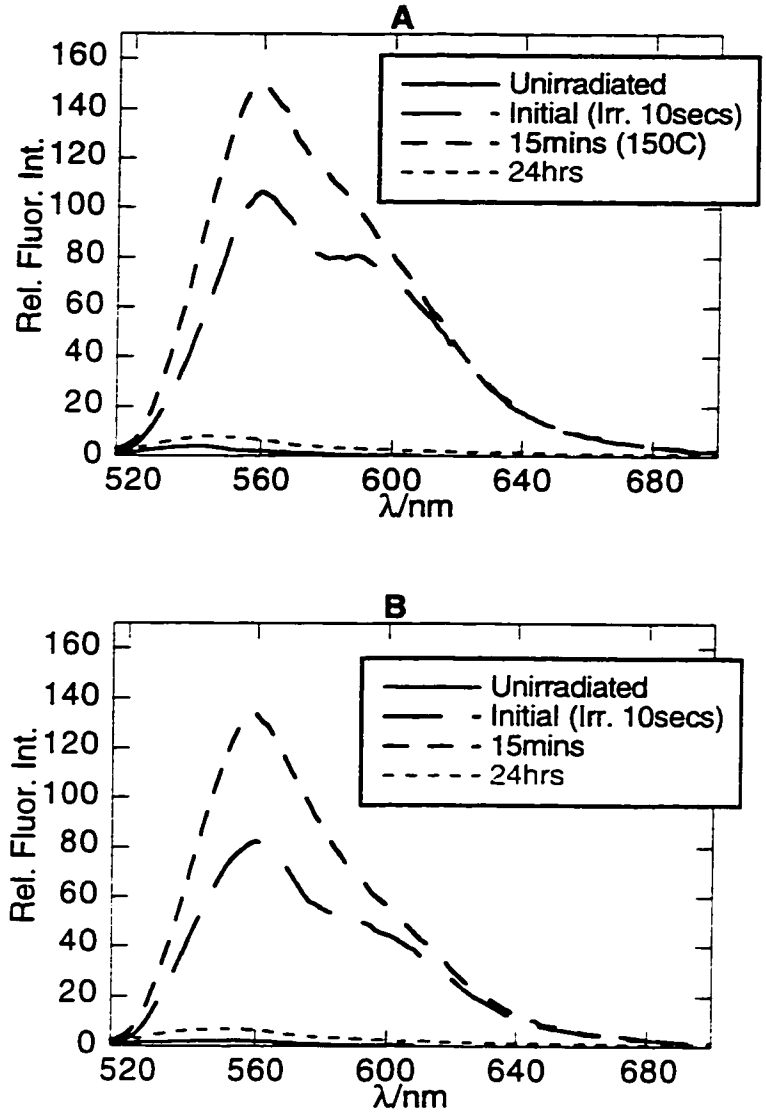

Figure 2.41: Diffusion experiment at 150°C. Fluorescence spectra of the A) reference and B) imaged sample were recorded at various intervals (λ_{ex} 535 nm). The samples were stored at 150°C in-between measurements. Samples consisted of 0.002 M Coumarin-6 with 0.062 M **9**. Samples were irradiated at 254 nm using the HTG unit for 10 sec (with either the blank or 1 μm lined mask placed on top).

These results were favorable, in the sense that a greater increase in fluorescence intensity of the imaged sample occurred. The blank sample only increased by 30%, whereas

the imaged sample increased by about 69%. This follows the trends that are expected from such experiments. However, the problem with this particular experiment was that at longer storage times at higher temperatures, the acid is lost from the film. The results from **Figure 2.41** show that after 24 hr. of storage, the acid was lost resulting in the decrease in fluorescence intensity at 560 nm, i.e., the dye reverts back to its unprotonated form. This effect was lessened when **7** and **8** were used.

Overall, these diffusion experiments were done as an initial test to determine the feasibility of such work. In the above work, problems of photodegradation and sample placement in the instrument were major restrictions. Another problem was that for the experiments done at higher temperatures the sample had to be removed every time. To rectify this problem, a built in temperature-controller has been built by Gerry Charette in our lab. This will allow samples to remain in the fluorimeter and be subjected to the higher temperatures as well. In terms, of the photodegradation of the dyes, additional dyes are being researched in our lab in the search for the perfect dye. In the meantime, some of the other dyes that were mentioned in this work could be used for such diffusion experiments.

2.3.3.7. Images Observed with Fluorescence Microscope

Figure 2.42 shows some of the photographs obtained by generating different sizes of images into the dye/polymer sample. These results are important because they indicate that such lines can be produced by this method, and that by the use of acid-sensitive dyes, the exact positions of the irradiated and non-irradiated regions can be observed. The figure shows that lines of varying thickness can be achieved by this method. We were able to achieve lines as small as 1 μm. Furthermore, the figures that have a plaid pattern were prepared in the same way but upon irradiation were irradiated in one direction and were rotated 180°C and irradiated again for an additional amount of time. The sample was irradiated in each direction for half the amount of time, i.e., 45 sec. in one direction and then 45 sec. rotated 180°C. By further

experiments, we hope to actually see the disappearance of these lines as a result of diffusion. In this work, experiments were done at 150°C to see if the lines would disappear before and after storage at 150°C. Upon viewing the samples under the fluorescence microscope the lines seemed to have broadened and faded. Although, photographs were taken of these, it is hard to see this effect from the pictures obtained.

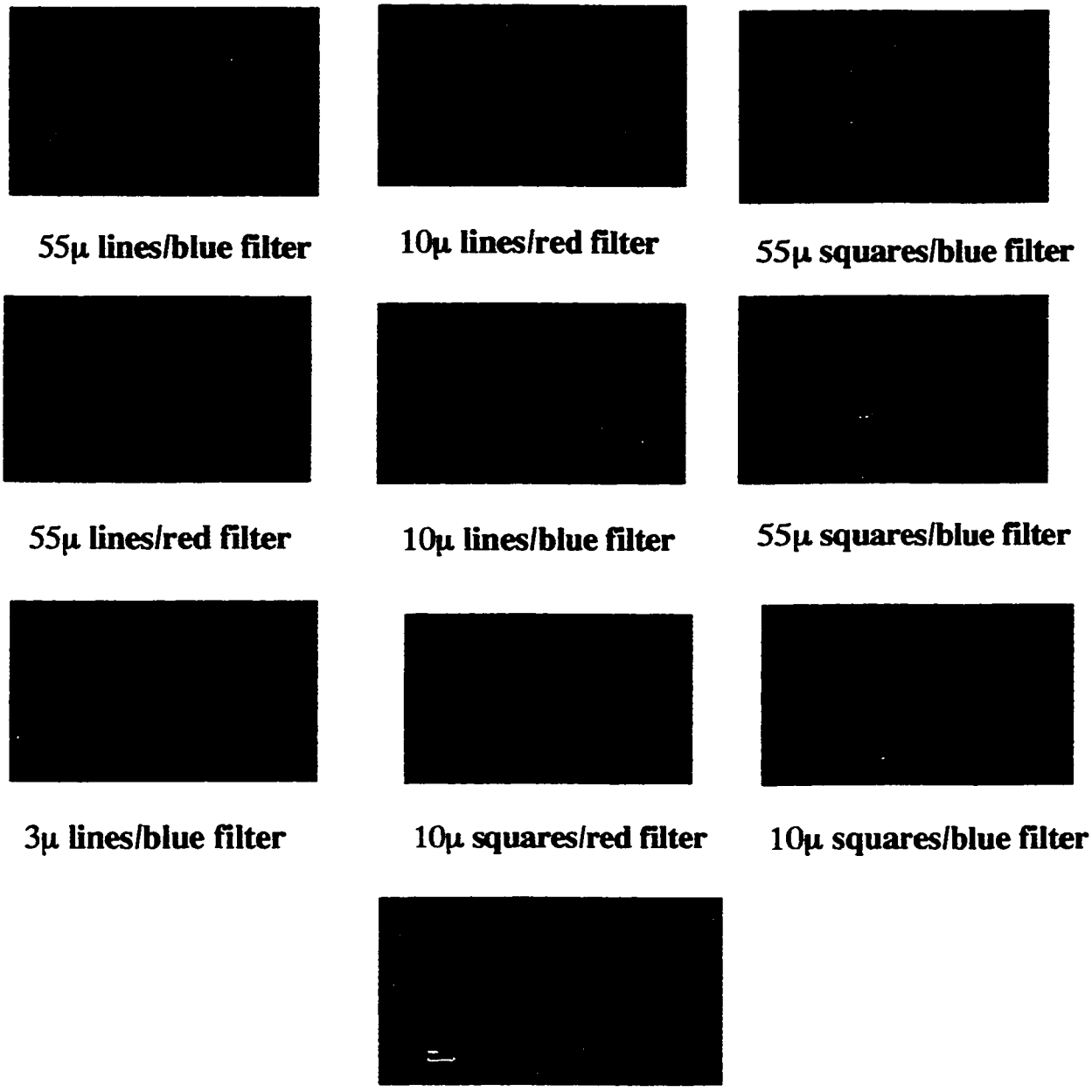

Figure 2.42: Scanned DSB/PAG/PHS film images obtained from the fluorescence microscope. Film samples were irradiated at 254 nm for 1.5 minutes and observed under the fluorescence microscope using a blue and a red filter.

2.4. Conclusions

In conclusion to all these studies, a number of comments and future considerations can be made with regards to monitoring diffusion in thin polymer films by the proposed method. For purposes of studying acid diffusion by fluorescence spectroscopy and microscopy, a specific criteria is needed for the ideal acid-sensitive probe. In this work, a number of compounds were studied to determine which would most ideally follow these parameters. The three categories of dyes studied were the aromatic monazines: specifically 2-phenylpyridine, 2-phenylquinoline and acridine: the xanthene dyes; fluorescein and rhodamine B base; and the benzothiazole derivatives; DSB, l-DSB, Coumarin-6, DSBS, DMBB, and a few others. By doing extensive absorption and fluorescence studies of each of the dyes, a great deal of insight has been obtained on the behavior of these dyes in film.

An investigation of the spectral properties of 2-phenylpyridine, 2-phenylquinoline and acridine in diglyme indicated that these aromatic monoazines can be protonated by p-toluenesulfonic acid in diglyme. The observed spectral changes and the increase in fluorescence quantum yield upon protonation make these compounds suitable sensors to monitor photoacid generation in PMMA films by fluorescence spectroscopy. 2-Phenylquinoline and acridine proved to be superior to 2-phenylpyridine, mainly because of the poor absorption / fluorescence characteristics of the latter which makes it unsuitable for an application in the phenolic polymers which are of industrial importance. Furthermore, acridine seems to be more favorable than 2-phenylquinoline because, the fluorescence of the protonated form does not overlap with the fluorescence emission of the polymer PHS.

The use of rhodamine B base and fluorescein are more favorable in the sense that the spectral ranges of these dyes do not overlap with the fluorescence of phenolic polymers. Furthermore, it is seen that both these dyes have a high fluorescence quantum yield and exhibit a significant change in absorption characteristics upon protonation if film. Also, both have a

high extinction coefficient. For purposes of this work, a high extinction coefficient at the excitation wavelength is needed to get a good signal-to-noise ratio in the thin polymer film. This problem cannot be solved by just increasing the sensor concentration since the acid consumption by the sensor cannot exceed a certain limit without influencing the effectiveness of the crosslinking process. In terms of these criteria, both fluorescein and rhodamine B base are quite good.

However, the problems with these xanthene dyes is that their lactone forms seem to open in PHS polymers. This opening results in an absorption at the wavelength of interest before any acid has been added or generated. This problem is more extreme for rhodamine B base due to its higher sensitivity to acid and thus the opening of the lactone form in PHS leads directly to the cationic form of the dye. For fluorescein, the initial absorption is quite small, and thus can be corrected for when monitoring the change in absorption spectra upon addition or generation of acid. In PMMA, both these dyes appear to be ideal sensors. The vertical diffusion experiment conducted with rhodamine B base indicated that it is an extremely sensitive dye. For this reason, both rhodamine B base and fluorescein can be used in PMMA to monitor diffusion as a comparison to the results obtained in PHS with other dyes.

The third set of dyes that were studied were the benzothiazole derivatives. These dyes are probably the most favorable of the three groups because they lead to a red-shift in absorption upon protonation. This phenomenon allows for the selective excitation of the protonated form, and thus, either the neutral or protonated forms can be monitored exclusively at specific wavelengths. In terms of the diffusion experiments proposed in this research, this is ideal because either the neutral or protonated forms can be monitored for changes in fluorescence intensity upon imaging. Upon imaging a 1 μm (or other size) lined dye/PAG/polymer sample, the neutral form can be monitored for a decrease in fluorescence or the protonated form for an increase in fluorescence upon subsequent storage times. Although,

most studies were done with DSB, 1-DSBS, DMBB, and Coumarin-6, some other dyes have been studied for their absorption and fluorescence properties. These included HSB, PSB, TSB and MBB. Either these or new dyes may possibly be studied for future research

Overall, the research conducted here indicated that the presence of acid can be monitored in thin polymer films of PHS and PMMA by the use of acid-sensitive probes. The overall objectives of this research was to set-up different probes that could be used for further diffusion experiments such that diffusion coefficients could be obtained. The initial diffusion work in this research indicates that the proposed method is quite feasible. The experiments done with DSB, 1-DSBS, DMBB, Coumarin-6 indicate that upon imaging a sample and comparing it to a reference, the fluorescence of the imaged sample is half as was expected. To conduct the proposed diffusion work, the initial ratio of fluorescence of the imaged to the reference sample should be half. This ratio should approach one upon subsequent storage times. The opposite holds true, if the fluorescence of the neutral form is monitored, i.e., the ratio will approach zero. The diffusion work conducted in this research showed that the general trend in the ratio approached one. This indicates that the acid in the imaged sample is diffusing, whereas, the reference sample remains constant.

In comparison to other studies on acid diffusion that have been done in film, we conclude that our method is better. Mckean *et al.*[32] employed acid-sensitive dyes, specifically the merocyanin dye to quantify acid in polymers by dissolving the polymer in a solution of dye. They obtained their diffusion coefficients by an acid diffusion model based on catalytic chain length. Since this model is based on an assumption, a correct representation of actual acid diffusion may not be achieved. Our study meets these requirements in the sense that acid-sensitive probes are being used to quantify the acid directly in the polymer. The study by Ohmori *et al.*[33] was similar in the sense that they reported a method for monitoring the migration of acid molecules in polymer matrices. They used an acid-catalyzed rearrangement

reaction to be able to monitor changes in absorption spectra. Specifically they used propargyl alcohol which gives an enone in acidic media, which subsequently leads to a change in UV spectra. Their study was different in the sense that they were limited to PMMA films. Furthermore, they used absorption spectroscopy whereas we used the more sensitive fluorescence microscopy. The study by Zhang *et al.*[30] used the pH-sensitivity of fluoresceinamine to monitor diffusion in film. However, they used acid vapor to quench the intensity of their pH sensor. Our study remains to be superior in the sense that we use the actual photoacid generation within the film that occurs upon irradiation. Furthermore, our study remains unique in the sense that we are able to observe the diffusion of the lines we generate by the use of these fluorescent probes. This is achieved by imaging the samples and then subsequently observing the lines under a fluorescence microscope for diffusion of the image.

Our vertical diffusion studies indicate that the use of acid-sensitive probes is an ideal way to conduct such an experiment. Other studies have looked at acid transfer between two polymer films by the use of acid-sensitive dye. However our study is unique in the dyes that we used. The other studies have been done with the use of the dye TBPB[34-37], however, the dyes used in our research are more favorable because they are more photostable. The results obtained in this study indicate that in addition to horizontal diffusion (i.e., diffusion between the boundaries of image and non-image), vertical diffusion or "acid loss" also occurs. Furthermore, the use of acid-sensitive dyes proves to be quite an ideal and sensitive technique.

Overall, the results obtained in this thesis have favorably moved toward being able to monitor diffusion in thin polymer films. The next step in this research is to obtain actual diffusion coefficients. For purposes of this M.Sc. thesis, these coefficients were not obtained. However, future studies within our lab will aim to obtain such diffusion coefficients. Either the method proposed in this thesis or by other methods that are being developed will be used.

References

(1) Mckean, D. R.; Schaedeli, U.; MacDonald, S. A. *J. Polym. Sci.: Part A Polym. Chem.* **1989**, *27*, 3927.

(2) Carey, W. P.; Jorgensen, B. S. *Appl. Spectrosc.* **1991**, *45*, 834.

(3) Pohlers, G.; Virdee, S.; Scaiano, J. C.; Sinta, R. *Chem. Mater.* **1996**, *8*, 2654.

(4) Mataga, N.; Tsuno, S. *Bull. Chem. Soc. Jpn.* **1957**, *30*, 368.

(5) Weller, A. Z. *Elektrochem.* **1957**, *61*, 956.

(6) Bowen, E. J.; Holder, N. J.; Woodger, G. B. *J. Phys. Chem.* **1962**, *66*, 2491.

(7) Kasama, K.; Kikuchi, K.; Yamamoto, S.; Uji-ie, K.; Nishida, Y.; Kokubun, H. *J. Phys. Chem.* **1981**, *85*, 1291.

(8) Diverdi, L. A.; Topp, M. R. *J. Phys. Chem.* **1984**, *88*, 3447.

(9) Kubin, J.; Testa, A. C. *J. Photochem. Photobiol. A: Chem.* **1994**, *83*, 91.

(10) Ueno, T.; Schlegel, L.; Hayashi, N.; Shiraishi, H.; Iwayanagi, T. In *SPE Regional Technical Conference on Photopolymers: Principles-Processes and Materials*; Society of Plastics Engineers Inc.: 1991; pp 121.

(11) Zanker, V. *Chem. Ber.* **1958**, *91*, 562.

(12) Sjoback, R.; Nygren, J.; Kubista, M. *Spectrochim. Acta Part A* **1995**, *51*, L7.

(13) Markuszewshi, R.; Diehl, H. *Talanta* **1980**, *27*, 937.

(14) Birks, J. B. *Photophysics of Aromatic Molecules*; Wiley-Interscience: New York, 1970.

(15) Ware, W. R.; Rothman, W. *Chem. Phys. Lett.* **1976**, *39*, 449.

(16) Pohlers, G.; Scaiano, J. C.; Sinta, R. *Chem. Mater.* **in press**,

(17) Huth, B. G.; Farmer, G. J.; Kagan, M. R. *J. Appl. Phys.* **1969**, *40*, 5145.

(18) Gaviola, E. *Z. Physik* **1927**, *42*, 862.

(19) Drexhage, K. H. *Topocs in Applied Physics, Vol. 1*; Springer: Berlin, .

(20) Drexhage, K. H. *Laser Focus* **1973**, *9*, 35.

(21) Diehl, H.; Horchak-Morris, N. *Talanta* **1987**, *34*, 739.

(22) Kubista, M.; Sjoback, R.; Nygen, J. *Anal. Chim. Acta* **1995**, *302*, 121.

(23) Martin, E.; Pardo, A.; Guijarro, M. S.; Fernandez-Alonso, J. I. *J. Mol. Str.* **1986**, *142*, 197.

(24) Klein, U. K. A.; Hafner, F. W. *Chem. Phys. Lett.* **1976**, *43*, 141.

(25) Faraggi, M.; Peretz, P.; Rosenthal, I.; Weinraub, D. *Chem. Phys. Lett.* **1984**, *103*, 310.

(26) Ferguson, J.; Mau, A. W. H. *Aust. J. Chem* **1973**, *26*, 1617.

(27) Arbeloa, I. L.; Ojeda, P. R. *Chem. Phys. Lett.* **1981**, *79*, 347.

(28) Arbeloa, I. L.; Ojeda, P. R. *Chem. Phys. Lett.* **1982**, *87*, 556.

(29) Sadkowski, P. J.; Fleming, G. R. *Chem. Phys. Lett.* **1978**, *57*, 526.

(30) Zhang, P. L.; Eckert, A. R.; Willson, C. G.; Webber, S. E.; Byers, J. *SPIE Adv. Res. Tech. & Proc.* **1997**, *3049*, 898.

(31) Pohlers, G.; Skene, W.; Scaiano, J. C.; Sinta, R. **to be published**,

(32) Mckean, D. R.; Allen, R. D.; Kasai, P. H.; Schaedeli, U. P.; MacDonald, S. A. *SPIE Adv. Res. Tech. & Proc.* **1992**, *1672*, 94.

(33) Ohmori, H.; Arimitsu, K.; Kudo, Y.; Ichimura, K. J. *J. Photopolym. Sci. and Tech.* **1996**, *6*, 25.

(34) Roeschert, H.; Eckes, C.; Endo, H.; Kinoshita, Y.; Kudo, T.; Masuda, S.; Okazaki, H.; Padmanaban, M.; Przybilla, K. J.; Spiess, W.; Suehiro, N.; Wengenroth, H.; Pawlowski, G. *Proc. of SPIE* **1993**, *1925*, 14.

(35) Thackeray, J. W.; Fedynyshyn, T. H.; Lamola, A. A.; Small, R. D. *J. Photopolym. Sci. Technol.* **1992**, *5*, 207.

(36) Thackeray, J. W.; Denison, M. D.; Fedynyshyn, T. H.; Kang, D.; Sinta, R. *ACS Symp. Ser.* **1995**, *614*, 110.

(37) Kihara, N.; Saito, S.; Ushirogouchi, T.; Nakase, M. *J. Photopolym. Sci. & Tech.* **1995**, *8*, 561.

Chapter 3

An On-Wafer Technique of Acid Quantification in Thin Polymer Films

3.0. Introduction:

Semiconductor microelectronic device manufacturers have been very successful in continuing to increase circuit densities. The increased density has been achieved by improvements in lithographic processing techniques, materials, and exposure tools which have permitted large reductions in the size of circuit elements [1]. A major focus in achieving these goals has been the incorporation of acid-catalyzed chemistry. Chemically amplified (CA) photoresists offer various outstanding properties with respect to photosensitivity, flexibility in resist design, and high resolution capability down to the quarter micron region [2].

Photoacid generation is of particular interest in chemically amplified systems. CA photoresist systems consist of a photoacid generating compound (PAG) and at least one acid sensitive derivative. In chemically amplified photoresist systems the photogenerated acid catalyzes the crosslinking or deblocking reaction to induce a solubility differential between the unexposed and exposed areas of the resist film [3]. Efficient photoacid generation is a very important factor in ensuring the success of a photoresist. Other factors, such as dissolution inhibiting/enhancing properties of the PAGs and the sensitizers can also have considerable effects on the overall performance of a resist but photoacid generation is of primary importance in chemically amplified systems [4]. This is true because the achievable photospeed for these photoresist formulations depends strongly on the efficiency of acid generation upon photolysis of the PAG. Photospeed is the rate at which the chemical reactions take place upon irradiation. It is a very important parameter when it comes to screening new compounds for PAG

efficiency in these formulations. For this reason a simple technique that enables quantification of the photogenerated acid in the photoresist would be extremely beneficial.

Quantification of acid in thin polymer films has proven to be a difficult and cumbersome task. A number of techniques exist but most involve quantifying the acid generated in film via a solution technique. One technique was the merocyanine dye technique used to quantify the acid efficiency of triphenylsulfonium salts [5]. This technique involved the irradiation of several resist-coated wafers and subsequent dissolution of the films. The quantification involves using merocyanine dye, which shows acid-sensitive visible absorption characteristics [5].

Similarly, another method previously used was the tetrabromophenol blue (TBPB) technique [4,6,7]. This was also a technique in which irradiated films were dissolved into a stock solution of the dye. Many solutions were prepared and the change in absorbance of TBPB at a given wavelength (610 nm) in the presence of acid was used to quantitatively monitor the amounts of acid generated. In order to correlate the amount of acid generated with the change in optical density of the TBPB, a calibration curve was required in which known amounts of acid were added to the dye and the change in optical density monitored by UV-Vis spectroscopy. As a result, a plot of absorbance vs. moles of acid provided a means of detecting the quantity of acid generated from the PAG. Model resist formulations consisting of PAG in a polymer matrix were spun onto wafers, UV-irradiated, and subsequently extracted with a fixed amount of solvent and TBPB solution. The detection limit of this technique was determined to be about 10^{-8} moles of acid. The high sensitivity of this technique can be attributed to the large extinction coefficient of TBPB (e.g. 58000 $M^{-1}cm^{-1}$ in diglyme).

Although the TBPB technique appeared to be quite sensitive to changes in acid generation in solution, there are some inherent problems that do not accurately define acid generation in films. The fact that films had to be dissolved in solution and then measured for

acid production is quite cumbersome and impractical. An on-wafer technique of measuring photoacid generation is more desirable. However, TBPB cannot be used in films due to poor photostability, i.e., the dye cannot be irradiated with the photoresist sample without undergoing extensive photodegradation. For this reason, the development of dyes that can be used in films is essential for the purposes of acid quantification.

A conductivity method of detecting photoacid generation within the film exists[8]. Furthermore, an *in situ* technique of acid quantification employing laser techniques was also developed by our lab [9]. This method proved to be quite sensitive. However, due to the use of a laser flash photolysis set-up, this method requires a more complicated experimental set-up.

This research proposes an on-wafer technique of acid quantification in thin polymer films. It is similar to the TBPB technique in that absorption spectroscopy was used to monitor the changes in photoacid generation by using acid sensitive dyes. Unlike the TBPB technique, these dyes were incorporated into the photoresist samples such that *in situ* measurements were monitored. For purposes of this study, the dyes that were characterized and utilized to test the acid generating efficiencies of various PAG systems included Fluorescein, Coumarin-6, Rhodamine B Base, DMBB, and DSBS. The structures of these dyes are given in **Figure 3.1**.

An introduction to these dyes was given in **Chapter 2**. Many of the spectra, and changes due to the presence of acid are outlined in the previous chapter. Most of the work reported in this chapter was a continuation of the proposed research of this thesis but was partially conducted at Shipley Co., in Marlboro, Mass.

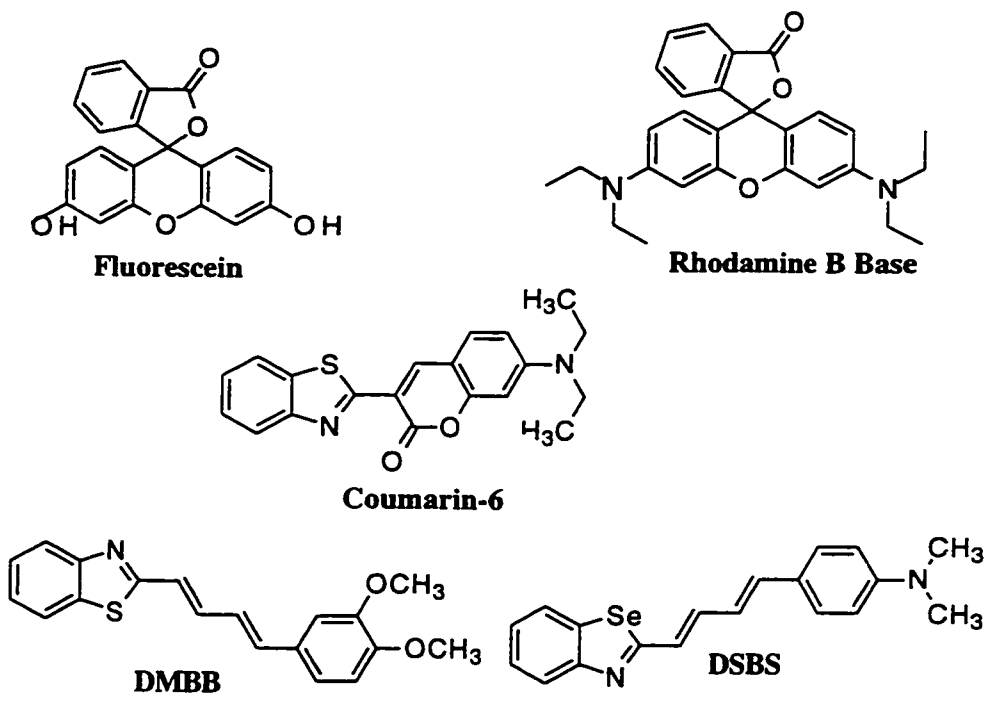

Figure 3.1: Structures of the dyes used.

These dyes can be utilized due to their changes in spectral absorptions upon protonation as discussed in **Chapter 2**. This change in protonation corresponds to an increase in acid production and thus a direct measurement of acid can be accomplished. The behavior of all five of these dyes have been studied in the previous chapter and the absorption (λ_{max}) values have been determined for the neutral, monocation and dication forms, depending on the dye structure. It was found that Coumarin-6 and DSBS form a dication in the presence of large amounts of acid. However, for purposes of this work, acid quantification does not reach sufficiently high acid concentrations to yield the dication. The changes in wavelength among the various prototopic forms of these dyes are summarized in **Table 3.1**.

DYE	$\lambda_{NEUTRAL}$	$\lambda_{MONOCATION}$	$\lambda_{DICATION}$
Rhodamine B Base*	NA	**560 nm**	
Fluorescein*	NA	**445 nm**	
Coumarin-6	**470 nm**	**530 nm**	**370 nm**
DMBB	**390 nm**	**460 nm**	
DSBS	**445 nm**	**370 nm, 590 nm**	**410 nm**

* Ring Opening Reactions

Table 3.1: Absorption wavelengths of the neutral and mono-protonated/diprotonated forms of 0.02 M dye in PHS or PMMA films.

3.1. Definition of Experimental Parameters

In order to conduct acid quantification experiments, a number of experimental parameters had to be defined. This analysis was necessary to be able to monitor the behavior of the dyes to see which ones would withstand the effects of photoresist processing. The parameters tested included: the background absorbances of the dye, solvent solubility, thermal stability, photostability, acid sensitivity, and compatibility with different polymers. These experiments were done to identify which dyes would behave suitably for acid quantification purposes under various conditions. In essence, the ideal dye would be thermally stable to withstand the baking process, photostable to withstand the irradiation process, sensitive enough to monitor the effects of acid generation, easily soluble in the solvents used in photoresist preparation, and compatible with the polymers used.

The next step involved the determination of acid calibrations of each dye with known amounts of acid. This would enable the detection of the changes in the absorption spectra of each dye. Subsequently, by monitoring the linear growth in absorbance at the λ_{max} of the

protonated forms, the sensitivity of each dye to the presence of acid (strong and weak) could be obtained.

Once the calibrations were done, it was easy to compare the efficiencies of acid generation for various PAG systems by comparing the rates of acid production for each PAG. In this work, a number of PAG systems were compared to test the validity of this acid quantification technique. This involved the comparison of photoefficiencies of various PAGs within the same family, as well as with other families of PAGs.

Experiments were also conducted to test the effects of changing the polymer matrix on photoacid generation. Also, acid loss experiments were done to compare with results obtained with the TBPB dye. This experiment was done to test the accuracy and sensitivity of these dyes in comparison to the TBPB dye.

3.2. Experimental:

3.2.1. Materials

Polymethylmethacrylate (PMMA), 2-methoxyethyl ether (diglyme), ethyl lactate, rhodamine B base, fluorescein, and Coumarin-6 were obtained from Aldrich. DSBS and DMBB were provided by Gerd Pohlers. Polyhydroxystyrene (PHS), photoresist compounds and all the PAGs were provided by Shipley Co.

3.2.2. Experimental Parameters

3.2.2.1. Solvent Solubility Characteristics

The solubility of each dye was tested in 2-methoxyethylether (diglyme) and ethyl lactate. Although, diglyme is a superior solvent in terms of its solubility characteristics, commercial photoresist samples are presently made in ethyl lactate. In the past, diglyme was the main solvent used in the preparation of photoresist formulations but due to its toxicity,

industry has switched to the less toxic solvent ethyl lactate. For purposes of acid quantification experiments were done in diglyme. Since industry currently uses ethyl lactate, the solubility of dye in both solvents is essential. In this work, 0.02 M dye concentrations were prepared in polymer solutions of 25% w/v PHS. For rhodamine B base the polymer used was 15% w/v PMMA.

3.2.2.2. Background Dye Absorbance

To identify the background absorbances of each dye, solutions of varying concentrations were analyzed. Solutions were made by adding increasing amounts of dye to solutions of 25% w/v polyhydroxystyrene (PHS) or 15.8% w/v polymethylmethacrylate (PMMA) in diglyme depending on the compatibility of the dye, i.e., rhodamine B base can only be analyzed in PMMA due to the opening of the lactone form, as discussed in **Chapter 2**. A stock solution of 25% (by weight) PHS in diglyme was prepared and filtered with a 0.2 μm filter to remove any existing dust particles. In order to have constant viscosities and thus consistent film thicknesses of the two different polymer solutions, the PMMA solution was made at a lower weight percentage. A 15.8% (w/v) PMMA solution made in diglyme was prepared. This solution was also filtered with a 0.2 μm filter.

Fluorescein, DSBS, DMBB were made at various concentrations in PHS. All were soluble at concentrations of 0.01 M, 0.015 M, and 0.02 M (Note: these molarity calculations were all converted to moles when plotting the graphs) in the PHS solution. Coumarin-6 was only soluble at concentrations lower than 0.01 M. Therefore, solutions of the following molarities were prepared: 0.005 M, 0.008 M, and 0.01 M. Solutions of Rhodamine B Base were tested at 0.01 M, 0.015 M and 0.02 M concentrations. However, this dye had to be done in 15.8% PMMA/diglyme due to its lack of polymer compatibility in PHS (i.e., opening of the lactone ring to the protonated form in this matrix) as discussed in **Chapter 2.**

Fluorescein was the only dye to be studied in both matrices, for purposes of acid quantification. In PMMA, the solubility of fluorescein decreases. Therefore, concentrations lower than 0.01 M were analyzed for the linear absorbance increase in PMMA samples i.e., 0.005 M, 0.008 M, and 0.01 M.

For all solutions, samples were prepared and spin-coated into thin polymer films for analysis. Samples were spin-coated onto 1 inch quartz disks at 3000 rpm for 20 sec., baked at 90°C, weighed, and analyzed by the Varian CARY-3 UV-Visible Spectrophotometer. Each sample was baked at 90°C on a hotplate for 1 minute because previous experiments had indicated that a 1 minute baking time on the hotplate was sufficient time to evaporate any remaining solvent. Samples were then weighed on an analytical balance to determine the weight of the film. The weight of the film was simply obtained by subtracting the weight of the uncoated quartz disk from the final weight of film and disk. Each sample was measured for film thickness using a Sloan Dektak IIA. Approximately three thickness trials were done for each film and then averaged. Typical film thicknesses were in the range of 0.72-0.82 μm for PHS films and 0.77-0.82 μm for PMMA films. Samples were scanned in the UV-Vis region of 200-700 nm and referenced to air. Spectra were recorded for each sample. Absorption values at wavelengths 248 nm, 254 nm, and corresponding protonated wavelength (λ_{max}) of each dye were recorded.

3.2.2.3 Thermal Stability

All dyes were tested for thermal stability. Fluorescein, DMBB, DSBS, rhodamine B Base solutions (0.02 M) and Coumarin-6 (0.01 M) incorporated into 25% PHS matrix or 15.8% PMMA (for rhodamine B Base) and spun onto one inch quartz disks. Samples were spun at 3000 rpm for 20 sec. and baked on a hotplate at increasing temperatures. The temperatures were 90°C, 100°C and 110°C for 60 sec.. Absorption spectra were recorded for each sample and the absorbance values at 248 nm, 254 nm, and the wavelengths of the

unprotonated and protonated forms of the dye (see **Table 3.1**) were recorded. Spectra were analyzed for thermal degradation characteristics, i.e., any decrease or change in the absorption spectra.

3.2.2.4. Photostability of Dyes

All dyes were also tested for photostability. Samples of each dye in 25% PHS matrices or 15.8% PMMA (for rhodamine B Base) were spun and baked at 90°C for 60 seconds on a hotplate. Each sample was then irradiated for varying times at 254 nm using a HTG imaging unit using a Hg/He arc lamp. Absorption spectra were recorded for each sample. At 248 nm, 254 nm, and the wavelengths of the unprotonated and protonated forms of the dye (see **Table 3.1**) absorbance values were recorded. Spectra were analyzed for photodegradation upon increasing amounts of irradiation at 254 nm. Samples were irradiated both with and without a 254 nm band-pass filter.

3.2.3. Calibration of Dyes:

In order to be able to quantify the acid generating efficiencies of the PAG samples, the "sensitivity" of each dye in a polymer matrix had to be obtained. This was done by preparing a stock solution of each dye in 25% PHS or 15.8% PMMA and adding increasing amounts of acid. The dye concentration in most cases was 0.02 M but varied with those dyes that were less soluble. Approximately 12-15 samples of varying acid concentrations with each dye were prepared. Usually, a concentration of 0.01 M was used instead. These values were chosen according to **Table 3.2**. Both a weak acid (camphorsulfonic acid/CSA) and a strong acid (perfluorooctanesulfonic acid/PFOS) calibration were done to report any differences in using different strengths of acid. Many of the resulting absorption spectra have been shown in **Chapter 2**.

Initially, we planned to use triflic acid for the strong acid calibration, but because of its high volatility, its use proved difficult and inaccurate. For this reason PFOS was used instead. However, although samples of PFOS are easily prepared, at high acid concentrations PFOS samples result in poor film quality leading to ripples and bumps over the film surface. Although, this is a problem, the area of lower acid concentrations (i.e., the linear portion of the growth) are of prime concern and therefore, the higher concentrated samples can be disregarded.

Samples were spin coated, baked at 90°C, weighed, and absorption spectra recorded. Samples were scanned in the UV-Vis region of 200-700 nm and referenced to air. Both spectra at each concentration and absorption values at wavelengths 248 nm, 254 nm, and corresponding protonated wavelength(s) of each dye were recorded to monitor the increase in monocation (protonated) species of the dye.

3.2.3.1. Carboxylic Acid Sensitivity of Dyes

Rhodamine B Base, Fluorescein and Coumarin-6 were also used to test the sensitivity to carboxylic acids. DSBS and DMBB were not used due to lack of availability of dye. These experiments were done because the sensitivity to carboxylic acids is important in the photoresist industry since the polymers may contain carboxylic acid functionalities. Samples were prepared with increasing amounts of triphenylacetic acid. Samples were spin coated, baked at 90°C, and analyzed by UV-absorption. Samples were scanned in the UV-Vis region of 200-700 nm and referenced to air. Spectra at each concentration and absorption values at wavelengths 248 nm, 254 nm, and corresponding protonated wavelength(s) of each dye were recorded to monitor the increase in monocation (protonated) species.

3.2.4. Acid Quantification:

In order to study the acid generating efficiencies of PAGs, a number of PAG systems were studied. The first experiment involved looking at the effect of varying the anion of the PAG systems. This was done by comparing three photoacid generators (PAGs). An example of the type of PAG compared is shown in **Figure 3.2**. The structural name of this PAG is di-(4-t-butylphenyl)iodonium camphorsulfonate (**1**). The other PAGs could not be included due to the confidential nature of such compounds.

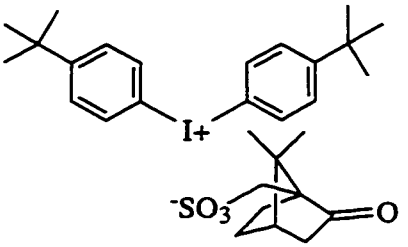

1

Figure 3.2: Structure of the PAG di-(4-t-butylphenyl)iodonium camphorsulfonate (**1**). Note: Structures of PAGs **2** and **3** could not be shown due to their confidential nature.

These PAGs all belong to the same family, differing only in the anionic component. The comparison of the PAGs was done with 0.02 M fluorescein in a 25% PHS matrix (the overall weight % of solids was 25.5%-fluorescein + PHS). A 1:1 molar dye/PAG loading was also utilized. The weight percent of **2** was 4.62%, for **1** it was 4.56%, and for **3** was 6.41%. Samples were prepared, spin coated as before, baked, weighed and absorption spectra recorded. Samples were then irradiated at 254 nm (with a 254 nm band-pass filter) for varying amounts of time, and subsequent absorption spectra were recorded until acid generation reached its plateau level. Doses up to 200 mJ/cm^2 (see **Appendix 1** calculation) were administered. The thicknesses of the films were also obtained. Absorption values at 248 nm, 254 nm, and 445 nm were recorded for each irradiation. Plots of dose (mJ/cm^2) vs.

absorbance/μm were plotted. The initial absorption of the unirradiated samples of PAG with dye in polymer was subtracted from subsequent irradiated values (i.e., data was normalized to zero). Using the weak acid (CSA) and strong acid (PFOS) "sensitivity values" for 0.02 M fluorescein in 25% PHS (see **Table 3.3**), the amount of acid generated at each dose was calculated via Beer's Law. Plots of individual results for each PAG were plotted. These were made by plotting dose (mJ/cm^2) vs. moles of acid, and dose (mJ/cm^2) vs. moles acid/moles PAG. A subsequent comparison of the three PAG efficiencies was done.

To test the effect of changing the ratio of dye/PAG, a 2:1 molar solution of 0.02M fluorescein and PAG **1** was also made. This solution had a 2.37% weight percent of PAG and a 2.52% weight percent of fluorescein. The 1:1 molar solution had a 4.62% weight percent of PAG and a 2.48% weight percent of fluorescein.

To further test, the acid generating efficiencies of different PAGs, different PAG classes were compared at 254 nm. The different PAGs that were compared were PAGs **1**, **4**, **5**, **6**, **7**. The PAGs **4**, **5**, **6**, **7** are depicted in **Figure 3.3**. PAG **5** generates perfluorooctane sulfonic acid (PFOS) upon irradiation at 254 nm and the PAGs **1**, **4**, **6**, **7** generate camphorsulfonic acid (CSA). Note: Other PAG classes were studied but due to their confidential nature could not be included in this thesis.

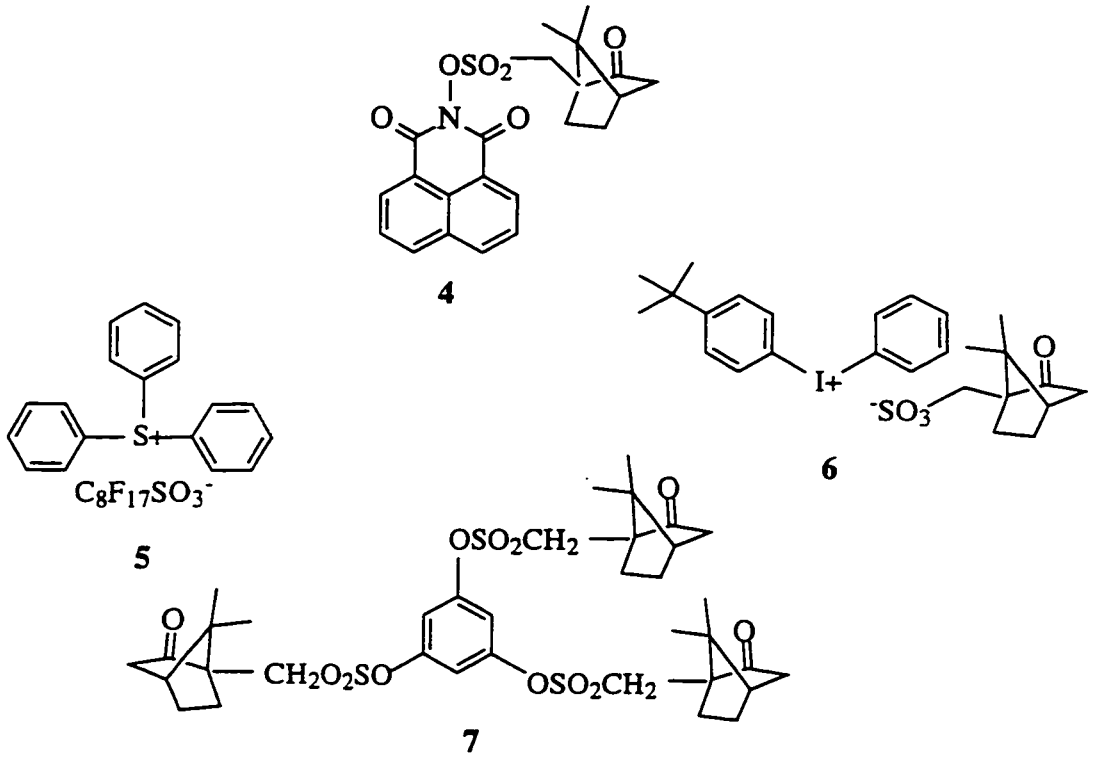

Figure 3.3: Structures of the different PAG classes

These PAGs were quantified using 0.01 M fluorescein in a 25% PHS matrix. This was done at this concentration such that a comparison could be made to samples evaluated in PMMA (i.e., fluorescein is only soluble at lower concentrations in PMMA). Again, all samples were made with a 1:1 molar dye/PAG loading.

Data were obtained and analyzed similar to before. Samples were spin coated onto 1 inch quartz disks, baked at 90°C, and absorption spectra recorded. Samples were scanned in the UV-Vis region of 200-700 nm and referenced to air. Both spectra at each concentration and absorption values at wavelengths 248 nm, 254 nm, and corresponding protonated wavelength(s) of each dye were recorded to monitor the increase in monocation (protonated) species.

Another set of experiments was done to compare matrix effects on acid generation efficiency. The first experiment involved comparing the photoacid generation of a PFOS PAG in both PHS and PMMA matrices. The PAG that was compared were **6** (see **Figure 3.3**). PAG samples were prepared as before with 1:1 molar dye/PAG loading. Data was obtained at various doses and plotted to compare the acid generating efficiencies of the two matrix systems.

Matrix effects were also compared by comparing the acid generation efficiency of a PAG (**2**) in a *p*-hydroxystyrene matrix versus a *m*-hydroxystyrene matrix. The backbone of each of these polymers is illustrated in **Figure 3.4** .

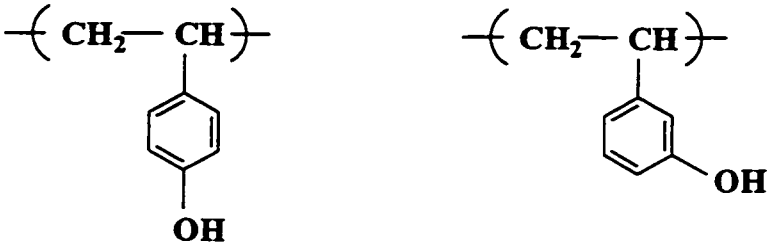

poly(PHS) "para" **poly(PHS) "meta"**

Figure 3.4: Structure of *p*-poly(hydroxystyrene) vs. *m*-poly(hydroxystyrene) backbones.

Samples were made using 0.02 M fluorescein in both cases. In each sample, the mole ratio of dye to PAG was matched. The amount of PAG added to the two polymers was also matched. Samples were prepared and analyzed as before.

3.2.5. Acid Loss Studies

The purpose of these experiments were to compare the values of acid loss obtained from the technique proposed in this work, to those that were obtained by the TBPB technique. The technique, similar to that discussed in **Chapter 2** is shown in **Figure 3.5**.

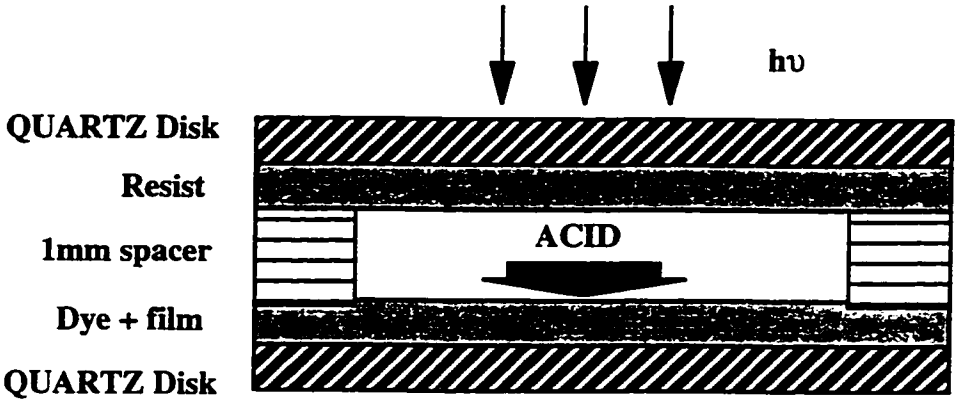

Figure 3.5: Diagram of the experimental method to quantify the acid loss from a resist.

The dye used for the capture layer was fluorescein, made in a formulation of 2.59% (weight percent of solids) in a 25% (by weight) solution of PHS made in diglyme. DMBB was also used since fluorescein does not dissolve in the solvents that were used for the TBPB method. The photoresists used were APEX-E-2408 and UVIIHS. Since direct comparison of the methods is required, the DMBB experiment was made to mimic the experimental conditions of the TBPB method. 2% DMBB was prepared in a polymer matrix of 10% partially hydrogenated PHS. The solvent used was propylene glycol methyl ether acetate (PGMEA). The experiment was conducted with and without a 254 nm band-pass filter to see if the results would vary.

3.3. Results and Discussion:

3.3.1. Experimental Parameters

In this work, each dye was studied to determine a number of experimental parameters and conditions under which the dye works most favorably. The results of the experiments are shown in **Table 3.2**. Once these conditions were determined they were utilized for the acid calibration and acid quantification experiments were carried out.

ACID QUANTIFICATION									
Dye	Polymer System	Range of Linearity (diglyme)	Solubility		Thermal-Stability	Photo-Stability 254 filter	Acid Calibration		
			Diglyme	Ethyl Lactate			Camphor Sulfonic	PFOS	Phenyl Acetic
Fluorescein (Red)	PHS PMMA	✓	0.02M 0.01M	x	<110°C	✓	✓ ✓	✓ ✓	not sensitive
DSBS	PHS	✓	0.015M		✓	✓	✓	✓	
DMBB	PHS	✓	0.015M	0.02M	✓	✓	✓	✓	
Coumarin-6	PHS	✓	0.008M		✓	✓	✓	✓	not sensitive
Rhodamine B Base	PMMA	✓	0.02M		✓	✓	✓	✓	sensitive

Table 3.2: Characterization of Rhodamine B base, Fluorescein, DSBS, DMBB and Coumarin-6 in terms of polymer used, solubility, photostability, thermal stability, acid calibration, sensitivity to carboxylic acid, linear absorbance increase as a function of concentration. Note: Check marks indicate that the experiment has been conducted. All other entries indicate the conditions concerning that dye.

The parameters described above will be discussed in more detail in the following sections.

3.3.1.1. Solubility of the Dyes

All dyes were soluble in diglyme, however, Coumarin-6 has a lower solubility than others. The same trend was observed in ethyl lactate where fluorescein also had a decreased solubility. Yellow fluorescein or the zwitterionic form of fluorescein has been shown to be more soluble than red fluorescein (*p*-quinoid structure) in ethyl lactate. However, all experiments done for purposes of this report were done in diglyme, and the solubility of red fluorescein is better in this solvent. Therefore, yellow fluorescein was not used. If experiments are required in ethyl lactate in the future, fluorescein can be easily converted from red fluorescein to yellow fluorescein by acidification and then reprecipitation[10]. Furthermore, by changing the matrix from PHS to PMMA, the solubility of all dyes also decreases.

For purposes of the acid calibration and quantification experiments, a concentration of 0.02 M dye was used in most cases, as a result of the solubility study. The DSBS and DMBB were used in concentrations of 0.015 M but these dyes are soluble at higher concentrations than this. Furthermore, Coumarin-6 was only soluble to concentrations of 0.01 M, so was used in concentrations of 0.008 M. Rhodamine B base/PMMA and fluorescein/PHS were used in concentrations of 0.02 M because they are quite soluble in diglyme. However, fluorescein was used a concentration of 0.01 M in PMMA/diglyme solution.

3.3.1.2. Dye Absorbance Range:

Spectra of each dye was recorded at each concentration. From these spectra the absorption value at wavelengths 248 nm, 254 nm and the wavelengths of the protonated forms of the dyes (see **Table 3.1**) were recorded. By plotting the points at each concentration (or moles of dye) as a function of Absorbance/μm, linear plots can be obtained showing the change of absorbance of the dye as a function of increasing the concentration. The absorbance at each of these wavelengths is important. Ideally the absorbance at 248 nm and 254 nm should be low enough, such that it will not interfere with the irradiation of the photoresist. Furthermore,

in terms of the neutral form of the dye, the initial absorbance recorded is also important. For fluorescein and rhodamine B base, it would be ideal for the neutral form to have a low absorbance. In terms of the other dyes that show a shift upon protonation, it is necessary that we have a high enough absorbance to get decent spectra. The results obtained are similar for all dyes. A representative plot of fluorescein absorbances recorded in PHS at the three concentrations are shown in **Figures 3.6**. Similar plots were obtained for the other dyes but are not shown here differing only in the moles of dye. The results show that all dyes seem to behave linearly upon increasing the concentration in a polymer matrix within the chosen concentration range. This indicates that any of the three

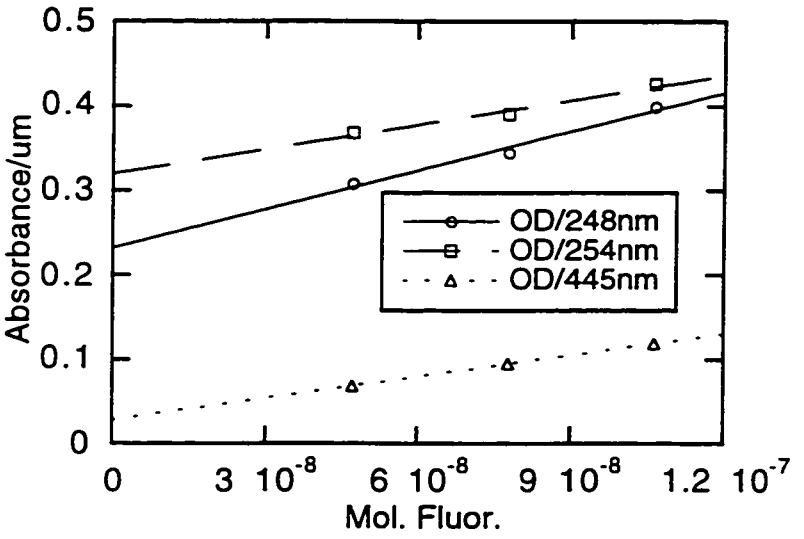

Figure 3.6: Plot of the change in absorbance of each fluorescein in 25% PHS as a function of concentration at three wavelengths: 248 nm, 254 nm, and λ_{max} (neutral form).

concentrations can be used for acid quantification studies. The middle range value was chosen for further studies. However, since only three points have been chosen, only an assumption of

linearity can be assigned. For fluorescein in PMMA, the result was not linear and therefore, lower concentrations had to be used.

3.3.1.3. Thermal Stability:

All dyes appeared to be thermally stable at these temperatures (90-130°C) except fluorescein which shows a slight broadening of its spectra if baked at temperatures greater than 110°C. **Figure 3.7** depicts the broadening the spectra of fluorescein upon baking at higher temperatures.

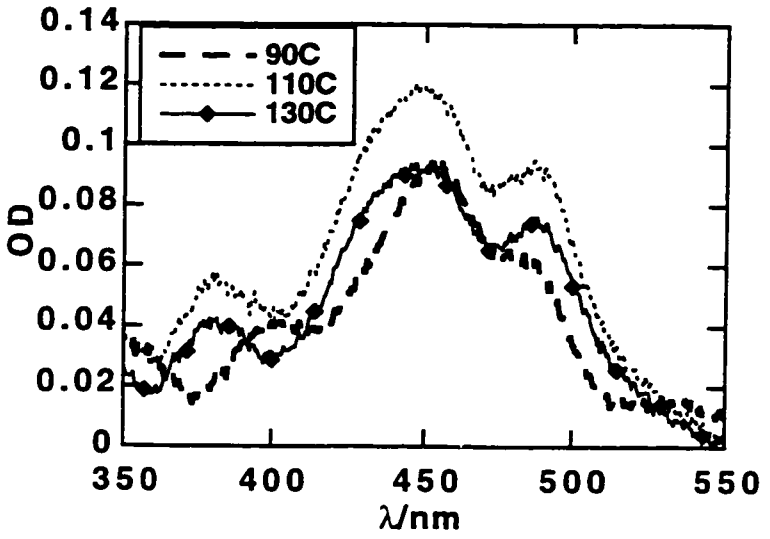

Figure 3.7: Broadening of the absorption spectra of 0.02 M fluorescein in a PHS polymer matrix at temperatures higher than 110°C and concurrent decrease in intensity at 445 nm. Samples were stored at each temperature for a few minutes.

These results indicate that the dyes can withstand the baking process. The only dye that showed an effect upon heating to higher temperatures, was fluorescein. At temperatures greater than 110°C, it showed a broadening in its spectra. The results of all other dyes indicate, that spectral changes do not occur at the temperatures studied.

3.3.1.4. Photostability:

Without using a 254 nm band-pass filter, DMBB appeared to be photobleaching upon irradiation. All other dyes did not show any significant change in spectral absorption upon longer irradiation times. When the band-pass filter was used, all dyes are photostable at the irradiation doses tested.

3.3.2. Acid Calibration

Upon protonation, each dye leads to changes at particular wavelengths (see **Table 3.1**). With increasing amounts of acid the absorption of the protonated form of the dye also increases. It is seen that the absorption of the cations of both fluorescein and rhodamine B base are markedly different from lactone forms, and thus result in a large bathochromic shift. The benzothiazole derivatives show a red shift upon protonation of the ring nitrogen.

For these experiments, each dye was monitored by absorption spectroscopy using a CARY spectrophotometer. The change in absorption at the wavelength of the protonated form was recorded and plotted against the moles of acid that was present. These values were calculated by knowing the weight of film and the weight percent of the acid in each sample. This plot of moles of acid vs. Absorbance/μm yielded values of "sensitivities (or slopes) " for both the strong and weak acid experiments. Basically, this plot is a calibration plot for which the photoacid generation of PAGs can be quantified. Although, these values were studied for all the dyes, we have shown representative plots of fluorescein in a PHS and PMMA matrices. The values obtained for all the other dyes are presented in **Table 3.3**. The calibration plots for fluorescein in PHS, for both strong and weak acids are given in **Figures 3.8 (A-C)**.

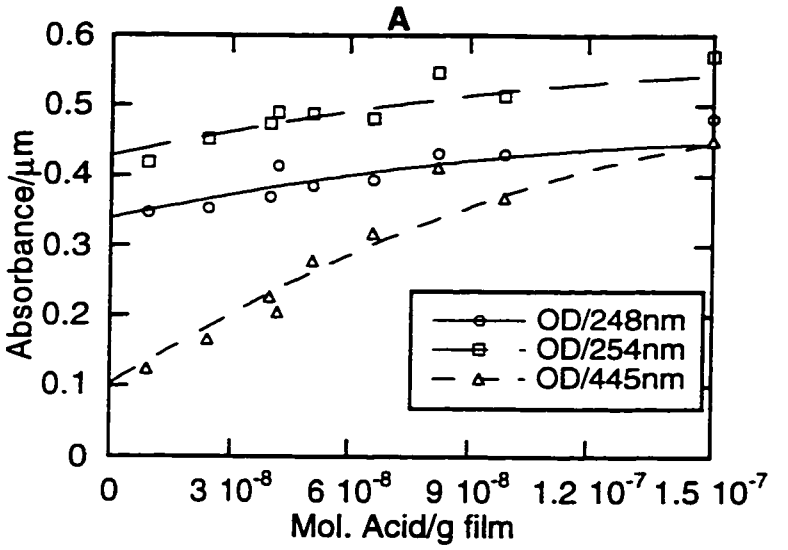
A
Absorbance/µm
0.6
0.5
0.4
0.3
0.2
0.1
0
0
3 10-8
6 10-8
9 10-8
1.2 10-7
1.5 10-7
Mol. Acid/g film
OD/248nm
- OD/254nm
- OD/445nm

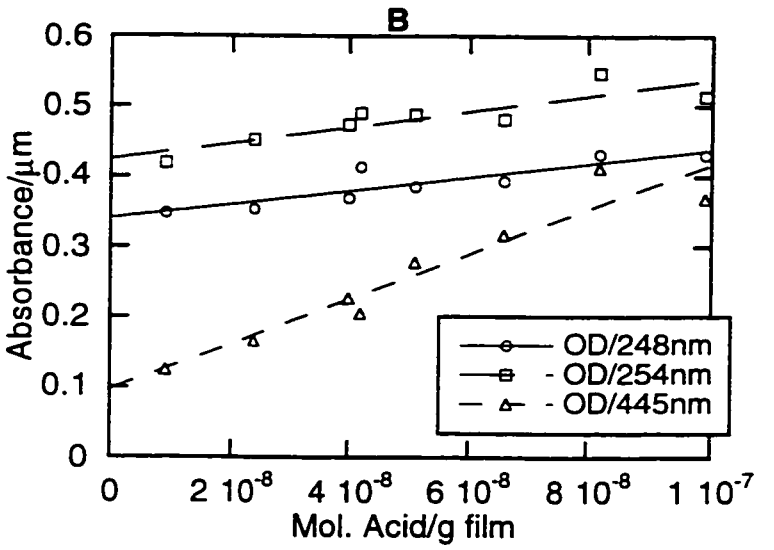
B
Absorbance/µm
0.6
0.5
0.4
0.3
0.2
0.1
0
0
2 10-8
4 10-8
6 10-8
8 10-8
1 10-7
Mol. Acid/g film
OD/248nm
- OD/254nm
- OD/445nm

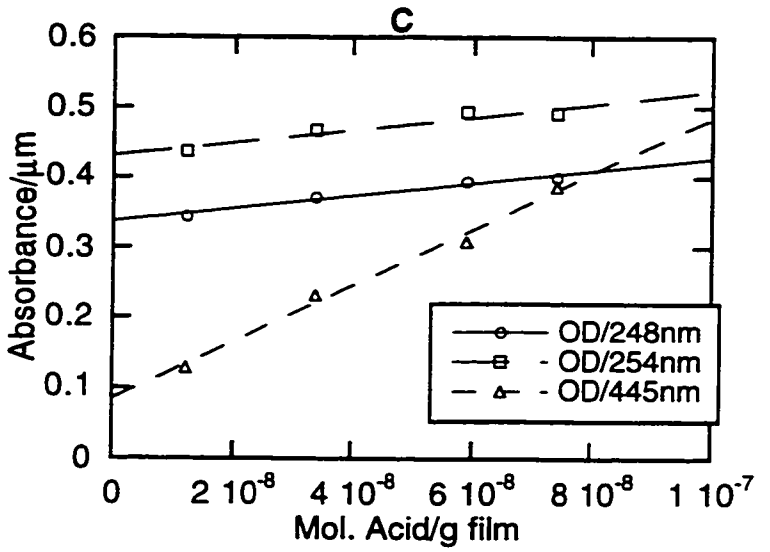

Figure 3.8: Acid calibration of 0.02 M Fluorescein in a 25% PHS matrix with **A)** & **B)** camphorsulfonic acid, and **C)** perfluorooctanesulfonic acid. Plot **A** shows the plateau region of the photoacid generation trend. Plots **B** and **C** and show the corresponding linear regions from which "sensitivities" can be compared. This value is 3.67×10^6 for the CSA calibration and for PFOS calibration is 4.08×10^6.

The calibration plots for fluorescein in PMMA, for both strong and weak acids are given in **Figures 3.9 (A-B).**

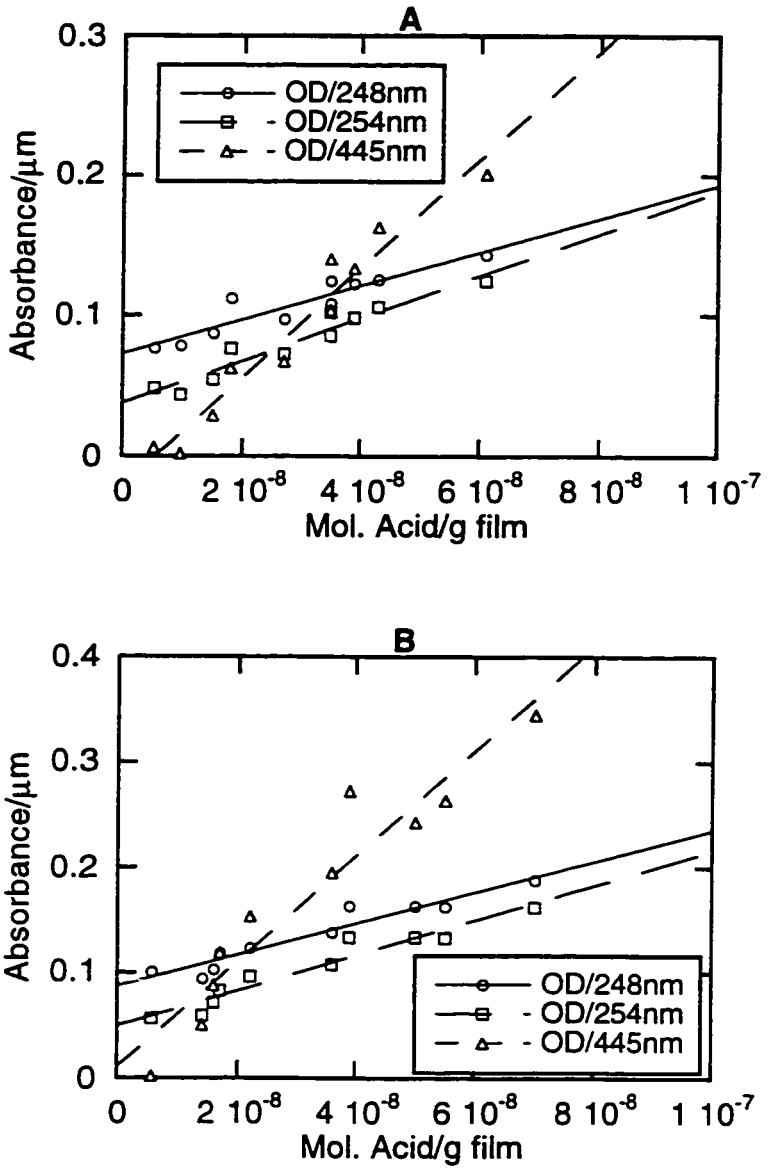

Figure 3.9: Acid calibration of 0.02 M Fluorescein in a 25% PHS matrix with **A**) camphorsulfonic acid, and **B**) perfluorooctanesulfonic acid. The sensitivity value is 3.56×10^6 for the CSA calibration and for PFOS calibration is 4.99×10^6.

To make such a plot, the absorbances obtained for each acid concentration were normalized to account for the differences in film thickness of each sample. Therefore, the absorbances are reported in absorbance per micron of film. Furthermore, in each case, moles

of acid were calculated by knowing the exact amount of acid relative to total weight of solids. By knowing the weight percentage of acid relative to the whole, the exact weight of acid was calculated from the weight of the film and then subsequently converted into moles of acid/per gram of film. A detailed description of this analysis is given in **Appendix 1**.

The representative "sensitivities" of each dye are shown in the Sensitivity Table (**Table 3.3**). For the DSBS samples, an "sensitivity" could not be obtained for the strong acid calibration due to precipitate formation in the solutions upon addition of PFOS. Similarly, rhodamine B base and camphorsulfonic acid in PMMA/diglyme lead to precipitate formation due to the insolubility of the protonated form (salt) of the dye. In all other cases, precipitate formation was not observed. Furthermore, the "sensitivities" between the strong acid and weak acid calibrations varied only to a small extent . The values obtained for fluorescein when comparing the PHS and PMMA matrices were also comparable. These values were close enough to assume that similar acid quantities can be detected, irrespective of whether a strong or weak acid is used. This similarity in values indicates that a true representation of acid quantification may be achieved.

3.3.2.1. Carboxylic Acid Sensitivity of Dyes:

Both fluorescein and Coumarin-6 were found not to be sensitive to the presence of carboxylic acid. The spectra did not show any change upon the addition of triphenylacetic acid. However, Rhodamine B Base showed an increase in absorption at 560 nm upon addition of triphenylacetic acid indicating a sensitivity to the presence of this acid. This increase in the protonated form of rhodamine B Base can be observed in **Figure 3.10**.

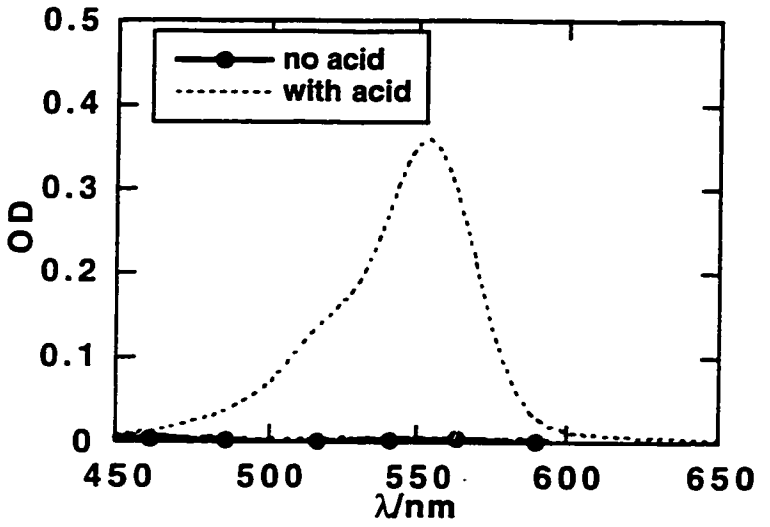

Figure 3.10: Spectra of 0.02 M rhodamine B Base with and without 0.08 M triphenylacetic acid in a PMMA matrix.

This result is of importance due to the possibility of the presence of carboxylic groups in the backbone of the some of the polymers used in the photoresist industry. Basically, this result indicates that rhodamine B base cannot be used to quantify acid generation in the certain polymer matrices due to its sensitivity to the presence of carboxylic acids. Both fluorescein and Coumarin-6 remain potential dyes to be used for such polymers.

Dye/ polymer	Acid	"Sensitivities"/Y-INTERCRPTS				
Fluorescein/ PVP 0.02M	CSA PFOS	248 nm 8.79e05/0.35 1.13e06/0.43	254 nm 1.25e06/0.42 1.23e06/0.43		445nm (protonated) 3.67e06/0.09 4.07e06/0.09	
Fluorescein/ PMMA 0.01M	CSA PFOS	248 nm 1.17e06/0.07 1.49e06/0.09	254 nm 1.36e06/0.04 1.67e06/0.05		445 nm (protonated) 3.56e06/0.01 5.00e06/0.01	
DMBB/ PVP 0.015M	CSA PFOS	248 nm -2.17e05/0.27 -3.54e05/0.27	254 nm -4.71e05/0.35 -6.60e05/0.36	390 nm (neutral) -2.59e06/0.27 -1.94e06/0.27	460 nm (protonated) 3.66e06/0.05 2.77e06/0.03	
DSBS/ PVP 0.015M	CSA PFOS(ppt)	248 nm -7.06e05/0.30	254 nm -5.72e06/0.43	445 nm (neutral) -3.55e06/0.24	370 nm (protonated) 2.35e06/0.09	590 nm (protonated) 1.04e06/0.01
Coumarin-6/ PVP 0.008M	CSA PFOS	248 nm -7.49e05/0.25	254 nm -5.09e05/0.41 1.71e05/0.36	470 nm (neutral) -3.50e06/0.23 -4.30e06/0.23	530 nm (protonated) 8.52e06/0.05 8.25e06/0.02	
Rhodamine B Base/PMMA 0.02M	CSA(ppt) PFOS	248 nm -3.10e06/0.46 -1.00e06/0.50	254 nm -2.13e06/0.34 8.50e05/0.36		556 nm (protonated) 1.77e05/0.07 1.32e07/0.02	

Table 3.3: Table of "sensitivities" and y-intercepts calculated for each dye using a strong (PFOS) and weak acid (CSA). The rate of changes are given for each wavelength of importance for each dye.

3.3.3. Acid Quantification

The first experiment compared the effect of varying the anion of a certain class of photoacid generator. The PAG class under study were the iodonium salts and the results can be observed in **Figure 3.11 (A&B)** . The results are shown for three different iodonium PAGs differing in anionic component. Although, only the structure for one of the PAGs (**1**) is given, the spectra of all three acid generating efficiencies are compared.

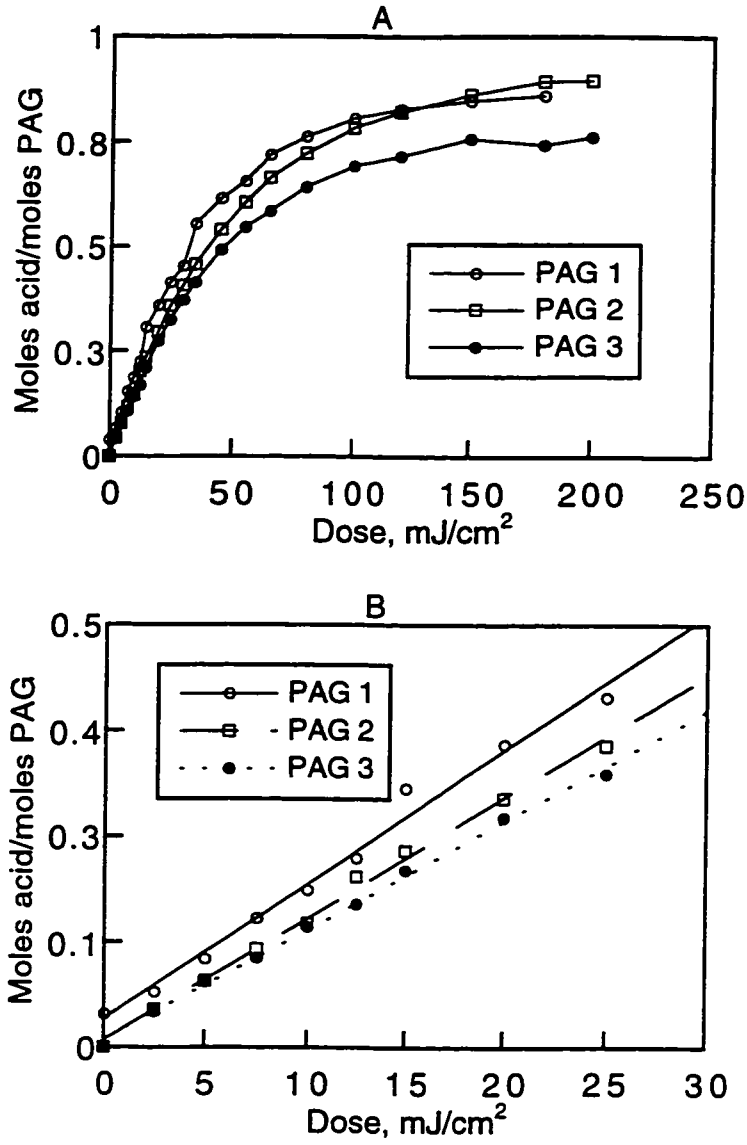

Figure 3.11: Comparison of acid generating efficiencies of three Iodonium PAGs; **A)** shows the plateau level of acid generation, **B)** shows the linear region from which slopes (efficiencies) can be obtained.

The small difference in slope indicates that there is a small difference in the rates of photoacid generation for each of the three PAGs. This indicates that changing the anion of the PAG does not considerably change the acid generating efficiency.

The effect of changing the ratio of Dye/PAG is shown in **Figure 3.12**. The spectra obtained show that with half the amount of PAG, the rate of acid production is also reduced accordingly. This further indicates that the technique is reliable.

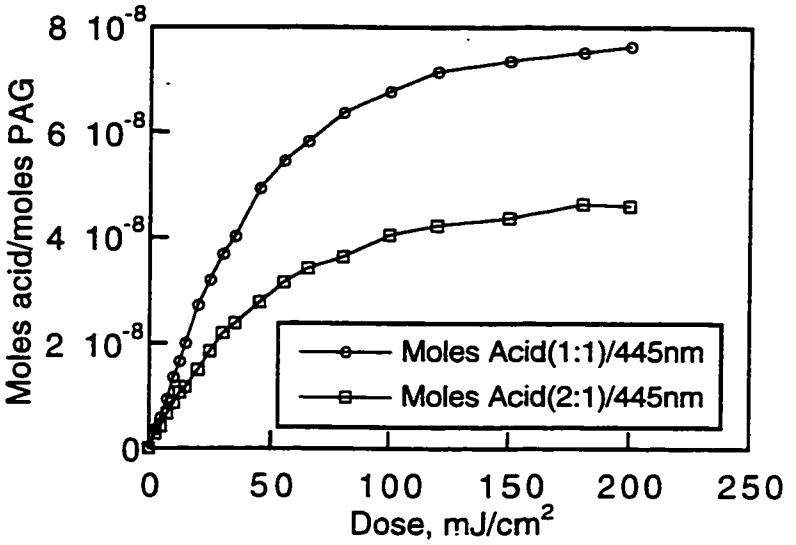

Figure 3.12: Plot of Irradiation dose versus moles of acid generated. Comparison of changing the ratio of Dye/PAG. The dye used was fluorescein and the PAG was compound **1**.

The comparison of different photoacid generators can be observed in **Figure 3.13** . The plots (both polynomial and linear) comparing dose vs. moles acid/moles PAG clearly show the differences in the acid generation efficiency of the five PAGs. It is seen that, and **1**, **6** are fairly similar in efficiency. Compound **5** although slightly lower is fairly close in efficiency as well. Phlouroglucinol(tris)camphorsulfonate (**7**) and camphor sulfonyl napthalimide (**4**) show slower acid-generating efficiencies. This effect clearly shows that the efficiencies of different PAG classes can be detected.

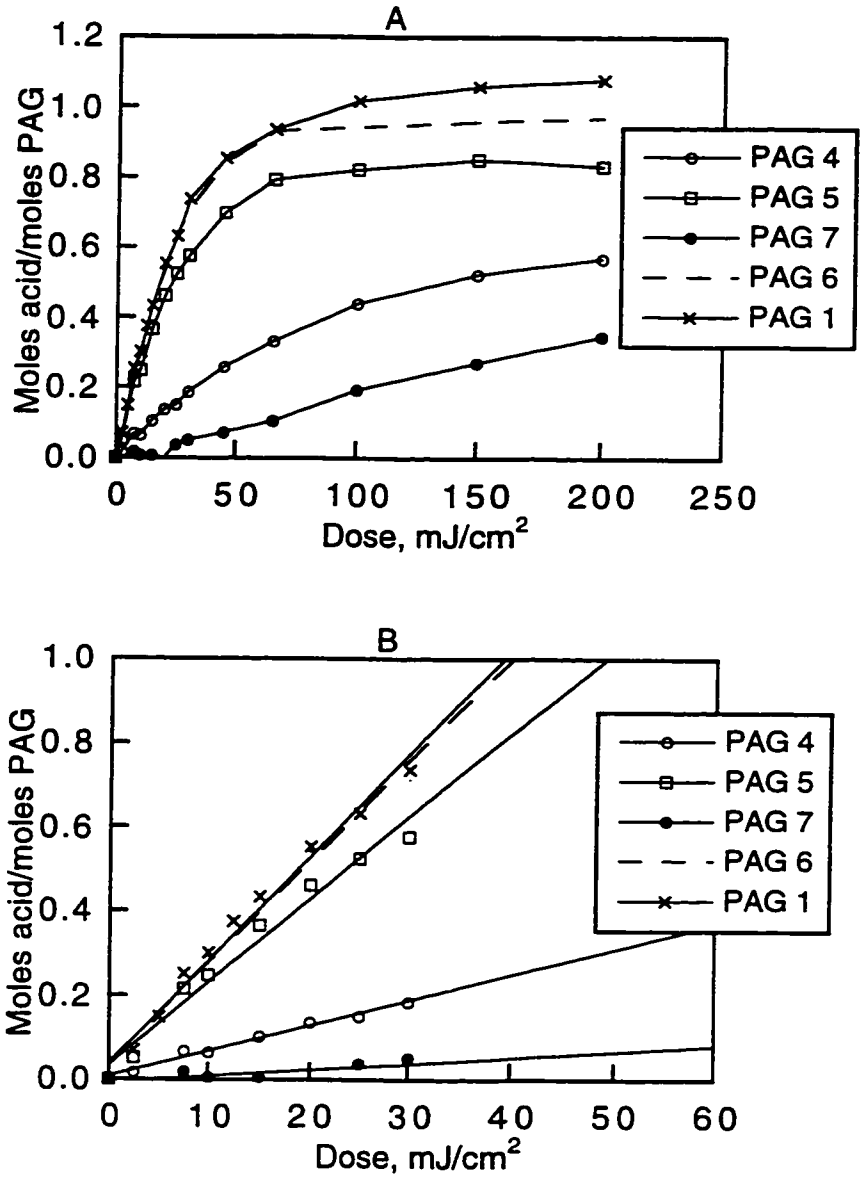

Figure 3.13: Comparison of acid generating efficiencies of different PAG classes in a PHS matrix: **A)** shows plateau levels of each PAG; **B)** shows linear region of each PAG.

From the results comparing acid generating efficiencies in a PHS versus a PMMA matrix, the differences are can be clearly observed in **Figure 3.14**.

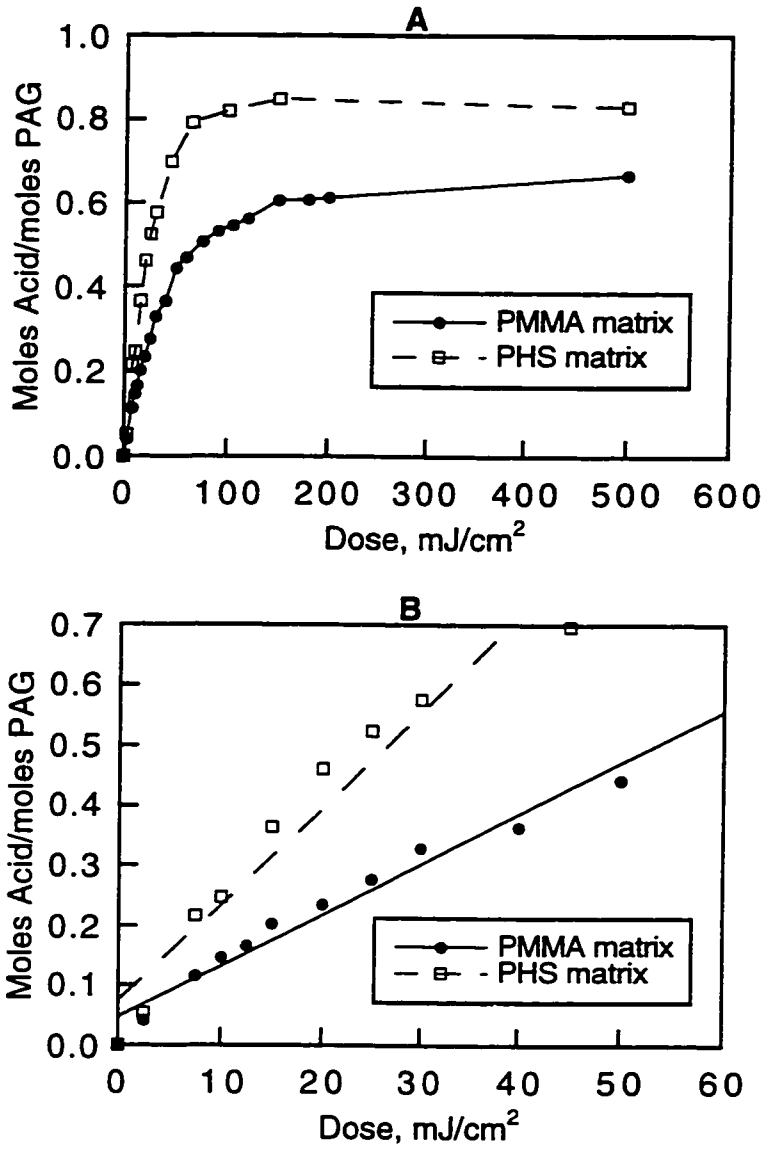

Figure 3.14: Comparison of the different acid generating efficiencies of PAG **5** in PHS and PMMA: **A)** plateau region and **B)** linear region. A dye concentration of 0.01 M fluorescein was used.

Comparison of results of the PFOS PAGs in PHS and PMMA matrices shows that the acid generation efficiencies of the PAG are greater in PHS than PMMA. The results clearly

show that the rate of acid formation is faster in a PHS matrix. It has been assumed that phenolic matrices can sensitize photoacid generation by being the source of electrons needed in mechanisms which involve electron transfer and thus this may explain the results.

Matrix effects on the efficiency of acid generation were also tested by comparing meta PHS versus para substituted polymer. Spectra obtained show a decreased acid generating efficiency in the meta polymer as compared to the para polymer, as depicted in **Figure 3.15** .

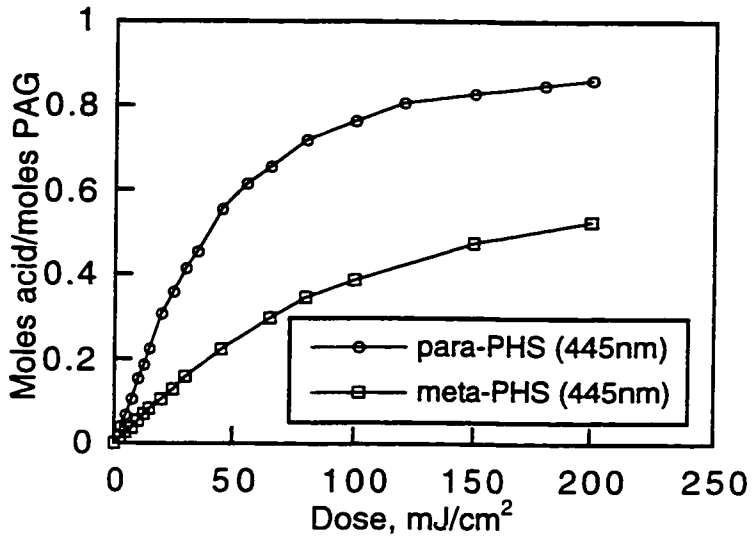

Figure 3.15: Comparison of meta-PHS vs para-PHS on the effects of acid generation. The PAG used in both cases was compound **1**. Fluorescein concentration was 0.02 M. Both samples were irradiated at 254 nm for varying amounts of time (Intensity 0.05 mJ/cm^2).

The differences observed between the two differently substituted polymers could be attributed to the fact that a calibration was not done using the meta PHS. The calibration of the para-PHS was used to quantify the moles of acid generated in both cases. In any cases, this result is interesting because it shows that there is a potential for the substituents of the polymer

to have an effect on acid-generating abilities of the PAG. In order to distinguish this relationship, further studies will have to be done.

3.3.4. Acid Loss Studies

The results obtained from this experiment are summarized in **Table 3.4.**

Resist Used	Dye Used	Moles Acid Loss	254nm Filter	Solvent/Matrix
APEX-E-2408	Fluorescein	6.0×10^{-11}	No	diglyme/PHS
APEX-E 2408	Fluorescein	1.9×10^{-10}	Yes	diglyme/PHS
APEX-E 2408	DMBB	7.7×10^{-10}	Yes	PMA/DAA/hyd.PHS
UVIIHS	Fluorescein	7.1×10^{-10}	No	diglyme/PHS

Table 3.4: Values of the moles of acid lost from the resist sample and captured by the dye/polymer layer. Fluorescein was made in a PHS/diglyme solution, and DMBB was made in a hydrogenated PHS/propylene glycol methyl ether acetate solution. The type of photoresists were APEX-E 2406 and UVIIHS.

The results obtained for the fluorescein dye were found to be comparable to previous acid loss studies . However, in the case of fluorescein, the results are likely to be more reliable due to the high sensitivity and better photostability than TBPB.

Overall, the results of these experiments show that fluorescein can be used to study acid loss. The use of fluorescein is more favorable due to the fact that the Na TBPB dye was photobleachable, had problems with stability, purity and reproducibility. Fluorescein is more advantageous due to its high sensitivity and stability.

3.4. Conclusion:

In this work, an *in situ* method of acid quantification in polymer films was developed. In order to test the applicability and subsequent validity of this method, a number of experiments were done. From the results obtained, all dyes that were tested appear to be appropriate for use in acid quantification. With the exception of rhodamine B base in the presence of carboxylic acid, all behave as desired. Furthermore, the fact that fluorescein shows a broadening in its spectra at temperatures greater than 110°C, can be ignored due to the small difference observed. Overall, the results of the characterization of the dyes are summarized in **Table 3.2.**

The next section of experiments dealt with the generation of calibration curves of the dyes both with a weak (CSA) and strong acid (PFOS). Representative plots were shown for fluorescein. In the cases of DSBS and rhodamine B Base, problems with precipitate formation occurred with one of the acids used. This precipitate formation was assumed to be because of the insolubility of the protonated (salt) form of the dye. All calibration results, acid generating 'sensitivites" and y-intercepts, are summarized in **Table 3.3** for each dye.

The acid calibration results of fluorescein were then used to quantify the amounts of acid generated for a number of PAG systems. Acid generating efficiency of each PAG was obtained by using the amount (moles) of PAG present in each mixture. This was calculated by knowing the change in absorbance and knowing the "sensitivity" of the dye mixture. This value of moles yields an efficiency measurement in terms of moles of acid generated per moles of PAG used. A plot of dose versus moles acid/moles PAG yields curves from which the linear portion of different PAGs can be compared.

The comparison of PAGs differing only in anion, resulted in similar acid generating efficiencies, as expected. When comparing different PAG classes, different acid generating efficiencies were observed. This indicates that the structure of the acid effects the photoacid

generation. The result of this study is essential in understanding PAG systems such that new PAG structures can be synthesized. Furthermore, matrix effects clearly showed that acid generating efficiencies are higher in a PHS matrix than a PMMA matrix, again these results were expected. This effect has been attributed to the sensitization effects of PHS.

The matrix effect of using *p*-poly(hydroxystyrene) versus *m*-poly(hydroxystyrene) was also studied. The results obtained indicate that there is higher acid generating efficiency of the PAG in *p*-poly(hydroxystyrene). Although, there were inherent problems with this experiment, further studies would be essential in determining whether substitution in a matrix, effects the acid generating properties of PAGs.

From the acid loss studies, further confirmation was given of the validity and sensitivity of this method of acid quantification. The results showed that fluorescein was sensitive enough to detect acid loss from a resist sample by changes in its absorption spectra. Overall, the objectives of this study were met. The results obtained appear to agree with previous methods (i.e., TBPB method) and hypothesized results.

This technique has a number of advantages over its predecessors. The advantages of this technique are that: acid generated can be quantified within the polymer matrix, dyes are very sensitive to acid; dyes are not photo or thermally-labile. This method can be used for any PAG system, and work is easily done using conventional UV-Vis spectrophotometer. Although this method, is at an initial stage of use, it appears to be working well. Further studies including use of the dyes in solution as was done with TBPB may be beneficial in comparing the results between the two methods. Furthermore, additional PAG classes should be tested.

Another aspect that may be considered is that absorption spectroscopy was used for the purposes of this work, since a fluorimeter was not available at Shipley Co. In terms of

sensitivity of the two methods, absorption spectroscopy versus fluorescence spectroscopy, fluorescence spectroscopy is a more sensitive technique, as discussed in the introduction. The results of this acid quantification study indicate that absorption spectroscopy is sensitive enough to monitor the rate of acid generation in PAG systems. However, in future studies it may be beneficial to do fluorescence studies to compare the difference in acid quantification capabilities.

Appendix I

Calculations

Calculations:

In this work, to quantify the exact amount of moles of acid in the samples a number of calculations had to be made. In solution samples this is an easy task but when working with polymer films this becomes a difficult task. The method in this work used the technique of calculating weight percents of each component such that the ratio of acid in the sample could be calculated and thus the exact number of moles could be obtained. Due to the large amounts of data obtained for purposes of this work, Microsoft Excel Spreadsheets were used for all the calculations. And due to the large sizes of these spreadsheets, they could not be included in this thesis. This appendix will go over the steps that were used to obtain the moles of added acid in the polymer samples, and further the moles of acid produced by the PAG, using the "sensitivities" obtained from the calibrations of a weak and a strong acid.

The calculations involved a weight analysis of all species present in the dye/acid or PAG/polymer systems. the weight percent of each compound was obtained by taking into the weight of the total solids, and each individual weight. The weight of total solids did not include the weight of the solvent, since an assumption that all solvent evaporated during the baking step. Although, this may not be the case the values obtained were consistent throughout the analysis. In this work there were a number of calculations involved, these included: weight percent of fluorescein, moles of acid in the sample, weight percent of PAG (or moles of PAG), moles of acid generated from the PAG, the absorption as a function of film thickness, and irradiation dose.

Steps Involved:

1) Weight % of Dye

- usually a stock solution of 25% polymer was made from which a sub-stock solution of dye in polymer was made

e.g. 0.02 M fluorescein in a 25% (by weight) PHS polymer solution

- for 75 mls of 25% PHS solution, 0.4986 g of fluorescein are needed to make a 0.02 M solution:

- from this the weight percentage of fluorescein relative to the total weight of the solids in the solution could be obtained, i.e, for 75 g of 25% PHS solution, the weight of solids (PHS) would be 18.75 g PHS and 56.25 g diglyme. Therefore, the ratio of fluorescein in relation to the total weight of solids is:

$$\frac{0.4986g}{18.75g + 0.4986} x100 = 2.59\% fluor.$$

And the ratio of the total weight of solids in relation to the total weight of solution is:

$$\frac{18.75g + 0.4986g}{75g + 0.4986g} x100 = 25.5\% solids$$

- by knowing the exact weight of spin-coated film, the % solids could be calculated, from which the % fluorescein by weight could be calculated and the moles of added fluorescein could be calculated.

2) Moles of Acid Added (CSA or PFOS)

- in most cases 1.5-2.0 g of the above dye/polymer solution was used to make solutions of varying acid concentration for the acid calibration curves

e.g. 0.01M PFOS ($CF_3(CF_2)_7SO_3H$ in the fluorescein/PHS solution

- for 1.5 mL of PHS solution, 0.0075 g of acid (PFOS) are needed to make a 0.01 M solution:

- in a 1.5 g solution of the above 0.3825 g (25.5%) is solids,

∴ the ratio of acid to total solids would be calculated as was done for the % Dye:

$$\frac{0.0075g}{0.3825g + 0.0075g} x100 = 1.92\%acid$$

- thus, for a spin coated film that has a measured weight of 0.0012 g

$$\frac{0.0012gx0.0192}{500.13g/mo} = 4.6068x10^{-8} \text{moles of acid (PFOS)}$$

This conversion was done for every concentration of added acid and thus the plots were plotted as moles of acid versus OD instead of molarity.

3) Moles of PAG Used

In most cases the PAG was loaded 1:1 in terms of mole ratio with the dye.

e.g. 1:1 molar PAG **1** loading (M.W. 624.59 g/mo),

- for 1.5 g of solution, 0.3825 g is the amount of solids (25.5% from above) and of this amount 2.59% is fluorescein (i.e. approx. 0.0099 g or 2.98 x 10^{-5} moles). Therefore, approx. 2.98 x 10^{-5} moles or 0.0186 g of PAG are required:

- From this, the exact weight percentage of PAG on the film can be calculated and the exact number of moles, as before:

$$\frac{0.0186g}{0.3825g + 0.186g} x100 = 4.63\%PAG$$

-on a film that weighs 0.0012 g, the moles of PAG would be:

$$\frac{0.0012gx0.0463}{624.59g/mo} = 8.895x10^{-8}\text{moles PAG}$$

This value would be constant throughout the samples because one disk was irradiated for varying amounts of time yielding increasing values of absorption at the wavelength of protonated form (i.e. 445 nm for fluorescein).

4) Normalized Absorption Values

Since every spin-coated polymer film differs in film thickness, all absorption (OD) values were normalized to a film thickness of 1 μm. To obtain these values these absorption values recorded at specific wavelengths were divided by the film thickness. Film thicknesses ranged from (0.65 μm to 0.88 μm)

5) Irradiated Dose

Before using the HTG Imaging Unit for the irradiations, the intensity of the instrument was checked with a dose-meter. In most cases the intensity was 0.05 mJ/scm^2. By irradiating the sample for different amounts of time, the total dose at 254 nm could be calculated.

The formula is: Time (s) X 0.05 MW/ scm^2 = Dose (mJ/cm^2)

6) Moles of Acid Generated by the PAG

These calculations were made using the calibration curves generated with known amounts of acid. Basically, by knowing the absorbance of samples of known acid concentration, Beer's Law was used to relate the absorbance values obtained from photoacid generation to the expected values of moles of acid produced. Depending on what type of acid was generated either the CSA (weak acid) calibration or PFOS (strong acid) calibration was used.

e.g. for the PAG **1** which generates camphorsulfonic acid, the CSA calibration would be used.

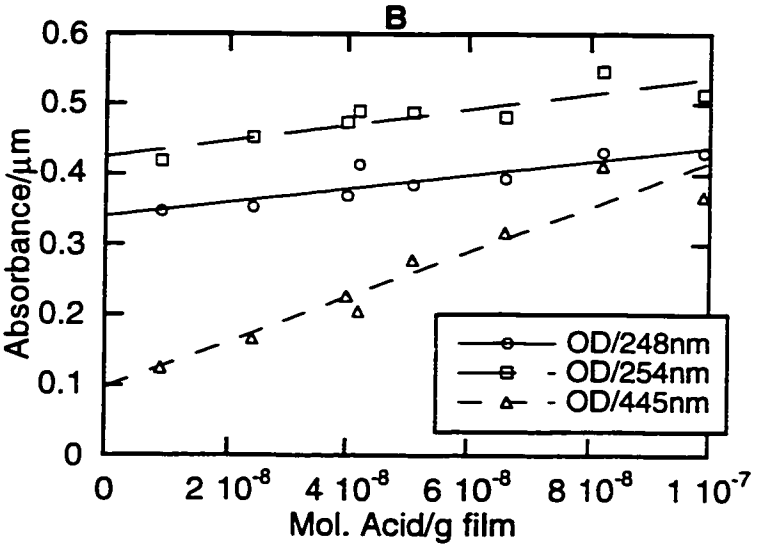

Figure 3.9B

From the calibration of fluorescein with increasing amounts of CSA (**Figure 3.9B**), the slope or "sensitivity" was found to be $3.67X10^6$ for the absorbances at 445 nm. This slope is in relation to ε. Thus by knowing this slope, it can be used by Beer's Law to find the corresponding acid amounts for a particular absorption (OD/µm) of the PAG.

e.g. for PAG **1** with fluorescein,

- at 15 mJ/cm^2, the OD obtained of the protonated form was 0.1502. Since fluorescein has an initial absorption at 445 nm before any acid is present, the absorption of the protonated form had to be corrected for:

$$\frac{\text{Final OD - Initial OD}}{\text{"Efficiency Value"}} = \text{moles of acid generated}$$

$$\frac{0.1502 - 0.077}{3.6676x10^6 mo^{-1}} = 2.00x10^{-8}\,\text{moles of acid generated}$$

These values were calculated for every irradiation ranging from a dose of 2.5-200 mJ/cm^2. Furthermore, these values were given in moles of acid generated per mole of PAG used. In the example given above, this would merely be obtained by:

$$\frac{\text{moles of acid generated}}{\text{moles of PAG added}} = \frac{2.00x10^{-8}mo}{8.95x10^{-8}mo} = 0.22$$

As more and more acid is generated this value would reach closer to 1.

References

(1) McKean, D. R.; Schaedeli, U.; MacDonald, S. A. In *Polymers in Microlithography*; American Chemical Society: Washinton, DC, 1989; pp 27.

(2) Roschert, H.; Eckes, C.; Endo, H.; Kinoshita, Y.; Kudo, T.; Masuda, S.; Okazaki, H.; Padmanaban, M.; Przybilla, K. J.; Spiess, W.; Suehiro, N.; Wengenroth, H.; Pawlowski, G. *SPIE* **1993**, *1925*, 14.

(3) Thompson, L. F.; Willson, C.; Bowden, M. J. *Introduction to Microlithography, 2nd edition*; American Chemical Society: Washington, DC, 1994.

(4) Malenfant, P. "Synthesis of Specialty Polymers for Microlitographic Applications and Spectrophotometric Determination of Acid in Thin Polymer Films", Co-op Report, University of Ottawa, 1994.

(5) Mckean, D. R.; Schaedeli, U.; Mcdonald, S. A. *J. Polym. Sci.: Part A: Polym. Chem.* **1989**, *27*, 3927.

(6) Thackeray, J. W.; Denison, M. D.; Fedynyshyn, T. H.; Kang, D.; Sinta, R. *ACS Symp. Series* **1995**, *614*, 110.

(7) Orellano, A. "Development and Study of Shipley's Experimental Deep UV Photoresists," Co-op Report, University of Ottawa, 1995.

(8) Takeyama, N.; Ueda, Y.; Kusumoto, H.; Ueki, H.; Hanabata, M. *ASC Symposium Series* **1994**, *537*, 53.

(9) Pohlers, G.; Scaiano, J. C.; Sinta, R. *Chem. Mater., in press* **1997**,

(10) Markuszewski, R.; Diehl, H. *Talanta* **1980**, *27*, 937.

* Note : Definitions of keywords are given in Appendix II

Chapter 4

Toxicological Properties of Some Photoresist Components Including the Acid Sensitive Dyes

4.0. Background:

This chapter is a non-experimental chapter discussing the toxicological properties of some of the components that comprise photoresist samples. Some of the dyes proposed in **Chapter 2** will also be discussed in terms of their toxicity. This chapter was written to meet the requirements to obtain a Specialization in Chemical and Environmental Toxicology. This chapter is followed by an appendix where some of the specialized terms used are defined.

4.1. Introduction

In the broadest sense, the science of toxicology involves all aspects of the adverse effects on biological systems, including mechanisms of harmful effects, conditions under which these harmful effects occur, socioeconomic considerations and legal ramifications[1]. Basically, a poisonous substance is any chemical that is capable of producing detrimental effects on a living organism. As a result of damage, there is an alteration of structural components or functional processes which may produce injury or even death. An important principle is that any chemical may be poisonous at a given dose and route of administration. In a sense, all chemicals are potentially toxic under the proper conditions. For this reason, toxicological studies are done, such that the exact elements of chemical "risk" can be determined.

Adverse or toxic effects in a biological system are not produced by a chemical agent unless that agent or its metabolite breakdown (biotransformation) products reach appropriate sites in the body at a concentration and for a length of time sufficient to produce a toxic

manifestation. Many chemicals are of relatively low toxicity in the "native" form but, when acted on by enzymes in the body, are converted to intermediate forms that interfere with normal cellular biochemistry and physiology. Whether a toxic response occurs is dependent on the chemical and physical properties of the agent, the exposure situation, how the agent is metabolized by the system, and the overall susceptibility of the biological system or subject. Thus, to fully characterize the potential hazard of a specific chemical agent; the type of effect, the dose required to produce that effect, the exposure, and the disposition of the subject are required. Overall, a typical risk assessment is made up of hazard, an intensive factor, used to describe the property of the agent i.e. its capacity or capability to do harm, and exposure, an extensive factor used to define the property of the context or environment. When these properties are described, the potential risk of the chemical can be characterized.

The purpose of this chapter, is to discuss the risk of the chemicals used for photoresist manufacture. This chapter will be divided into three main categories: toxicity of photoresist polymers, toxicity of the solvents used in photoresist samples, and the toxicity of incorporated dyes.

4.2. Toxicity of Incorporated Dyes:

In the previous chapters, a number of dyes were used to quantify and monitor acid production and diffusion in photoresist samples. The toxicological properties of these dyes, as well as any other compound, are important knowledge when the compounds are used for industrial purposes. The possible toxicity of these dyes could help in choosing which dyes should be preferred for photoresist technology. Due to the lack of toxicological studies in the literature only some of the compounds could be reviewed. The dyes that were reviewed for toxicological studies were acridine, 2-phenylquinoline, 2-phenylpyridine, rhodamine B, and fluorescein.

4.2.1. Acridine

Acridine (dibenzo[b,e]pyridine) is a nitrogen-containing analogue of anthracene and is an aza-rene. The structure is in **Figure 4.1**. Although, there have been few studies investigating the mammalian toxicity of acridine, those that have been done suggest that it only

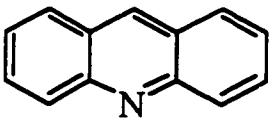

Figure 4.1: Structure of acridine.

causes mild toxic responses. An early study on the acute toxicity in rabbits provided LD_{50}'s of 1-1.5g/kg body weight for oral administration and 100 mg/kg bw for intravenous[2]. The LD_{50} for subcutaneous administration was found to be 300-400 mg/kg bw[3], while an oral LD_{50} of 2g/kg bw for rats and 500 mg/kg bw for mice was reported[4]. In a subchronic 90 day mouse study, it was reported that twice-weekly dermal application of acridine in a solution of liquid paraffin produced no tumors[5]. A study in rats which investigated the carcinogenicity of various nitrogen-containing polycyclic aromatic hydrocarbons involved a one-time, direct injection of 0.2, 1.0 or 5.0 mg of acridine per rat into the left lobe of the lung[6]. Of the 35 rats per dose level, one of the middle dose group (about 4 mg/kg bw) developed a pulmonary adenocarcinoma and one of the high dose group (about 20 mg/kg bw) manifested a pleomorphic sarcoma. Acridine has been shown to be mutagenic in *Salmonella typhimurium* [7,8].

Furthermore, a recent subchronic toxicity study on acridine has been done to investigate the systemic toxicity in rats through dietary exposure at 0, 1, 10, 100 and 500 ppm for 13 weeks [9]. After 13 weeks the rats were killed and various tissues, including the liver, brain, heart, lung, spleen, kidney, as well as others, were excised and analyzed for abnormalities and

acridine residue. This was done by HPLC and fluorescence measurements. They used an excitation wavelength of 250 nm and an emission wavelength of 405 nm to monitor the fluorescence. They also assayed the supernatant of the samples for ethoxyresorufin O-deethylase (EROD) and pentoxyresorufin O-dealkylase (PROD) activities, two enzymes involved with the metabolism of acridine.

Over the course of 13 weeks, all animals appeared to be normal i.e. no overt signs of toxicity were observed, with no effect on body weight or food consumption. There were some slight effects on organ weights with spleen in the male control animals being significantly heavier than those in the 500 ppm dose group. In females, thymus weight showed a response across the treatment groups with the two highest dose groups having significantly heavier weights.

Both hepatic ethoxyresorufin O-deethylase (EROD) and pentoxyresorufin O-dealkylase (PROD) activities were slightly, but significantly, elevated in females in the 500 ppm dose group. However, males did not show any signs of induction of PROD or EROD. This result indicates there is some difference in gender sensitivity to the presence of acridine. Consistent across all groups were the normal levels of the serum enzymes alkaline phosphatase and aspartate amino transferase. Increased levels of these enzymes have been used as indicators of hepatotoxicity and normal levels are evidence for minimal affect of treatment on the liver. Also unaffected were serum levels of creatine and urea nitrogen. These analytes have been markers for altered renal function; normal levels are indicators of unimpaired renal activity.

Treatment related histopathological changes were seen in the thyroid, liver and kidney and included hepatic anisokaryosis and vesiculation of nuclei and glomerular adhesions, reticulin sclerosis and nuclear pyknosis in the kidney. In the thyroid, there were also some degree of papillary proliferation and inspissation of colloid in males, but all of the thyroid changes were slight and likely to be reversible. The most prominent change in the liver, was

anisokaryosis. Unlike the thyroid, these changes are likely to result in a permanent increase in connective tissue. In the kidney, the epithelial injury and the presence of interstitial changes point to the ability of acridine to cause permanent injury. However, overall, the histopathological changes were very mild in nature, even at the highest dose.

Residue analysis was performed on representative liver, kidney and fat samples and acridine was found to have accumulated to only a slight extent, with levels being about 60 ng/g in the adipose tissue of males of the highest dose group. Females had residues of about half that value. Basically, the lack of accumulation of acridine under conditions of high loading , as was the case in this study, indicates rapid elimination and/or rapid metabolism of this compound. In a previous study[10], acridine was reported to be metabolized by the S-10 fractions from rat liver homogenates to 9-acridone and by PCB-induced enzymes to a dihydrodiol. They calculated the V_{max} and K_M for 9-acridone. V_{max} and K_M are values for the kinetic constants of the enzymes involved, where, V_{max}, is the maximum enzyme activity and K_m, is the Michaelis constant. These were found to be $7x10^{-7}$ mol/min.-mg and $5x10^{-4}$ M or 89.5 mg/L. From this an estimate of the V_{max} for acridine scaled to a 1 kg rat could be determined. This value would be 9.3 mg/h or 52 µmol/h which would indicate that rats are capable of metabolizing more than 200 mg of acridine per day, which far exceeds the daily intake in the highest dose group of both sexes. Overall, these numbers support the rapid metabolism of acridine and explain the very low accumulation of the dosed material. In summary, acridine was seen to cause only mild toxic responses, likely due to the rapid metabolism and/or elimination. Based on the data for the gross, biochemical and histological changes, the no observable adverse effect level (NOAEL) of acridine was judged to be 100 ppm or 12 mg/kg bw/day.

4.2.2. Fluorescein

Fluorescein (3', 6'- dihydroxyspiro[isobenzofuran-1(3H), 9'-[9H]xanthen]-3-one, is a fluorescent organic dye used for a variety of purposes besides that proposed in this thesis. The structure of this xanthene dye is shown in **Figure 4.2.**

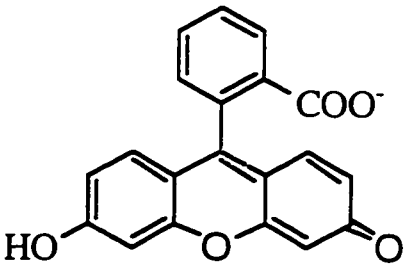

Figure 4.2: Structure of fluorescein.

Fluorescein and its sodium salt (uranin), have proved inactive in a variety of mutagenicity tests. These include the Ames assay with and without activation , other bacterial systems without activation, the Kada *rec* assay and the *B. subtilis* transforming DNA system after light activation. The dyes were also inactive when tested for petite induction with yeast[11].

Fluorescein is used for tracing the course of underground streams and of factory effluents and sewage sources that contaminate underground water supplies[12]. It is also used to ascertain connections between streams and sea or to determine the approximate volume of water delivered by a spring. The toxicity of fluorescein to fish has been studied, which demonstrated that certain species are more susceptible to fluorescein toxicity. The turbot species of fish was seen to develop irritability, decreased spontaneous motor activity, ataxia and decreased rates of respiration similar to the effects of fluorescein on rats in another study[13]. Basically, fish show toxic effects at fluorescein concentrations greater than 0.9 g/L. But since most field applications use concentrations of 1 mg/ml which do not lead to deaths, the authors concluded that fluorescein is not harmful to fish.

Sodium fluorescein is also widely used for diagnostic procedures in medicine. It is commonly used as a quantitative tracer for studying physiologic functions of tissues and the eye[14]. Since introduced in 1934, the determination of the distribution of the intravenously administered dye has also become an important means of documenting human skin microcirculation[15]. The appearance of epithelial cell fluorescence is considered a diagnostic marker of damaged epithelial cells or ocular surface disorders. Clinicians generally consider fluorescein to be completely safe to the corneal epithelium and for use in humans. However, a number of adverse effects to parenterally administered fluorescein have been reported; these include allergic reaction, hypertensive crisis, and myocardial infarction, as well as photosensitizing effects[16]. The most common frequent side-effect is urticaria, which occurs in 0.5% of the patients[17,18]. In contrast, the photosensitizing effects of fluorescein are less common. After systemic administration, fluorescein is widely distributed to body tissues and is excreted by the kidney and also conjugated by the liver. Its excitation spectrum shows a peak at 495 nm (19). *In vitro* studies have shown that fluorescein is a photosensitizer by producing singlet oxygen, which acts as a reactive intermediate[19]. These reactive intermediates can lead to oxidative damage to cellular materials causing phototoxic or photoallergic reactions. The phototoxic reactions of fluorescein have occurred in people but only to a small extent[16,20]. Overall, the toxicity of fluorescein is quite low and in terms of its benefit to risk ratio, the benefits far outweigh the risks.

4.2.3. Rhodamine B

There are very few papers dealing with the toxicological properties of rhodamine B base (Solvent Red). The only papers found in the literature dealt with the toxicity of rhodamine B. Rhodamine B (or Food Red 15) is a xanthene dye commonly used for coloring textiles, paper, soap, leather, drugs etc., as well as a dye in food. The structure of this dye can be seen in **Figure 4.3.**

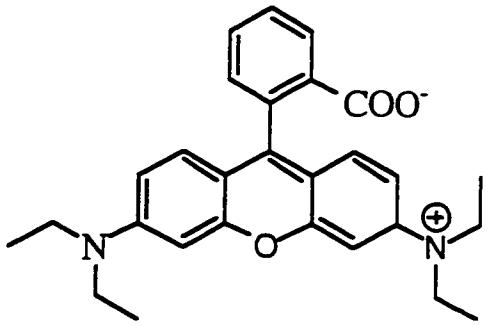

Figure 4.3: Structure of Rhodamine B.

The use of this dye is an issue of whether the benefits outweigh the risks. Rhodamine B is known to be a carcinogen in rats, producing local sarcomas following subcutaneous injections[21].

Rhodamine B has been reported to be mutagenic in salmonella[22], in the *Bacillus subtilis rec*-assay[23] and in the *Saccharomyces cerevisiae* mitotic gene conversion assay[24]; it was also mutagenic in *Escherichia coli* [25]. In the Drosophila sex-linked recessive lethal test, following adult feeding, the outcome was inconclusive[26]. Furthermore, the clastogenicity and DNA damaging effects of rhodamine B in Chinese hamster ovary cell *in* vitro have been established[22,27]. Also, in the fibroblast cells of *Muntiacus muntjac* in culture, rhodamine B induced chromosomal aberrations[28].

Another study looked at the genotoxicity of rhodamine B in the somatic and germ line cells of *Drosophila melanogaster* following chronic larval exposure in comparison to another red dye, amaranth[29]. They tested for genotoxic effects of the dyes following the wing spot and the sex-linked recessive lethal tests. Second- and third-instar larvae, carrying suitable genetic markers, were subjected to chronic exposure to different concentrations (0, 5, 10, 25 mM) of the test dyes. Upon exposure the wings of the flies were screened under a compound

microscope to detect the size and type of each spot (i.e. mutations). The data obtained were evaluated statistically following a conditional binomial test.

The results obtained from the wing spot test following chronic larval exposures shows that rhodamine B base causes the appearance of both small and large single spots, evidence of mutations. However, small single spots were positive only at the doses of 10 and 25 mM, whereas the large single spots were only positive at 25 mM dose. The frequency of induction of spots for amaranth was negative. The data on the frequency of lethal induction in the sex-linked recessive lethal test indicated that exposure to rhodamine B at the higher concentrations led to the induction of lethals in significantly higher frequencies. At the lowest dose tested (5 mM), however, the lethal frequency was not significantly different from the control. The sex-linked recessive lethal test is supposed to be the best-validated mutagenicity test in Drosophilia. A lethal originates following the induction of gene mutations, deletions of small chromosome parts or other types of chromosomal aberrations[26]. Overall, from these studies, in agreement with other studies, it can be said that rhodamine B is genotoxic in both the somatic and germ cell lines of Drosophilia. This result leads to the potential risk in humans when using this dye as food coloring or other uses.

4.2.4. 2-Phenylpyridine

The compound, 2-phenylpyridine has been shown to induce mitotic aneuploidy as well as mitotic recombination in strain D61.M of *Saccharomyces cerevisiae*[30]. Pyridine has previously been found to induce mitotic chromosome loss in the same strain and also to inhibit the assembly in vitro of brain tubulin[31]. However, a number of studies have shown that different pyridine derivatives induce aneuploidy and inhibit tubulin assembly to different extents[30]. The structure of 2-phenylpyridine is in **Figure 4.4**.

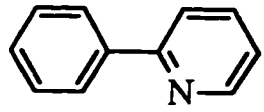

Figure 4.4: Structure of 2-phenylpyridine.

Studies have shown that it is more effective than pyridine in inducing aneuploidy, mitotic recombination, point mutations, and deletion of chromosomal fragments[30]. However, this study looked at various pyridine derivatives and found that 4-acetylpyridine had the highest frequency of inducing aneuploidy. By studying a number of pyridine derivatives with the same groups inserted in different positions of the pyridine ring, they were able to study the relation between structure and aneuploidy-inducing effect. Their results indicated that the induction of aneuploidy at least in yeast required structural specificities.

Other studies have shown that 2-phenylpyridine as well as other pyridine analogues interact and inhibit human aromatase activity in microsomal suspensions[32]. The aromatase cytochrome P-450 enzyme catalyzes a unique three-step oxidative removal of the 19-methyl group from androst-4-ene-3,17-dione or testosterone as formic acid and aromatization of ring A to form the estrogens. The high degree of specificity for androgens and the stereospecific nature of the reactions effected suggest that the androgen substrate is oriented in a unique configuration within the active site. It is seen that the substrates or the inhibitors (i.e., pyridine derivatives) interact with P-450 enzymes and can be characterized by spectral changes. To determine the nature of the androgen-aromatase interaction, the various pyridine derivatives were studied for their spectral interaction with partially purified human placental aromatase and for their kinetic inhibition of aromatase activity in microsomal suspensions. Their spectral and kinetic results indicated that 2-phenylpyridine, as well as the other analogues function through a ligation to the heme iron of $P\text{-}450_{arom}$ and hydrophobic interaction with the steroid-binding site. This study also found that the position of the substituent relative to the pyridine nitrogen

and the relative conformational rigidity are major determinants in the inhibition of aromatase activity. Basically, there is a requirement for a pyridinic nitrogen for the effective competitive inhibition of aromatase activity. Furthermore, the structural features essential for effective nonsteroidal inhibitors of aromatase are heme ligation and extensive hydrophobic overlap with the steroid ring plane.

Another study looked at the effects of various substituted pyridine and imidazole compounds on the induction of hepatic microsomal heme oxygenase (HO) and cytochrome P450 in rats[33]. Cytochrome P450 consists of a superfamily of various P450 gene products which play important roles in the detoxification and metabolic activation of endogenous and exogenous substrates, including various drugs and environmental chemicals. They found that the position of the lipophilic moiety bound to the pyridine ring could influence the HO induction response and P450 synthesis. They found that the substituted pyridines at the 2-position with some aromatic derivatives (i.e., 2-phenylpyridine), generally showed more potent abilities to induce HO than the other 3- and 4-positional isomers.

Furthermore, another study showed that 2-phenylpyridine inhibit oxidative phosphorylation in isolated mitochondria from the rat and decrease locomoter activity in the mouse[34]. Overall, these studies show that 2-phenylpyridine has the potential to cause a number of toxic effects in rats, mice and human. Therefore, precaution must be used when handling this compound.

4.2.5. 2-Phenylquinoline

The literature on 2-phenylquinoline is quite sparse. To date very little, if any, pharmokinetic and toxicological studies have been done with this compound. The structure of 2-phenylquinoline is seen in **Figure 4.5**. This compound is similar in structure to 2-

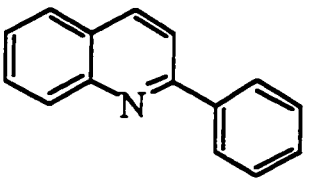

Figure 4.5: Structure of 2-phenylquinoline.

phenylpyridine but seems to be less toxic. 2-Phenylquinoline has been proposed to be an effective antileishmanial drug in one research study[35]. The authors of this study found that treatment with 2-phenylquinoline administered orally at 50 mg/kg twice daily for 15 days decreased the lesions in the infected animals by 68% ($P < 0.001$). However, they noted that intralesional injections of 2-phenylquinoline at 50 mg/kg did not suppress the parasite burden. In summary, this study indicated a potential use of 2-phenylquinoline against leishmaniasis. Overall, this indicates that 2-phenylquinoline is fairly non-toxic since it can be used against disease but until specific toxicological studies are done, some risk still exists.

4.3. Solvent Toxicity

In the preparation of photoresist samples, the polymer, photoacid generator, and all the other components of the formulation must first be dissolved in a compatible solvent. The presence of the solvent eases the step of spin casting and helps to produce a consistent, non-bumpy surface. Upon spin casting the polymer solution, the sample is baked, such that the solvent is evaporated. Although, not a specific part of the photoresist, the solvent is still an important part of its manufacture. For this reason the toxicity of the solvent is very important to the people that must handle these materials. Upon spin coating the wafers, they come in contact with the vapors of the solvent. Initially, the solvent used in the preparation of photoresist samples was bis(2-methoxyethyl) ether or diglyme. Within the last ten years, a number of studies has shown that diglyme is quite toxic and for this reason photoresists

industries has opted to change the solvent. The most solvent most commonly used is ethyl lactate which is considerably less toxic than diglyme.

4.3.1 Bis(2-Methoxyethyl) Ether

Bis(2-methoxyethyl) ether (or dimethylene glycol dimethyl ether, diglyme) belongs to a family of compounds classified as glycol ethers. The structure is in **Figure 4.6.**

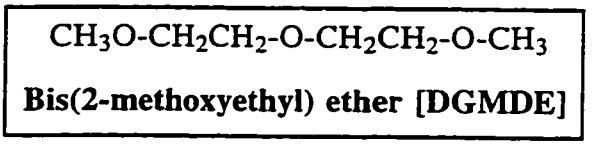

Figure 4.6: Structure of diglyme.

Diglyme is an aprotic solvent used in a variety of industrial products, where potential occupational exposure would occur by inhalation and dermal contact. Diglyme has been shown to be a reproductive toxicant in male rats and male mice and a developmental toxicant in pregnant mice and in rabbits[36]. Diglyme has been shown to cause significantly reduced male rat fertility[37], as well as adverse effects on fetal growth, viability, and morphological development[38]. It has been shown that the metabolism of diglyme in Sprague-Dawley rats results in four major metabolites [36]. These are illustrated in **Figure 4.7.**

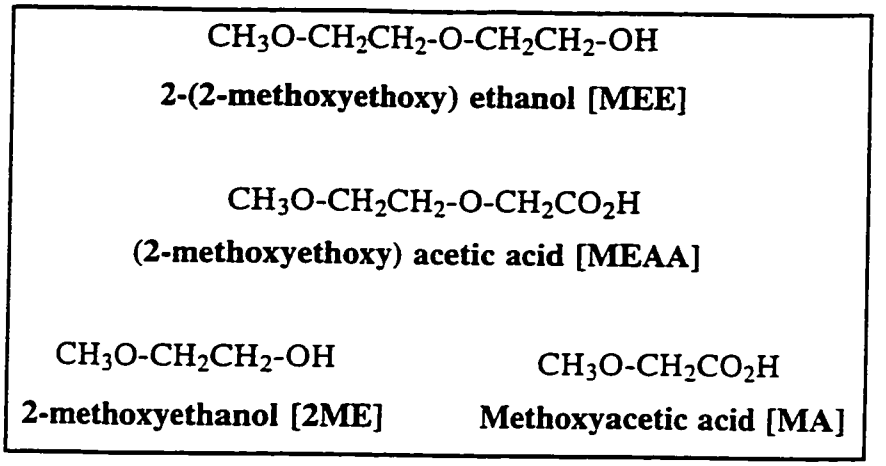

Figure 4.7: Metabolites of Diglyme.

The metabolic scheme of diglyme has been proposed to occur via two separate pathways[39]. The primary pathway involves a single O-demethylation step to form MEE, which is then oxidized first to (2-methoxyethoxy) acetaldehyde by alcohol dehydrogenase and subsequently to MEAA by aldehyde dehydrogenase. A secondary pathway proceeds by cleavage of the interior ether bond to form 2ME, which, in part, undergoes similar enzymatic oxidation to form MAA.

The principal metabolite of diglyme has been shown to be (2-methoxyethoxy) acetic acid [MEAA][36]. However, the observed toxicity of diglyme, as discussed above, has been attributed to the metabolite, methoxyacetic acid (MAA). Exposure to 2-methoxyethanol or methoxyacetic acid, the minor metabolites of diglyme, have been reported to cause encephalopathy and erythocyte hemolysis as well as reduced leucocyte count in man[40]. Similar blood effects have been noted for 2-methoxyethanol in rats, dogs, and mice[40]. Reproductive effects in rats exposed to 2-methoxyethanol or methoxyacetic acid have been repeatedly demonstrated[40] as well as developmental toxicity. For these compounds, the earliest sign of testicular tubular atrophy is depletion of the pachytene spermatocytes, with prolonged exposure

resulting in depletion of spermatocytes and spermatids. Other studies have indicated that the principal reproductive toxicant is methoxyacetic acid. This metabolite has been identified in the rats given single potent doses of diglyme[39] and in the blood and urine of pregnant mice given embryotoxic oral doses of diglyme as well as in embryonic tissue taken from the exposed dams[41].

The metabolic pathway involving the cleavage of the central ether bond is thought to be mediated by certain cytochrome P-450 isozymes, as first evidenced by the finding that MAA is formed in significantly greater amounts in rats treated with phenobarbital than in rats given no such pretreatment[42]. More recently, it was reported that the metabolism of diglyme to 2ME, a precursor of MAA in rat liver microsomes was NADPH-dependent. Overall, in the male rat, diglyme undergoes complete metabolism with greater than 83% of the dose excreted as urinary metabolites within 96h of administration[40]. The urinary MAA accounted for only 6.2% of the administered dose, whereas the principle metabolite, identified as (2-methoxyethoxy)acetic acid (MEAA), represented 67.9% of the dose.

Overall, most of the studies indicate that the metabolism of diglyme results in the formation of methoxyacetic acid, a known developmental toxicant. Harmful effects include fetal malformations in pregnant mice, as well as tubular atrophy in the testis of males leading to reduced fertility. One study has suggested that the acid metabolite may produce the reproductive effects in the rat either through interference as a "false substrate" in the tricarboxylic acid cycle or as an inhibitor of sarcosine metabolism[40]. Although the mechanism of action is not yet clear, it is quite clear that methoxyacetic acid is responsible for the toxic effects observed for diglyme.

4.3.2. Ethyl Lactate

In the photoresist industry, ethyl lactate was the solvent that was used to replace diglyme. The structure of ethyl lactate is shown in **Figure 4.8.**

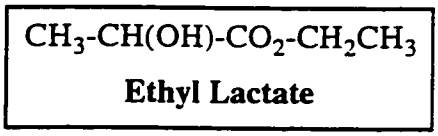

Figure 4.8: Structure of ethyl lactate.

Overall, it is a fairly non-toxic and can be used without risk in industrial settings. Studies have shown that ethyl lactate breaks down into ethanol and lactic acid in the blood. The average lethal doses (LD_{50}) for ethyl lactate and ethanol are reported to be 618 mg/kg and 2.0 g/kg respectively[43]. The toxicity of ethyl lactate is low enough that is has been used as a cosolvent for intravenous administration of theophylline, a drug employed in the use of asthma therapy[44]. Furthermore, ethyl lactate has been shown to be an effective treatment for acne[45] with only minimal reported cases of allergic contact dermatitis[46]. Overall, these uses of ethyl lactate indicate that it is a fairly non-toxic solvent and can be used with much less worry than diglyme.

4.4. Photoresist Polymers

In the manufacture of photoresists, a polymer is required. For these purposes a number of different polymers are utilized to make the different photoresist samples. The people that manufacture these photoresists have to synthesize the polymer, conduct various experiments with the polymer produced, and use it for photoresist manufacture. In terms of the toxicological properties of these polymers, it has been shown that most plastics produce severe tissue reaction in their particulate forms. They also produce tumors in rats[47,48]. Although, a

number of polymers are used to make the photoresist samples, only polymethylmethacrylate was reviewed for the purposes of this chapter.

4.4.1 Polymethylmethacrylate

Polymethylmethacrylate is a polymer that is used for a variety of industrial and medical purposes. It has been used as a biomaterial for the manufacture of cemented prosthetic joints and due to evidence of toxicity a number of studies have looked at the toxicity of PMMA particulates[49,50]. It has been shown that implanted biomaterials induce various degrees of non-specific foreign body inflammatory response, which are critical to their integration and susceptibility to infection[49]. A major part of this inhibitory response involves macrophage interaction with biomaterials. Exposure of macrophages to various biomaterials alters the physiology and biochemistry of the macrophages. One study showed that the exposure of macrophages to poly(methyl methacrylate) particles, *in vitro*, inhibited DNA synthesis, impaired their cytolytic ability and induced death[51]. Overall, this study showed the potential toxicity that PMMA can cause when used as a biomaterial. Although, the use of PMMA in the photoresist industry does not endanger the person in such ways, there is still possible risk in breathing the dust particles.

4.5. Conclusion

Risk assessment is the systematic scientific characterization of potential adverse health effects resulting from human exposure to hazardous agents or situations[52]. Risk is made up of hazard, an intensive factor, used to describe the property of the agent i.e. its capacity or capability to do harm, and exposure, an extensive factor used to define the property of the context or environment. Therefore, characterizing the risk of a chemical requires knowing what dose of chemical causes which effects (dose-response assessment) and the dose to which worker's are exposed (exposure assessment)[53].

The characteristics of exposure are that adverse or toxic effects in a biological system are not produced by a chemical agent unless that agent or its metabolite breakdown (biotransformation) products reach appropriate sites in the body at a concentration and for a length of time sufficient to produce a toxic manifestation. Many chemicals are of relatively low toxicity in the "native" form but, when acted on by enzymes in the body are converted to intermediate forms that interfere with normal cellular biochemistry and physiology. Thus, whether a toxic response occurs is dependent on the chemical and physical properties of the agent, the exposure situation, how the agent is metabolized by the system, and the overall susceptibility of the biological system or subject. Thus, to characterize fully the potential hazard of a specific chemical agent, the type of effect, the dose required to produce that effect, the exposure, and the disposition by the subject are required. The major factors that influence toxicity as it relates to the exposure situation for a specific chemical are the route of administration and the duration and frequency of exposure.

The term "hazard" is a measure of the strength or thermodynamic properties of the agent, measured as percent detriment per unit dose. Hazard identification is considered the final step in risk assessment[54]. It involves the qualitative determination of whether exposure to a chemical causes an increased incidence of an adverse effect in a population of test animals. and an evaluation of the relevance of this information to the potential for causing similar effects in humans. A test agent's structure, solubility, pH sensitivity, electrophilicity, and chemical reactivity can represent important information for hazard identification. It has been seen that certain key molecular structures have provided regulators with some of the most readily available information on which to assess hazard potential[52]. In order to determine these structures the detailed steps of hazard identification may include: epidemiology, toxicology, *in vitro* tests, and structure-activity analysis.

In doing dose-response assessment, acute and chronic affects are assessed. Acute toxicity occurs within minutes, hours or days and is much easier to observe. On the other hand, chronic toxicity especially cancer assessment is very difficult to assess. Society has decided that no more than one additional cancer in 100,000 or one million exposed people is acceptable, so assessment measures must be able to detect this small number[52]. Two types of evidence are utilized to determine the chemical dose that will result in an adverse health effect. One is derived from animal experiments with the use of mathematical models to predict the levels of a chemical that will cause one additional cancer in a million animals or a million humans. The other type of evidence utilized in chronic toxicity assessment is human exposure, better known as epidemiological evidence. With this type of study human populations are carefully observed and possible associations between specific chemical exposure and particular health effects are investigated.

In this chapter, a number of different studies were reviewed to determine the possible risk of some of the components used in the photoresist industry. Furthermore, some of the dyes that were used for purposes of acid diffusion and quantification were reviewed for their toxicity. This is very important because the use of the chemicals is used extensively in the industry. The decreased toxicity of the solvent ethyl lactate, is very important because diglyme has known reproductive effects. The further replacement of this solvent would be beneficial to all those people who may come in contact with such solvent. Although, the polymers used for photoresist manufacture cannot be replaced, the careful use of the particulate forms must be considered. Furthermore, the toxicity of these dyes is important to decide which are more preferable. This review indicated that fluorescein and 2-phenylquinoline are non-toxic enough to be used for medical purposes. However, it was seen that rhodamine B is used for food coloring. The use of this dye to should be re-considered due to its known carcinogenic effects. Furthermore, the use of acridine has found to be toxic in animals, but these effects have not been observed in humans. The dye 2-phenylpyridine has also found to have toxic effects.

When considering, which dyes are the most non-toxic, it should be remembered that many of these experiments have been done on animals, yeast or flies. When relating these effects to those in humans, it is not a direct process. Many of the experiments above did not relate the effects to humans, and thus it is very difficult to say whether these dyes are harmful to humans. And due to the lack of studies in the literature, it is often impossible to correctly correlate the effects to humans.

Toxicological studies are very important to those working with hazardous chemicals, and for this reason it is very important to conduct such experiments. In terms of the chemicals described above, further work is required for most cases to determine the effects on humans. However, many of the studies indicate possible risks and for this reason, they should be used with caution.

Appendix II - Definitions

- **Acute Exposure** - is defined as exposure to a chemical for less than 24 hours and usually refers to a single administration.

- **Ames test** - in this mutagenicity assay, bacterial cells that are deficient in DNA repair and lack the ability to grow in the absence of histidine are treated with several dose levels of carcinogenic agent, after which reversion to the histidine-positive phenotype is ascertained and mutations can be observed. See Salmonella typhimurium.

- **Aneuploidy** - DNA damage by changes in chromosome number. Specifically, deviation of chromosome number from an exact multiple to the haploid state.

- **Chromosomal Aberration** - DNA damage by gross change in chromosome structure.

- **Clastogenicity** - Ability to cause chromosomal aberrations.

- **Dose-Response Curve** - fundamental basis of the quantitative relationships between exposure to an agent and the incidence of an adverse response.

- **Exposure** - measures whether a compound of interest reaches appropriate sites in the body at a concentration and for a length of time sufficient to produce a toxic manifestation.

- **Exposure Assessment** - the determination of the source, type, magnitude and duration of contact with the agent of interest.

- **Genotoxicity** - deals with the mutagenic effects of chemicals and radiation and the consequences for human health of exposure to mutagens.

- **Germ Cells** - i.e. eggs, sperm, and their precursors. Genes located in the chromosomes of the germ cells transmit genetic information and modulate cell differentiation and organogenesis. Germ cells ensure the maintenance of structure and function in the organism in its own lifetime and from generation to generation.

- **Hazard** - refers to the intrinsic toxic properties of a chemical or substance, i.e., a test agent's stucture, solubility, stability, pH sensitivity, electrophilicity, and chemical reactivity.

- **Hepatotoxic** - compounds that are injurious to the liver

- **Interstitial Cells** - primary site of testosterone synthesis.

- **Intravenous Administration** - this route is used to introduce the toxicant directly into the bloodstream of the animal, eliminating the process of absorption.

- **LD_{50} (Median Lethal Dose)** - dosage of chemicals needed to produce death in 50 percent of treated animals.

- **Metabolism** - modification of a xenobiotic by biotransformation into a compund favoring excretion. This is catalyzed by enzymes in the liver or other tissues.

- **mg/kg** - typical units used to describe the dose of toxicant.

- **mg/kg bw** - units of dose in proportion to the body weight of the animal.

- **Mitotic Recombination** - genetic recombination or crossing-over of homologous DNA sequences during mitosis.
- **NOAEL** - no observed adverse effect level. It is the highest dose level that does not produce a significantly elevated increase in an adverse response.

- **Oxidative Phosphorylation** - or ATP formation. This process occurs by cellular respiration to produce ATP from ADP.

- **Point Mutation** - are also called gene mutations. They are changes in the DNA sequence in a gene and are restricted to a particular site.

- **Poison** - any agent capable of producing a deletrious response in a biological system, seriously injuring function or producing death.

- **Risk** - measure of the probability of an adverse outcome to occur.

- **Risk Assessment** - is the systematic scientific characterization of potential adverse health effects resulting from human exposures to hazardous agents or situations. This type of assessment includes qualitative information on the strength of the chemical and the nature of the outcomes and quantitative assessment of the exposure and the potential magnitude of the risks.

- **Salmonella typhimurium** - is the strain of bacteria that is used in the Ames mutagencity test. These bacteria lack the enzyme phosphoribosyl ATP synthetase, which is required for histidne symthesis. Several different strains have been generated to permit the detection of point mutations and frameshift mutations. See Ames test definition.

- **Sex-Linked Recessive Lethal (SLRL) Test** - this is a genetic assay that is done in Drosophila and it permits the detection of recessive lethal mutations at 600 to 800 different loci on the X chromosome by screening for the presence or absence of wild-type males in the offspring of specifically designed crosses.

- **Somatic Mutations** - refer to mutations in all other cell types and are not heritable but may result in cell death or transmission of a genetic defect to other cells in the same tissue through mitotic division.

- **Subchronic Exposure** - refers to repeated exposure to a chemical for 1 to 3 months.

- **Subcutaneous Administration** - toxicants are administrated directly into the general circulation.

- **Systemic toxicity** - requires absorption and distribution of a toxicant from its entry point to a distant site at which deletrious effects are produced.

- **Toxicity** - the ability of a chemical to illicit detrimental effects at target organs within the body.

- **Toxicology** - study of the adverse effects of chemicals on living organisms.

- **Tubulin** - principle protein of spindle fibres.

References:

(1) Gossel, T. A.; Bricker, J. D. *Principles of Clinical Toxicology, 2nd Edition*; Raven Press: New York, 1990.

(2) Dyson, G. M. *The Chemistry of Chemotherapy*; Ernest Benn Ltd.: London, UK, 1928.

(3) Rubbo, S. D. *J. Exp. Pathol.* **1947**, *28*, 1.

(4) Kapitul'skiy, V. B.; Kogan, F. M.; Dorinovskaya, A. P.; Pachaskev, E. N. *Gig. Truda Profess. Zabol.* **1970**, *14*, 56.

(5) Shubik, P. *Cancer Res.* **1950**, *10*, 13.

(6) Deutsch-Wenzel, R. P.; Brune, H.; Grimmer, G. *Cancer Lett.* **1983**, *20*, 97.

(7) Seixas, G. M.; Andon, B. M.; Hollingshead, P. G.; Thilly, W. G. *Mutation Res.* **1982**, *102*, 201.

(8) Probst, G. S.; McMahon, R. E.; Hill, L. E.; Thompson, C. Z.; Epp, J. K.; Neal, S. B. *Environ. Mutagen* **1981**, *3*, 11.

(9) Moir, D.; Poon, R.; Yagminas, A.; Park, G.; Viau, A.; Valli, V. E.; Chu, I. *J. Environ. Sci. Health* **1997**, *B32*, 545.

(10) McMurtey, K. D.; Knight, T. J. *Mutation Res.* **1984**, *140*, 7.

(11) Combes, R. D.; Haveland-Smith, R. B. *Mutation Res.* **1982**, *98*, 101.

(12) Pouliquen, H.; Algoet, M.; Buchet, V.; Le Bris, H. *Vet. Human Toxicol.* **1995**, *37*, 526.

(13) Yankell, S. L.; Loux, J. J. *J. Peridontol.* **1977**, *48*, 228.

(14) Novotny, H. R.; Alvis, D. L. *Circulation* **1961**, *24*, 82.

(15) Lange, K.; Boyd, L. J. *Bull. NYM Coll. Flower Fifth Ave. Hosp.* **1934**, *6*, 78.

(16) Lentner, A.; Bohler, U. *Photodermatol. Photoimmunol. Photomed.* **1995**, *11*, 178.

(17) Hochsattl, R.; Gall, H.; Weber, L.; Kaufmann, R. *Contact Derm.* **1990**, *22*, 42.

(18) Yannuzzi, L. A.; Rohrer, K. T.; Tindel, L. J. *Ophthalmol.* **1986**, *93*, 611.

(19) Riaz, M.; Pilpel, N. *J. Pharm. Pharmacol.* **1983**, *35*, 79.

(20) Jennings, B. J.; Mathews, D. E. *J. Amer. Optom. Assoc.* **1994**, *65*, 465.

(21) IARC *International Agency for Research on Cancer* **1978**, *16*, 221.

(22) Nestman, E. R.; Douglas, G. R.; Matula, T. I.; Grant, C. E.; Kowbel, D. J. *Canc. Res.* **1979**, *39*, 4412.

(23) Kada, T.; Tutikawa, K.; Sadaie, Y. *Mut. Res.* **1972**, *16*, 165.

(24) Ito, T.; Koboyashi, K. *Phochem. Photobiol.* **1977**, *26*, 581.

(25) Luck, H.; Wallnofer, P.; Bach, H. *Pathologia et Microbiologia* **1963**, *26*, 206.

(26) Lee, W.; Abrahamson, S.; Valencia, R.; Von Halle, E. S.; Wurgler, F. E.; Zimmering, S. *Mut. Res.* **1983**, *123*, 183.

(27) Au, W.; Hsu, T. C. *Environ. Mutagen.* **1979**, *1*, 27.

(28) Lewis, I. L.; Patterson, R. M.; McBay, H. C. *Mutat. Res.* **1981**, *88*, 211.

(29) Tripathy, N. K.; Nabi, M. J.; Sahu, G. P.; Kumar, A. *Fund. Chem. Tox.* **1995**, *33*, 923.

(30) Zimmerman, F. K.; Henning, J. H.; Scheel, I.; Oehler, M. *Mutat. Res.* **1986**, *163*, 23.

(31) Zimmerman, F. K.; Groschel-Stewart, U.; Scheel, I.; Resnick, M. A. *Mutat. Res.* **1985**, *150*, 203.

(32) Vaz, A. D. N.; Coon, M. J.; Peegel, H.; Menon, K. M. J. *Drug Metab. Disp.* **1992**, *20*, 108.

(33) Kobayashi, Y.; Yamamoto, T.; Okui, E.; Kotani, E.; Yoshida, T.; Kuroiwa, Y. *Jpn. J. Toxicol. Environ. Health* **1996**, *42*, 468.

(34) Hassan, M. N.; Thakar, J. H.; Grimes, J. D. *Adv. Neur.* **1990**, *53*, 219.

(35) Fournet, A.; ferreira, M. E.; De Arias, A. R.; De Ortiz, S. T.; Fuentes, S.; Nakayama, H.; Schinini, A.; Hocquemiller, R. *Antimicrob. Agents Chemo.* **1996**, *40*, 2447.

(36) Richards, D. E.; Begley, K. B.; DeBord, D. G.; Cheever, K. L.; Weigel, W. W.; Tirmenstein, M. A.; Savage Jr, R. E. *Arch. Toxicol.* **1993**, *67*, 531.

(37) McGregor, D. B.; Williams, M. J.; McDonald, P.; Neimeier, R. W. *Toxicol. Appl. Pharmacol.* **1983**, *70*, 303.

(38) Price, C. J.; Kimmel, C. A.; George, J. D.; Marr, M. C. *Fundam. Appl. Toxicol.* **1987**, *8*, 115.

(39) Cheever, K. L.; Richards, D. E.; Weigel, W. W.; Lai, J. B.; Dinsmore, A. M.; Daniel, F. B. *Toxicol. Appl. Pharmacol.* **1988**, *94*, 150.

(40) Cheever, K. L.; Weigel, W. W.; Richards, D. E.; Lal, J. B.; Plotnick, H. B. *Tox. & Indust. Health* **1989**, *5*, 1099.

(41) Daniel, F. B.; Cheever, K. L.; Begley, K. B.; Richards, D. E.; Weigel, W. W.; Eisenmann, C. J. *Fund. Appl. Tox.* **1991**, *16*, 567.

(42) Cheever, K. L.; Richards, D. E.; Weigel, W. W.; Begley, K. B. *Toxicol. Ind. Health* **1989b**, *5*, 601.

(43) Martin, A.; Paruta, A. N.; Adjei, A. *J. Pharm. Sci.* **1981**, *70*, 1115.

(44) Christensen, J. M.; Suvanakoot, U.; Ayres, J. W.; Tavipatana, W. *Res. Comm. Chem. Path. Pharm.* **1985**, *50*, 147.

(45) Prottey, C.; George, D.; Leech, R. W.; Black, J. G.; Howes, D.; Vickers, C. F. H. *Brit. J. Derm.* **1984**, *110*, 475.

(46) Willigen, A. H.; Dutree-Meulenberg, R. O. G. M.; Stolz, E.; Guersen-Reitsma, A. M.; Joost, T. *Contact Derm.* **1987**, *17*, 45.

(47) Oppenheimer, B. S.; Oppenheimer, E. T.; Stout, A. P. *Acta Unio Internationalis Contra Cancrum* **1959**, *15*, 659.

(48) Oppenheimer, B. S.; Oppenheimer, E. T.; Danishefsky, I. *Cancer res.* **1955**, *15*, 333.

(49) Giridhar, G.; Gristina, A. G.; Myrvik, Q. N. *Biomat.* **1992**, *14*, 609.

(50) Gelb, H.; Schumacher, R.; Cuckler, J.; Baker, D. G. *J. Orthop. Res.* **1994**, *12*, 83.

(51) Horowitz, S. M.; Frondoxa, C. G.; Lennox, D. W. *J. Orthop. Res.* **1988**, *6*, 827.

(52) Klaassen, C. D. *Casarett & Doull's Toxicology : The Basic Science of poisons, 5th Ed.*; McGraw-Hill Companies, Inc.: New York, 1996.

(53) Lu, F. C. *Basic Toxicology: Fundamentals, Target Organs, and Risk Assessment, 2nd Ed.*; Hemisphere Publishing Company: New York, 1991.

(54) Hodgson, E.; Levi, P. E. *A Textbook of Modern Toxicology*; Elsevier Science Publishing Company, Inc.: 1987.

Claims to Original Research

- We have developed the basic understanding of dyes to allow the for monitoring of acid diffusion in thin polymer films by fluorescence spectroscopy and fluorescence microscopy, by the use of acid-sensitive dyes.

1. Three different types of dyes; aromatic monozines, xanthene dyes and benzothiazole derivatives have been utilized to detect the presence of acid in PHS and PMMA systems.

2. Images as small as 1 μm have been observed by fluorescence microscopy, using the technique of acid-sensitive dyes.

- We have a developed an *in situ* technique of quantifying photoacid generation in polymer systems, and thus have contributed to the understanding of photoacid generation in photoresist samples. This understanding helps to screen new compounds for their acid generation efficiency.

3. DSBS, DMBB, Rhodamine B base, fluorescein, Coumarin-6 have been shown to be ideal sensors for purposes of acid quantification in film by absorption spectroscopy.

4. The rate of acid generation has been found to be slower in samples prepared in PMMA than PHS.

5. PAGs differing only in anionic component have similar PAG efficiencies.

IMAGE EVALUATION
TEST TARGET (QA-3)

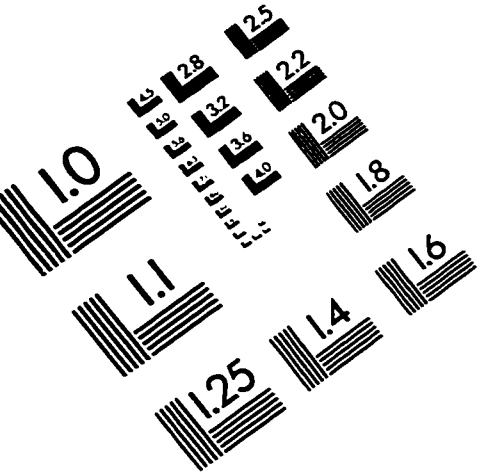

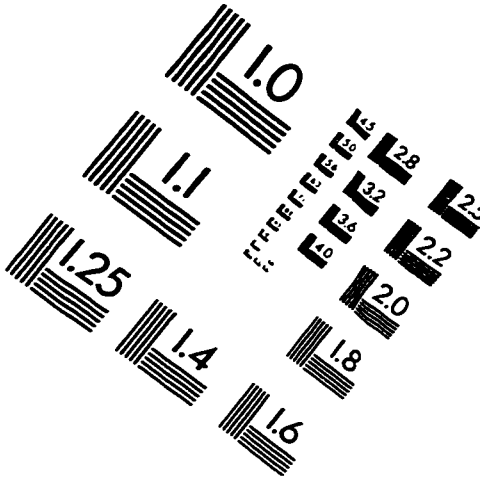

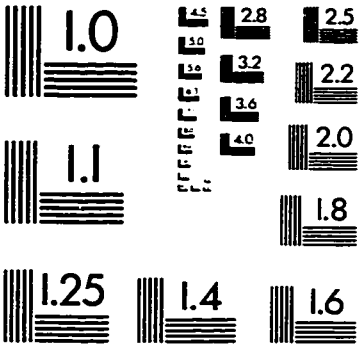

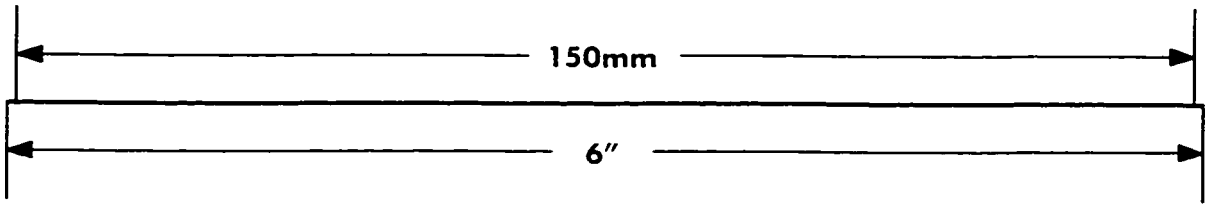

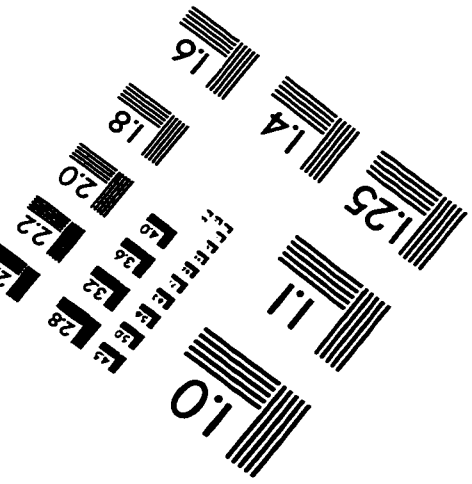

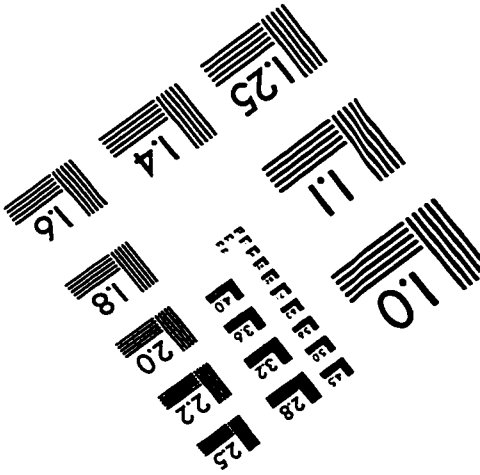

APPLIED IMAGE, Inc
1653 East Main Street
Rochester, NY 14609 USA
Phone: 716/482-0300
Fax: 716/288-5989